

## STATUS OF THESIS

Title of thesis NATURAL CONVECTIVE HEAT TRANSFER ANALYSIS NEAR A  
MOVING INFINITE VERTICAL POROUS PLATE WITH  
NEWTONIAN HEATING

I MUHAMMAD KAMRAN

hereby allow my thesis to be placed at the Information Resource Center (IRC) of Universiti Teknologi PETRONAS (UTP) with the following conditions:

1. The thesis becomes the property of UTP
2. The IRC of UTP may make copies of the thesis for academic purposes only.
3. This thesis is classified as

☐ Confidential

☒ Non-confidential

If this thesis is confidential, please state the reason:

\_\_\_\_\_  
\_\_\_\_\_  
\_\_\_\_\_

The contents of the thesis will remain confidential for \_\_\_\_\_ years.

Remarks on disclosure:

\_\_\_\_\_  
\_\_\_\_\_  
\_\_\_\_\_

Endorsed by

\_\_\_\_\_  
Signature of Author

\_\_\_\_\_  
Signature of Supervisor

Permanent address: House#13  
Street#01Muhalla chamba park near  
Kothi Haq Nawaz sultan Mehmood  
road, Baghbanpura, Lahore, Pakistan.

Name of Supervisor  
Dr. Marneni Narahari

Date : 18-08-2014

Date : 18-08-2014

UNIVERSITI TEKNOLOGI PETRONAS

NATURAL CONVECTIVE HEAT TRANSFER ANALYSIS NEAR A MOVING  
INFINITE VERTICAL POROUS PLATE WITH NEWTONIAN HEATING.

by  
MUHAMMAD KAMRAN

The undersigned certify that they have read, and recommend to the Postgraduate Studies Programme for acceptance this thesis for the fulfillment of the requirements for the degree stated.

Signature: \_\_\_\_\_

Main Supervisor: Dr. Marneni Narahari

Signature: \_\_\_\_\_

Co-Supervisor: Dr. Azuraïen Bt Japper

Signature: \_\_\_\_\_

Head of Department: Dr. Balbir Singh Mahinder Singh

Date: 18-08-2014

NATURAL CONVECTIVE HEAT TRANSFER ANALYSIS NEAR A MOVING  
INFINITE VERTICAL POROUS PLATE WITH NEWTONIAN HEATING

by

MUHAMMAD KAMRAN

A Thesis

Submitted to the Postgraduate Studies Programme

as a Requirement for the Degree of

MASTER OF SCIENCE

FUNDAMENTAL & APPLIED SCIENCE DEPARTMENT

UNIVERSITI TEKNOLOGI PETRONAS

BANDAR SERI ISKANDAR,

PERAK

AUGUST 2014

## DECLARATION OF THESIS

Title of thesis

# NATURAL CONVECTIVE HEAT TRANSFER ANALYSIS NEAR A MOVING INFINITE VERTICAL POROUS PLATE WITH NEWTONIAN HEATING

I \_\_\_\_\_ MUHAMMAD KAMRAN

hereby declare that the thesis is based on my original work except for quotations and citations which have been duly acknowledged. I also declare that it has not been previously or concurrently submitted for any other degree at UTP or other institutions.

Witnessed by

Signature of Author

Signature of Supervisor

Permanent address: House#13  
Street#01Muhalla chamba park near  
Kothi Haq Nawaz sultan Mehmood  
road, Baghbanpura, Lahore, Pakistan.

Name of Supervisor  
Dr. Marneni Narahari

Date : 18-08-2014

Date : 18-08-2014

## DEDICATION

To my father, *Muhammad Ishaq*

for his motivations and moral support.

## ACKNOWLEDGEMENTS

I would like to express sincere thanks to my supervisor Dr. Marneni Narahari for his direction, guidance and encouragement throughout the research work. I would also like to thank the academic and non-academic staff at the Fundamental & Applied Science Department (FASD) and the Centre of Graduate Studies (CGS), Universiti Teknologi PETRONAS for their kind assistance and financial support during my study and giving me a golden opportunity to complete this research work. Finally, I wish to send my regards and appreciations to my family whose support has been valuable.

## ABSTRACT

The natural convective flow due to heat and mass transfer along an impulsively started vertical porous plate has numerous applications in engineering and technology. For example, water filtration in agriculture engineering, distillation, oil cracking, in nuclear reactors, ionization of liquids, etc. In this thesis, the free convection heat and mass transfer flow past an impulsively started infinite vertical porous plate with Newtonian heating is studied. Different physical effects such as heat generation, viscous dissipation, magnetic field, thermal radiation, chemical reaction, Soret and Dufour effects have been examined in this research. The governing non-linear boundary layer equations are transformed to non-dimensional ordinary differential equations by using suitable dimensionless variables. The non-linear problems are then solved by Homotopy Analysis Method (HAM). HAM solution results are found to be in excellent agreement with the exact solution results for limiting cases. The velocity, temperature and concentration profiles as well as skin friction, rate of heat and mass transfer are analyzed through graphs and tables. It has been observed that, the dimensionless velocity increases as the Eckert number, heat generation parameter, Soret number or Dufour number increasing, while it decreases as the suction parameter, magnetic field parameter, radiation parameter or chemical reaction parameter increasing. The dimensionless temperature increases as the Eckert number, heat generation parameter, magnetic field parameter or Dufour number increasing, while it decreases as the suction parameter, radiation parameter or Soret number increasing. Similarly, the dimensionless concentration increases as the magnetic field parameter, Soret and Dufour number increasing, while it decreases as the suction parameter, radiation parameter or chemical reaction parameter increasing.

## ABSTRAK

Aliran olakan bebas disebabkan pemindahan haba dan jisim dengan desakan permulaan di sepanjang plat berlians menegak mempunyai banyak aplikasi dalam kejuruteraan dan teknologi. Sebagai contoh, penapisan air dalam bidang kejuruteraan pertanian, penyulingan, pemisahan minyak, dalam reaktor nuklear, pengionan cecair, dan lain-lain. Dalam tesis ini, aliran olakan bebas pemindahan haba dan jisim yang mengalir melalui desakan permulaan plat tegak berliang dengan pemanasan Newtonan dikaji. Kesan fizikal yang berbeza seperti penjanaan haba, pelepasan likat, medan magnet, sinaran haba, tindak balas kimia, kesan Soret dan Dufour diselidik dalam kajian ini. Persamaan penaklukan lapisan sempadan tak linear diubah kepada persamaan pembezaan biasa tak berdimensi dengan menggunakan pemboleh ubah tak berdimensi yang sesuai. Masalah-masalah tak linear kemudiannya diselesaikan dengan Homotopy Analysis Method (HAM). Keputusan penyelesaian HAM didapati menunjukkan persetujuan yang baik dengan keputusan penyelesaian tepat untuk kes yang terhad. Profil halaju, suhu dan kepekatan serta geseran permukaan, kadar pemindahan haba dan jisim dianalisis melalui graf dan jadual. Hasil pemerhatian bahawa halaju tak berdimensi bertambah apabila nombor Eckert, parameter penjanaan haba, nombor Soret atau nombor Dufour bertambah. Dan halaju berkurang apabila parameter sedutan, parameter medan magnet, parameter sinaran atau parameter tindak balas kimia bertambah. Suhu tak berdimensi pula bertambah apabila nombor Eckert, parameter penjanaan haba, parameter medan magnet atau nombor Dufour bertambah. Dan suhu berkurang apabila parameter sedutan, parameter sinaran atau nombor Soret bertambah. Begitu juga konsentrasi tak berdimensi bertambah apabila parameter medan magnet, nombor Soret dan nombor Dufour bertambah. Dan konsentrasi berkurang apabila parameter sedutan, parameter sinaran atau parameter tindak balas kimia bertambah.



In compliance with the terms of the Copyright Act 1987 and the IP Policy of the university, the copyright of this thesis has been reassigned by the author to the legal entity of the university,

Institute of Technology PETRONAS Sdn Bhd.

Due acknowledgement shall always be made of the use of any material contained in, or derived from, this thesis.

© Muhammad Kamran, 2014

Institute of Technology PETRONAS Sdn Bhd

All rights reserved.

## TABLE OF CONTENT

ABSTRACT.....	vii
ABSTRAK.....	viii
LIST OF FIGURES .....	xii
LIST OF TABLES.....	xv
CHAPTER 1 INTRODUCTION .....	2
1.1 Thesis Outlines .....	2
1.2 Heat Transfer .....	2
1.2.1 Conduction .....	2
1.2.2 Convection .....	3
1.2.2.1 Free Convection .....	3
1.2.2.2 Forced Convection .....	4
1.2.3 Thermal Radiation.....	4
1.3 Mass Transfer .....	5
1.4 Heat Transfer past a Porous Surface.....	6
1.5 Magneto-hydrodynamics (MHD) equations with Ohmic heating.....	7
1.6 Basic Idea of the HAM.....	10
1.7 Literature Review .....	13
1.7.1 Newtonian Heating.....	17
1.8 Problem Statement.....	18
1.9 Research Objectives.....	19
1.10 Significance of the Research .....	19
1.11 Scope of the Research.....	20
1.12 Chapter Summary .....	20
CHAPTER 2 EFFECTS OF HEAT GENERATION AND VISCOUS	
DISSIPATION.....	21
2.1 Introduction.....	21
2.2 Problem Description .....	22
2.3 Solution by HAM .....	25

2.4 Exact Analytical Solution .....	30
2.5 Result and Discussion.....	33
2.6 Chapter Summary .....	42
CHAPTER 3 THERMAL RADIATION AND VISCOUS DISSIPATION	
EFFECTS IN THE PRESENCE OF MAGNETIC FIELD .....	43
3.1 Introduction.....	43
3.2 Problem Description .....	45
3.3 Solution by HAM .....	48
3.4 Exact Analytical Solution .....	50
3.5 Result and Discussion.....	53
3.6 Chapter Summary .....	66
CHAPTER 4 SORET AND DUFOUR EFFECTS IN THE PRESENCE OF THERMAL RADIATION, VISCOUS DISSIPATION AND CHEMICAL REACTION .....	
4.1 Introduction.....	67
4.2 Problem Description .....	70
4.3 Solution by HAM .....	74
4.4 Exact Analytical Solution .....	77
4.5 Result and Discussion.....	82
4.6 Chapter Summary .....	102
CHAPTER 5 CONCLUSION.....	103
5.1 Conclusion .....	103
5.2 Recommendations for Future Work .....	104
APPENDIX A BOUSSINESQ APPROXIMATION .....	105

## LIST OF FIGURES

Figure 2.1: Physical Model .....	23
Figure 2.2: $\hbar$ curves at 20 <sup>th</sup> order of HAM .....	33
Figure 2.3: $\hbar$ curves at 20 <sup>th</sup> order of HAM .....	34
Figure 2.4: Comparison of temperature profiles for HAM and analytical solution at different $Pr$ when $Ec = 0$ . .....	34
Figure 2.5: Comparison of velocity profiles for HAM and analytical solution at different $Gr$ when $Ec = 0$ .....	35
Figure 2.6: Comparison of temperature profiles for HAM and analytical solution at different $s$ when $Ec = 0$ . .....	35
Figure 2.7: Comparison of velocity profiles for HAM and analytical solution at different $s$ when $Ec = 0$ . .....	36
Figure 2.8: Comparison of temperature profiles for HAM and analytical solution at different $Q$ when $Ec = 0$ . .....	36
Figure 2.9: Influence of $s$ on velocity profiles .....	37
Figure 2.10: Influence of $Gr$ on velocity profiles .....	37
Figure 2.11: Influence of $Pr$ on velocity profiles.....	38
Figure 2.12: Influence of $s$ on temperature profiles .....	38
Figure 2.13: Influence of $Q$ on temperature profiles .....	39
Figure 2.14: Influence of $Pr$ on temperature profiles .....	39
Figure 2.15: Influence of $Ec$ on temperature profiles.....	40
Figure 3.1: Physical Model .....	46
Figure 3.2: $\hbar$ curves at 20 <sup>th</sup> order of HAM .....	54
Figure 3.3: $\hbar$ curves at 20 <sup>th</sup> order of HAM .....	54
Figure 3.4: Comparison of temperature profiles for HAM and analytical solution at different $Pr$ when $Ec = 0$ . .....	55
Figure 3.5: Comparison of velocity profiles for HAM and analytical solution at different $Gr$ when $Ec = 0$ .....	55

Figure 3.6: Comparison of velocity profiles for HAM and analytical solution at different $M$ when $Ec = 0$ .	56
Figure 3.7: Comparison of temperature profiles for HAM and analytical solution at different $R$ when $Ec = 0$ .	56
Figure 3.8: Comparison of temperature profiles for HAM and analytical solution at different $s$ when $Ec = 0$ .	57
Figure 3.9: Comparison of velocity profiles for HAM and analytical solution at different $s$ when $Ec = 0$ .	57
Figure 3.10: Influence of $Pr$ on velocity profiles.	58
Figure 3.11: Influence of $Pr$ on temperature profiles. ....	59
Figure 3.12: Influence of $Gr$ on velocity profiles. ....	59
Figure 3.13: Influence of $M$ on velocity profiles. ....	60
Figure 3.14: Influence of $M$ on temperature profiles. ....	60
Figure 3.15: Influence of $R$ on velocity profiles. ....	61
Figure 3.16: Influence of $R$ on temperature profiles. ....	61
Figure 3.17: Influence of $s$ on velocity profiles. ....	62
Figure 3.18: Influence of $s$ on temperature profiles. ....	62
Figure 3.19: Influence of $Ec$ on temperature profiles. ....	63
Figure 4.1: Physical Model .....	71
Figure 4.2: $\hbar$ curves at 20 <sup>th</sup> order of HAM .....	83
Figure 4.3: $\hbar$ curves at 20 <sup>th</sup> order of HAM .....	83
Figure 4.4: Comparison of temperature profiles for HAM and analytical solution at different $s$ when $Ec = Du = 0$ .....	84
Figure 4.5: Comparison of Concentration profiles for HAM and analytical solution at different $s$ when $Ec = Du = 0$ .....	85
Figure 4.6: Comparison of velocity profiles for HAM and analytical solution at different $s$ when $Ec = Du = 0$ .....	85
Figure 4.7: Comparison of velocity profiles for HAM and analytical solution at different $M$ when $Ec = Du = 0$ .....	86
Figure 4.8: Comparison of temperature profiles for HAM and analytical solution at different $R$ when $Ec = Du = 0$ .....	86

Figure 4.9: Comparison of concentration profiles for HAM and analytical solution at different $\gamma$ when $Ec = Du = 0$ .....	87
Figure 4.10: Comparison of concentration profiles for HAM and analytical solution at different $Sr$ when $Ec = Du = 0$ .....	87
Figure 4.11: Comparison of temperature profiles for HAM and analytical solution at different $Pr$ when $Ec = Du = 0$ .....	88
Figure 4.12: Comparison of velocity profiles for HAM and analytical solution at different $Gm$ when $Ec = Du = 0$ .....	88
Figure 4.13: Comparison of concentration profiles for HAM and analytical solution at different $Sc$ when $Ec = Du = 0$ .....	89
Figure 4.14: Comparison of velocity profiles for HAM and analytical solution at different $Gr$ when $Ec = Du = 0$ .....	89
Figure 4.15: Influence of $s$ on the dimensionless velocity profile.....	90
Figure 4.16: Influence of $Sr$ on the dimensionless velocity profile.....	91
Figure 4.17: Influence of $R$ on the dimensionless velocity profile.....	91
Figure 4.18: Influence of $M$ on the dimensionless velocity profile. ....	92
Figure 4.19: Influence of $\gamma$ on the dimensionless velocity profile. ....	92
Figure 4.20: Influence of $Du$ on the dimensionless velocity profile. ....	93
Figure 4.21: Influence of $Gr$ on the dimensionless velocity profile.....	93
Figure 4.22: Influence of $Gm$ on the dimensionless velocity profile.....	94
Figure 4.23: Influence of $s$ on the dimensionless temperature profile. ....	94
Figure 4.24: Influence of $M$ on the dimensionless temperature profile. ....	95
Figure 4.25: Influence of $Sr$ on the dimensionless temperature profile. ....	95
Figure 4.26: Influence of $R$ on the dimensionless temperature profile. ....	96
Figure 4.27: Influence of $Du$ on the dimensionless temperature profile. ....	96
Figure 4.28: Influence of $Ec$ on the dimensionless temperature profile.....	97
Figure 4.29: Influence of $s$ on the dimensionless concentration profile.....	97
Figure 4.30: Influence of $Sr$ on the dimensionless concentration profile.....	98
Figure 4.31: Influence of $R$ on the dimensionless concentration profile.....	98
Figure 4.32: Influence of $\gamma$ on the dimensionless concentration profile. ....	99

## LIST OF TABLES

Table 2.1: Effects of Eckert number ( $Ec$ ) and heat source parameter ( $Q$ ) on velocity profile.....	40
Table 2.2: Skin Friction ( $\tau$ ) and Nusselt number ( $Nu$ ) variation .....	41
Table 3.1: Influence of Eckert number ( $Ec$ ) on fluid velocity.....	64
Table 3.2: Influence of thermal Grashof number ( $Gr$ ) on fluid temperature.....	64
Table 3.3: Skin Friction ( $\tau$ ) and Nusselt number ( $Nu$ ) variation .....	65
Table 4.1: Influence of $M$ on concentration profile $C(y)$ .....	99
Table 4.2: Influence of $Du$ on concentration profile $C(y)$ .....	100
Table 4.3: Influence of $\gamma$ on temperature profile $\theta(y)$ .....	100
Table 4.4: Skin Friction ( $\tau$ ), Nusselt number ( $Nu$ ) and Sherwood number ( $Sh$ ) effects .....	101

## LIST OF NOMENCLATURE

$B_0$	Magnetic Field ( $T$ )
$C$	Dimensionless Concentration
$C'$	Dimensional Concentration ( $Kgm^{-3}$ )
$c_p$	Specific Heat at Constant Pressure ( $JK^{-1}Kg^{-1}$ )
$c_s$	Concentration Susceptibility ( $Kgm^{-3}$ )
$C'_\infty$	Free Stream Dimensional Concentration ( $Kgm^{-3}$ )
$D_m$	Mass Diffusivity ( $m^2s^{-1}$ )
$Du$	Dufour Number
$Ec$	Eckert Number
$g$	Acceleration due to Gravity ( $ms^{-2}$ )
$Gm$	Mass Grashof Number
$Gr$	Thermal Grashof Number
$h$	Heat Transfer coefficient ( $Wm^{-2}K^{-1}$ )
$k$	Thermal Conductivity ( $Wm^{-1}K^{-1}$ )
$k_c$	Rate of Chemical Reaction
$k_T$	Thermal Diffusion Ratio
$M$	Magnetic Field Parameter, i.e., Square of the Hartmann Number
$Nu$	Nusselt Number
$P$	Pressure ( $Pa$ )
$Pr$	Prandtl Number
$Q$	Dimensionless Heat Source Parameter
$Q'$	Dimensional Heat Source ( $J$ )
$q_r$	Radiative Heat Flux ( $Wm^{-2}$ )
$R$	Thermal Radiation Parameter
$s$	Suction Parameter
$Sc$	Schmidt Number



$Sh$	Sherwood Number
$Sr$	Soret Number
$T'$	Temperature of the Fluid ( $K$ )
$T_m$	Mean Fluid Temperature ( $K$ )
$T'_\infty$	Free Stream Temperature ( $K$ )
$u$	Dimensionless Fluid Velocity
$u'$	Dimensional Fluid Velocity ( $ms^{-1}$ )
$u_0$	Velocity of the Plate ( $ms^{-1}$ )
$v_0$	Suction Velocity ( $ms^{-1}$ )
$x, y$	Dimensionless Cartesian co-ordinates
$x', y'$	Cartesian co-ordinates

#### Greek symbols

$\alpha$	Absorption coefficient
$\beta$	Thermal Expansion coefficient ( $K^{-1}$ )
$\beta^*$	Concentration Expansion coefficient ( $m^3 Kg^{-1}$ )
$\gamma$	Chemical Reaction Parameter
$\theta$	Dimensionless Fluid Temperature
$\mu$	Dynamic Viscosity ( $Pa.s$ )
$\nu$	Kinematic Viscosity ( $m^2 s^{-1}$ )
$\rho$	Fluid Density ( $Kgm^{-3}$ )
$\sigma$	Electrical Conductivity ( $Sm^{-1}$ )
$\sigma^*$	Stefan-Boltzmann Constant ( $Wm^{-2} K^{-4}$ )
$\tau$	Skin Friction
$\tau'$	Sheer Stress ( $Kgm^{-1} s^{-2}$ )

# CHAPTER 1

## INTRODUCTION

### 1.1 Thesis Outlines

In this thesis Homotopy Analysis Method (HAM) is applied to solve system of non-linear ordinary differential equations. In chapter 1, a brief introduction about heat and mass transfer, heat transfer through a porous plate, Magneto-hydrodynamic (MHD) equations of viscous incompressible fluid with ohmic heating, basic idea of HAM, literature review about the free convection along a porous plate, problem statement, research objectives, significance and scope of research are given. In chapter 2, an incompressible viscous fluid flow problem with heat generation parameter is considered to illustrate the application and scope of HAM. In chapter 3, we explore the solution of a viscous fluid flow problem in the presence of thermal radiation and transverse magnetic field. Chapter 4 deals with MHD fluid flow to study the Soret and Dufour effects. In addition, all chapters incorporate the HAM solution of the respective problem and the validation of results with the exact analytical solution results for limiting cases. Chapter 5 presents the main findings of the present study and recommendations for future work.

### 1.2 Heat Transfer

Heat transfer deals with the study of rates at which exchange of heat takes place between a source and a receiver. Energy, as heat, is transfer from one place to another within the system or between the systems due to temperature difference. When two bodies at different temperature are brought into thermal contact, heat transfer takes place from higher temperature region to lower temperature region. The net flow of the heat is always in the direction of lower temperature region. The energy, in heat transfer

process, cannot be measured or observed directly. However, its effects can be identified and quantified through measurements and analysis. Heat-transfer phenomena occur in many industrial and environmental processes, particularly in energy utilization, thermal processing and thermal control. The purpose of thermal processing is to force a temperature change in the system that enables or disables some material transformation; e.g., in food pasteurization, cooking, steel tempering or annealing. Heat transfer encompasses all phenomena occurring in the environmental sciences like meteorology, oceanography, pollutant dispersion, forest fires, urban planning, building, etc. In manufacturing industry heat transfer plays fundamental role to manufacture the energy conversion devices, like solar collectors, combustors, incandescent lamps, radiators, refrigerators, heat exchangers, etc. Heat transfer problems are encountered in many chemical reactions such as crystallization, distillation, ionization and oil cracking. The study of heat transfer may arise in materials processing like casting, welding, hot shaping and crystal growth. It has wide range of applications in high speed air craft, missiles, re-entry vehicles, cooling of turbine blades, air conditioning and in nuclear reactors. A heat transfer analysis must also be made in the design of electric machines, transformers, computer assemblies, electronic chips and bearings to avoid conditions that will cause overheating and damage the equipment.

When temperature difference exists, heat transfer is classified into three basic mechanisms, namely conduction, convection and thermal radiation.

### **1.2.1 Conduction**

Conduction is a heat transfer mechanism in which heat is transferred from higher energetic particles to lower energetic particles as a result of their lattice or random collision. In conduction heat transfer, atoms or molecules physically interact by elastic and inelastic collisions to transfer their energy from higher temperature region to lower temperature region. In conduction, usually termed as molecular phenomenon, energy transfer takes place in all form of ponderable matter, such as solids, liquids, gases and ionized plasmas. In opaque solids conduction rate is high as compared to liquids and gases. Heat is transferred by conduction in numerous examples such as flow of heat

through bricks of a furnace, metallic sheet of a boiler, metallic wall of a heat exchanger tube, etc. A monograph [1] on the heat conduction explores the various aspects of thermal conduction in the heat transfer process.

### **1.2.2 Convection**

The transverse of energy from one region to another due to macroscopic motion in a fluid, added on the energy transfer by conduction is called heat transfer by convection. In other words, convection is the heat transfer mechanism in which heat transfer takes place between the solid surface and the adjacent moving fluid. In convective heat transfer phenomenon, physical mixture of hot and cold portion of fluid and solid is responsible for the flow of heat from one region to another region. Numerous practical applications of convective heat transfer in chemical process industries involve either heat transfer from a fluid or heat transfer to a fluid. A detailed tract [2] on the convective heat transfer explains numerous aspects in the study of heat transfer. In the literature, it has been observed that convection on a surface merely depends upon the three fundamental factors that play a major role in convective heat transfer: (i) fluid motion, (ii) nature of the moving fluid, and (iii) surface geometry. The convection mode of heat transfer actually classified into two basic phenomena, free convection and forced convection.

#### ***1.2.2.1 Free Convection***

Free or natural convection is a phenomenon, a type of convective heat transfer, in which heat flows with the fluid motion generated by the density variation occurring in the fluid due to temperature gradient. Free convection actually consists of two mechanisms operating simultaneously, (i) gravitational force, and (ii) density gradient. Due to density gradient, caused by temperature difference, fluid closer to the body receives heat, become less dense and rises, meanwhile surrounding cooler fluid then moves to replace it. In this way, density difference creates an ascendant movement of the fluid closer to the body. The driving force for free convection is the buoyancy force due to combined gravitational force and density gradient of the fluid. Hence in free convection

flow, momentum and energy equations are depend on each other. Free convection flows have been studied extensively because of their numerous applications in science and engineering. Practical applications of free convection are such as heat transfer from the surface of a pipe to the ambient air and in transmission lines as well as from various electronic devices and finned surfaces, as heat sinks, that are designed to use in microelectronics cooling systems.

#### *1.2.2.2 Forced Convection*

A convection process in which fluid motion is generated by an external mean (such as pump, fan, suction device, etc.) is called forced convection. In such type of flow, heat transfer rate at the surface of fluid can be enhanced by pressure gradient. So, the most common perception is that higher the pressure gradient, higher the forced convection, and therefore higher the cooling rate of the moving fluid. In forced convection flow, momentum equation is independent of the energy equation but the energy equation depends on the momentum equation. Forced convection plays a fundamental role in daily use appliance, including air conditioning, cooling of computer's assemblies, micro-wave ovens, etc. Forced convection is also used in engineering practices to provide the best design of heat conducting devices such as heat exchangers, rocket nozzles and shuttle wings are few among the examples.

#### **1.2.3 Thermal Radiation**

The mode of heat transfer in which energy is generated by charged particles of matter in the form of electromagnetic waves (or photons) as a result of the changes in the electronic configurations of that charged particles (such as atoms or molecules), is called thermal radiation. In this heat transfer mechanism, electromagnetic radiations are emitted from solid surfaces, emission may also occur from liquids and gases, which have temperature above absolute zero. The energy of the radiation field is transported by electromagnetic waves or photons, which does not require a physical medium for their propagation. While other modes of heat transfer require the presence of a material medium for their heat transmission. In fact, radiation transfer occurs most efficiently in

vacuum and therefore it suffers no attenuation in space. This is exactly how the sunlight reaches the earth in the form of thermal radiation. When these radiations are incident on the earth's surface, a portion of the total energy is absorbed in the surface, a portion is reflected from the surface, and the remainder is transmitted through the surface. The earth's absorption of solar radiation and its outgoing thermal radiation cause to create a temperature difference on the surface of earth. Due to this temperature difference a change in the earth's climate occur. When temperatures are uniform, the radiative heat flux between objects is in equilibrium and there is no net heat transmission between them. The balance is disturbed when temperature difference become non-uniform and thermal energy is transported from higher temperature region to lower temperature region. Generally, two limiting cases of radiative heat transfer mechanism are considered in literature, namely (i) optically thick limit and (ii) optically thin limit. The ratio of the characteristic physical dimension to the penetration length of radiation is termed as the optical dimension of a system. For an optically thick medium, radiation can be considered as a diffusive process in which penetration length is small and is equivalent to the radiation mean free path. On the other hand, a reverse trend can find for an optically thin medium. Many researchers have studied the thermal radiation for the heat transfer phenomena - Siegel et al. [3], Modest [4], etc.

### **1.3 Mass Transfer**

The phenomenon in which constituent of matter moves from a region of higher concentration to that of lower concentration is called mass transfer. In mass transfer, constituent transports to the direction of reducing concentration gradient and when concentration gradient is zero then equilibrium takes place. In other words wherever the concentration difference exists, mass transfer takes place.

Mass transfer processes may be divided into two categories: molecular diffusion and convective mass transfer. Diffusion pertains to the transport of constituents through the action of random motions and its rate depends on the temperature, velocity of the fluid and size of the particles. Molecular diffusion takes place in solids, liquids or gases.

Convection refers to transport of the constituents with the mean fluid flow along with the molecular diffusion. Convective mass transfer is carried out in liquids and gases.

Mass transfer operation plays an important role in nature and industries. For example, evaporation of the water from the surface to the atmosphere, diffusion of chemical impurities in the water, separation of chemical particles in the distillation process, elimination of toxic gases and deodorization of air, humidification, drying, crystallization and number of other techniques.

#### **1.4 Heat Transfer past a Porous Surface**

A porous medium is a material that contains interconnected voids or spaces through which fluid (liquid / gas) can pass. Physically, porosity of porous mediums depends on the size of pores. Materials with smaller size of pores are less permeable, while materials with high porosity have large pore size and are easily permeated. Sand, soil and some type of stones are general examples of naturally occurring porous medium. On the other hand, ceramics and foams are manufactured to use as porous media. There are numerous applications of porous media in science, engineering and everyday life. Among all these applications filtration is the most common one. In industries, porous materials can be used to filter gases or liquids from certain compounds, e.g., petroleum refining, heat transfer from preserved agriculture products, water filtration in which carbon filters are used to filter undesirable organic compounds and metals from the water, etc.

A literature survey reveals that the boundary layer flow past a porous surface has been studied by a number of researchers. Kim [5] reported the heat transfer through moving vertical porous plate in a micropolar fluid. He found that by increasing the permeability parameter, velocity increases rapidly near the porous plate and then decreases to the relevant free stream velocity. Jaiswal and Soundalgekar [6] studied the temperature effects on a viscous incompressible dissipative fluid flow past an infinite vertical porous plate embedded in a porous medium under the influence of constant suction. Kim and Fedorov [7] examined the thermal radiation effects on unsteady mixed convection flow of a micro polar fluid along a vertical porous plate. They used

Rosseland approximation to study the radiation effects for an optically thick fluid. Makinde [8] studied the free convection interaction with thermal radiation in a boundary layer flow past a moving vertical porous plate using shooting method. An analytical series solution for unsteady mixed convection stagnation point flow along a vertical surface in a porous medium was investigated by Liao et al. [9]. Seddeek and Salama [10] investigated the effects of variable viscosity and thermal conductivity on unsteady laminar flow past a semi-infinite vertical porous plate using shooting method. In the presence of thermal radiation, effects of variable suction and thermophoresis on combined free-forced convective flow over an inclined porous plate have been examined by Aslam et al. [11]. An analytical study for a first order homogenous chemical reaction and electrically conducting viscous fluid past a moving vertical porous plate with time dependent variable suction velocity has been reported by Ibrahim et al. [12]. Damseh and Shannak [13] used the Crank-Nicolson method to investigate the unsteady free convection flow of an incompressible visco-elastic fluid past an infinite continuously moving vertical porous plate in the presence of first order chemical reaction.

### **1.5 Magneto-hydrodynamics (MHD) equations with Ohmic heating**

Magneto-hydrodynamics deals with the study of moving fluid in an electromagnetic field. The basic equations of MHD, in fluid dynamics, consist of the modified electro-dynamic and hydrodynamic equations. In MHD modified equations, Maxwell's electro-dynamic equations remain same. The ohm's law in which electric current is proportional to the potential difference across the ends of a conductor has been modified to the induced current. The modified momentum equation has to include the Lorentz force into account. The inclusion of the ohmic/joule heating modifies the energy equation. Charge density is negligible for neutral fluids. Also in MHD, when the velocity of the moving fluid is very slow in comparison with the velocity of light then the Maxwell displacement current can be neglected and the fluid may be treated as a continuum, without mean-free-path effects. In the same case, convection current can also be neglected as compared to the conduction current.



The basic equations for viscous incompressible MHD fluid flow can be summarized in the form of the continuity, momentum and energy equations.

The equation of continuity is

$$\nabla \cdot \vec{V} = 0, \quad (1.1)$$

where  $\vec{V}$  is the fluid velocity vector. The equation of the continuity basically is a statement about the law of conservation of the mass. According to this law mass of the fluid within the specified region is conserved.

The momentum equation for MHD fluid is

$$\rho \left[ \frac{\partial \vec{V}}{\partial t} + (\vec{V} \cdot \nabla) \vec{V} \right] = -\nabla p + \mu \nabla^2 \vec{V} + (\vec{j} \times \vec{B}) + \rho g, \quad (1.2)$$

where  $\rho$  is the fluid density,  $p$  the modified fluid pressure including centrifugal force,  $\mu$  the coefficient of viscosity,  $\vec{j}$  the current density vector,  $\vec{B}$  the magnetic induction vector and  $g$  the acceleration due to gravity. In the above equation (1.2) the term  $(\vec{V} \cdot \nabla) \vec{V}$  represents the convective acceleration which is usually caused by a change in fluid velocity over position,  $\nabla p$  the pressure gradient,  $\mu \nabla^2 \vec{V}$  the viscous force and  $\vec{j} \times \vec{B}$  the Lorentz force term. The equation (1.2) is the modified form of the Navier-Stokes' equation.

The equation of state for the incompressible viscous fluid under the Boussinesq approximation can be written as

$$\rho = \rho_0 [1 - \beta(T' - T'_0)] \quad (1.3)$$

where  $\beta$  is the thermal expansion coefficient,  $T'$  the fluid temperature,  $T'_0$  the reference temperature and  $\rho_0$  the fluid density at temperature  $T'_0$ .

The Maxwell's equations are

$$\nabla \times \vec{B} = \mu_e \vec{j} \text{ (Ampere's law),} \quad (1.4)$$

$$\nabla \times \vec{E} = -\frac{\partial \vec{B}}{\partial t} \text{ (Faraday's law of magnetic induction),} \quad (1.5)$$

$$\nabla \cdot \vec{B} = 0 \text{ (Gauss's law for magnetism),} \quad (1.6)$$

$$\nabla \cdot \vec{D} = \rho_e \text{ (Gauss's law),} \quad (1.7)$$

where  $\mu_e$  is the magnetic permeability,  $\vec{E}$  the electric field vector,  $\vec{D}$  the displacement vector and  $\rho_e$  the electric charge density.

By the Ohm's law,

$$\vec{j} = \sigma(\vec{E} + \vec{V} \times \vec{B}) \quad (1.8)$$

From the Navier-Stokes' equation, the magnetic induction equation can be modified as

$$\frac{\partial \vec{B}}{\partial t} = \nabla \times (\vec{V} \times \vec{B}) + v_m \nabla^2 \vec{B}, \quad (1.9)$$

where  $v_m = \frac{1}{\sigma \mu_e}$  is the magnetic diffusivity and  $\sigma$  the electrical conductivity of the fluid. Generally, the equation (1.9) holds for all compressible or incompressible fluids and it is quite independent from the Lorentz or Coriolis forces.

The energy equation including viscous dissipation and ohmic heating is

$$\rho c_p \left[ \frac{\partial T'}{\partial t} + (\vec{V} \cdot \nabla) T' \right] = k \nabla^2 T' + \mu \phi + \frac{\vec{j}^2}{\sigma} \quad (1.10)$$

where  $k$  is the thermal conductivity of the material,  $c_p$  the specific heat at constant pressure,  $\phi$  the viscous dissipation term and  $\frac{\vec{j}^2}{\sigma}$  the ohmic heating.

The combination of the momentum equations of fluid dynamics and Maxwell's equations of electromagnetism generally describe the MHD effects in the heat and mass transfer problems. Magneto-hydrodynamics and ohmic heating have numerous applications in science and engineering. MHD plays a fundamental role in plasma physics. The applications of MHD has been found in problems related to power generation, space research, cooling of nuclear reactor and many other engineering fields. Applications of ohmic heating are very broad ranging from science to industry. In the literature [14] it has been found that the applied electric field under ohmic heating causes electroporation of cell membranes. The principles of ohmic heating also used in blanching, evaporation, dehydration, sterilization, and pasteurization.

## 1.6 Basic Idea of the HAM

Consider a non-linear differential equation in the general form

$$N[u(y)] = 0 \quad (1.11)$$

where  $N$  represents a non-linear differential operator and  $u(y)$  is a solution of that non-linear differential equation. Let  $u_0(y)$  denote the initial guess of  $u(y)$ , which satisfies the initial and boundary conditions of the equation (1.11). To illustrate the idea of HAM, a continuous mapping can be defined as

$$u(y) \rightarrow \phi(y; q)$$

where  $q \in [0,1]$  represents the so-called embedding parameter or sometimes it is called as homotopy parameter that increases from 0 to 1, as a result unknown function  $\phi(y; q)$  varies from initial guess  $u_0(y)$  to the solution of equation (1.11), i.e.,  $u(y)$ . To ensure this, Liao [15] constructed a so-called zero-order deformation equation as

$$(1 - q)L[\phi(y; q) - u_0(y)] = q\hbar H(y)N(\phi(y; q)) \quad (1.12)$$

where  $L$  is an auxiliary linear operator which may be a linear differential operator of any order from equation (1.11),  $\hbar$  is a non-zero auxiliary parameter,  $H(y)$  is the auxiliary function and  $N(\phi(y; q))$  is a non-linear differential operator.

when  $q = 0$ , the zero-order deformation equation gives,

$$\phi(y; 0) = u_0(y) \quad (1.13)$$

and at  $q = 1$ , the zero-order deformation equation gives,

$$\phi(y; 1) = u(y) \quad (1.14)$$

It would be noted that there is a great freedom to choose the initial guess  $u_0(y)$ , auxiliary linear operator  $L$  [15], auxiliary parameter  $\hbar$  [16-18] and auxiliary function  $H(y)$  [19, 20] and this criteria plays an important role in the convergence of the HAM solution [21, 22]. However, the Taylor's series expansion of  $\phi(y; q)$  about  $q$  gives,

$$\phi(y; q) = \phi(y; 0) + \sum_{n=1}^{\infty} D_n(\phi(y; q)) q^n \quad (1.15)$$

where  $D_n(\phi)$  is the  $n^{\text{th}}$  order deformation derivative, i.e.,

$$D_n(\phi(y; q)) = \frac{1}{n!} \left. \frac{d^n \phi(y; q)}{dq^n} \right|_{q=0} \quad (1.16)$$

It is assume that all the auxiliary variables are properly chosen so that the solution  $\phi(y; q)$  to the zero-order deformation exists for all  $q \in [0, 1]$ ; and the series (1.15) converges at  $q = 1$ . Then, the solution will be given by

$$u(y) = u_0(y) + \sum_{n=1}^{\infty} u_n(y). \quad (1.17)$$

To get the unknowns, i.e.,  $u_n(y)$  in (1.17), so-called  $n^{\text{th}}$  order deformation equation can be obtained by  $n$  times differentiating the equation (1.12) with respect to the embedding parameter  $q$ , and after setting  $q = 0$  and finally dividing by  $n!$ , we have

$$L[u_n(y) - \chi_n u_{n-1}(y)] = \hbar H(y) R_n(u_{n-1}(y)) \quad (1.18)$$

where

$$\chi_n = \begin{cases} 0 & n \leq 1 \\ 1 & n > 1, \end{cases}$$

and

$$R_n(u_{n-1}(y)) = D_{n-1}(N(\phi(y; q))|_{q=0}).$$

It is important to note that the  $R_n(u_{n-1}(y))$  only depend upon the  $u_0(y), u_1(y), u_2(y), \dots, u_{n-1}(y)$ . Hence, from the  $n^{\text{th}}$  order deformation equation (1.18), the  $n^{\text{th}}$  order solution of equation (1.11) can be written as

$$u(y) \approx u_0(y) + \sum_{m=1}^n u_m(y).$$

Numerous types of non-linear problems have been successfully solved by using HAM. In 1992 HAM was proposed by Liao in his PhD dissertation to solve the linear and non-linear differential equations. In this method, there is a lot of freedom to accelerate the convergence of series solution by choosing suitable solution parameters [15] namely, auxiliary linear operator, auxiliary parameter and auxiliary function. Auxiliary parameter plays an important role to enhance the convergence of series solution [18, 23]. A delineate description on auxiliary linear operator, auxiliary function and auxiliary parameter has been reported in [17-20]. HAM has advantage over homotopy perturbation method [24, 25] and many others; in most cases it gives the best approximated analytical solution for nonlinear differential equations [21, 22, 26]. Srinivas and Muthuraj [27] investigated the effects of thermal radiation and space porosity on MHD mixed convection boundary layer flow past a vertical channel by using HAM. Zheng et al. [28] used HAM to analyze the unsteady mixed convection boundary layer flow and radiation heat transfer of Maxwell fluid over a stretching porous plate in the presence of boundary slip and heat source/sink.

## 1.7 Literature Review

Many researchers investigated the thermal radiation effects on porous surfaces by using analytical, approximate analytical or numerical methods. Laplace transformation, finite difference method, perturbation technique, shooting method and many other techniques were applied to solve porous plate problems.

Hossain et al. [29] investigated the radiation effects on vertical porous plate with variable temperature depended viscosity by using Keller box method. Kim and Fedorov [7] studied the thermal radiation effects on transient mixed convection flow of a micro-polar fluid past a moving semi-infinite vertical porous plate. They used Rosseland approximation to delineate the radiative heat flux with the constant velocity of porous plate. Naby et al. [30] reported the thermal radiation effects on MHD unsteady free convective flow over a vertical porous plate by using a finite difference method in the presence of transverse uniform magnetic field. Makinde [8] reported a study of boundary layer flow with thermal radiation and mass transfer past a vertical porous plate in a gray absorbing-emitting fluid. Thermal radiation interaction with unsteady MHD flow past a vertical porous plate immersed in a porous medium was analyzed by Samad and Rehman [31]. They used the Nachtsheim-Swigert iteration technique to solve the governing equations with the time dependent suction velocity of the porous plate. Network simulation method was applied to study the thermal radiation and viscous dissipation effects on MHD unsteady free convective flow over a vertical porous plate by Jordan [32]. Makinde and Ogulu [33] investigated the thermal radiation effects on a vertical porous plate in the presence of transverse magnetic field with time dependent variable viscosity. They used shooting method to solve the boundary layer equations with the consideration of first order homogenous chemical reaction. In the presence of thermal radiation, variable suction and thermophoresis, the combined free-forced convective flow over an inclined porous plate have been examined by Aslam et al. [11]. An analytical study for a first order homogenous chemical reaction and electrically conducting viscous fluid past a moving vertical porous plate with time dependent variable suction velocity was reported by Ibrahim et al. [12]. Mohamed and Abo-Dahab [34] analyzed the effects of thermal radiation and chemical reaction on free convective MHD heat and mass transfer for a micro-polar fluid flow over a vertical

moving porous plate with the heat generation. They studied these effects with time-dependent variable suction velocity of the porous plate in the presence of a uniform transverse magnetic field. Pal and Talukdar [35] studied the thermal radiation and first order chemical reaction effects on unsteady mixed convection heat and mass transfer boundary layer slip flow over a vertical porous plate by using perturbation technique. An interaction of thermal radiation and  $n^{\text{th}}$  order homogenous chemical reaction with MHD mixed convection heat and mass transfer flow past a vertical porous plate with constant heat flux and viscous dissipation has been investigated by Makinde [36].

In nature and engineering, free convection flow is very common and has been studied extensively by many researchers. When heat and mass transfer takes place simultaneously in a moving fluid, the relations between fluxes and driving potentials are more complex in nature. An energy flux generated by composition gradient is termed the Dufour or diffusion-thermo effect. On the other hand, mass flux generated by temperature gradient is termed the Soret or thermal-diffusion effect. Generally, Soret and Dufour effects in heat and mass transfer process are neglected due to smaller order of magnitude than the effects described by Fourier's and Fick's laws. However, when the density difference occurs Soret and Dufour effects play an important role in the flow regimes. These effects are considered as second order phenomena and may become important, for instant, Soret effect has been utilized for isotope separation from a mixture of gasses of light molecular weight ( $\text{H}_2$ ,  $\text{He}$ ) and medium molecular weight ( $\text{N}_2$ , air), the Dufour effect can't be ignored due to its importance in certain kind of conditions [37]. Due to significance of Soret (thermal-diffusion) and Dufour (diffusion thermo) effects for the fluids with light molecular weight as well as medium molecular weight, many researchers have been studied and reported results for such type of flows.

Postelnicu [38] investigated the influence of chemical reaction on free convection heat and mass transfer flow past a vertical surface in porous medium by considering Soret and Dufour effects using finite difference technique. It was observed that by increasing chemical reaction parameter concentration profile increases. Mansour et al. [39] studied the effects of chemical reaction and thermal stratification on MHD free convection heat and mass transfer flow over a vertical stretching surface embedded in a porous medium in the presence of Soret and Dufour effects by shooting method. They

found that the velocity, temperature and concentration decrease with an increase in chemical reaction parameter. Chamkha and Nakhi [40] reported the MHD mixed convection radiation interaction along a permeable surface immersed in a porous medium in the presence of Soret and Dufour effects. They observed that in the presence of thermal radiation local Nusselt number increases and local Sherwood number decreases. Thermophoresis particle deposition in a non-Darcy porous medium under the influence of Soret-Dufour effects was analyzed by Partha [41]. He found that increasing concentration distributions, Soret effect has significant influence not only in aiding but also in opposing buoyancies. A numerical study of free convection magneto-hydrodynamic heat and mass transfer flow past a stretching surface embedded in a saturated porous medium with Soret and Dufour effects was studied by Beg et al. [42]. Partha [43] examined the suction and injection effects on thermophoresis particle deposition in a non-Darcy porous medium under the influence of Soret and Dufour effects. Mahdy [44] presented a study of non-similar boundary layer non-Darcian mixed convection heat and mass transfer flow of a non-Newtonian fluid past a vertical isothermal plate embedded in a porous medium with the Soret and Dufour effects using Newton-Raphson shooting technique. He found that local heat transfer rate increases and local mass transfer rate decreases for the increase of Soret number. Kumar and Murthy [45] analyzed the Soret and Dufour effects on heat and mass transfer double-diffusive free convection boundary layer flow past a corrugated vertical surface embedded in a non-Darcy porous medium using finite difference scheme. A numerical study of Soret and Dufour effects on the combined laminar free convection flow of non-Newtonian fluids along a vertical plate embedded in a porous medium with thermal radiations was studied by Tai and Char [46]. Vempati and Gari [47] used the finite element method to investigate the Soret and Dufour effects on unsteady MHD flow past an infinite vertical porous plate with thermal radiation and oscillatory suction velocity. For electrically conducting fluid, a free convective chemically reacting MHD boundary layer flow of heat and mass transfer problem along a vertical plate in the presence of suction and injection with Soret and Dufour effects was reported by Olanrewaju and Makinde [48]. Using Runge Kutta Gill integration scheme with shooting technique, Kandasamy et al. [49] examined the Soret and Dufour effects with thermophoresis and chemical reaction on free convection heat and mass transfer flow past a porous



stretching surface in the presence of heat source and sink. Arasu et al. [50] studied the Lie group analysis for Soret and Dufour effects on free convective heat and mass transfer flow over a vertical porous stretching surface with time depended fluid viscosity embedded in a porous medium in the presence of thermophoresis particle deposition. Cheng [51], making use of the cubic spline collocation method, Soret and Dufour effects on the free convection boundary layer flow past a vertical plate embedded in a porous medium saturated with a non-Newtonian power law fluid were studied. Prasad et al. [52] carried out an implicit numerical study of Soret and Dufour effects on MHD free convective heat and mass transfer flow past a vertical porous plate embedded in a non-Darcian porous medium in the presence of uniform magnetic field. Makinde and Olanrewaju [53] employed a shooting iteration technique with the forth order Runge-Kutta integration scheme to examine the Soret and Dufour effects on unsteady mixed convection flow over a vertical porous flat plate moving through a binary mixture of chemically reacting radiative fluid. A numerical study of Soret and Dufour effects on unsteady MHD free convective flow of an electrically conducting fluid over a vertical plate embedded in a non-Darcy porous medium was studied by Odat and Ghamdi [54]. They employed an implicit finite difference scheme of a Crank Nicolson type and found that the skin friction and Sherwood number decreases either by increasing Dufour number or by decreasing Soret number. Turkyilmazoglu and Pop [55] investigated a numerical study for the Soret and heat source effects on the unsteady MHD free convection flow of an electrically conducting fluid past an impulsively started infinite vertical plate. Hayat et al. [56] used the homotopy analysis method to analyze the Soret and Dufour effects on the unsteady free convection heat and mass transfer flow of a third grade non-Newtonian fluid past a stretching sheet in the presence of chemical reaction. Prakash et al. [57] accounted for the Dufour and radiation effects on unsteady MHD free convection flow past an impulsively started an infinite vertical plate embedded in a porous medium with variable temperature and uniform mass diffusion in the presence of transverse magnetic field, employing the Laplace transform method. A numerical study of thermophoresis particle deposition and Soret-Dufour effects on MHD free convective heat and mass transfer flow past a non-isothermal wedge in the presence of thermal radiation and ohmic dissipation was studied by Pal and Mondal [58]. Sharma et al. [59] used a finite difference method to investigate the Soret and

Dufour effects on unsteady MHD mixed convection flow past an infinite vertical porous plate embedded in a porous medium in the presence of heat source, ohmic dissipation and chemical reaction. Turkyilmazoglu [60] carried out an analytical and numerical study of Soret and Dufour effects on MHD mixed convection flow of an electrically conducting, viscoelastic fluid over a stretching vertical porous surface embedded in a porous medium in the presence of uniform magnetic field.

### **1.7.1 Newtonian Heating**

In the literature, Merkin [61] pointed that there are four common heating processes, generally specified as the wall-to-ambient temperature distributions, namely, (i) prescribed wall temperature distributions; (ii) prescribed surface heat flux distributions; (iii) conjugate conditions, where heat is supplied through a bounding surface of finite thickness and finite heat capacity. The interface temperature is not known a priori but depends on the intrinsic properties of the system; and (iv) Newtonian heating, in which the heat transfer rate from the bounding surface with a finite heat capacity is proportional to the local surface temperature and it is usually termed conjugate convective flow.

Among these four heating processes, many researchers investigated the boundary layer problems with Newtonian heating. Chaudhary and Jain [62] investigated the unsteady free convection boundary layer flow over an infinite vertical plate with Newtonian heating using Laplace transform technique. Salleh et al. [63] examined the steady forced convection boundary layer flow near a forward stagnation point past an infinite plane wall with Newtonian heating using finite difference scheme. They investigate the effects of large range of values of Parandtl number on temperature profiles. Mebine and Adigio [64] analyzed the thermal radiation effects on unsteady free convection flow past a vertical porous plate with Newtonian heating by using Laplace transform technique. Salleh et al. [65] studied the free convection boundary layer flow over a solid sphere with Newtonian heating. In the presence of thermal radiation, Narahari and Nayan [66] investigated an analytical study of free convection boundary layer flow resulting from heat and mass transfer over an infinite vertical plate

with Newtonian heating. Salleh et al. [67] examined the forced convection heat transfer over a circular cylinder with Newtonian heating. Singh and Makinde [68] investigated the combined effects of transverse magnetic field and volumetric heat generation on boundary layer flow of a viscous incompressible electrically conducting fluid past an inclined plate with Newtonian heating by using shooting method. Narahari and Dutta [69] reported the effects of thermal radiation and mass transfer on unsteady free convection boundary layer flow of an optically dense viscous incompressible fluid past a vertical plate with Newtonian heating using Laplace transform technique. Das et al. [70] examined the radiation effects on unsteady free convection flow over a vertical plate with Newtonian heating using finite difference scheme. They found that temperature decreases with an increase in radiation parameter and Prandtl number, while the velocity increases with an increase in either Grashof number or time.

In the above all cited work, the problem of free convection flow past an infinite vertical porous plate with Newtonian heating has not been investigated even though this problem involves in numerous practical applications.

## **1.8 Problem Statement**

The aim of this study is to investigate the free convection heat and mass transfer flow past an impulsively started infinite vertical porous plate with Newtonian heating. In this research, the problems considered are

1. Heat generation and viscous dissipation effects.
2. Thermal radiation and viscous dissipation effects in the presence of transverse magnetic field.
3. Soret and Dofour effects in the presence of thermal radiation, viscous dissipation and chemical reaction.

Additionally these effects are not yet explored on infinite moving vertical porous plate with Newtonian heating but interesting to be investigated.

## **1.9 Research Objectives**

Objectives of the proposed research work are

1. To obtain the solution of system of non-linear ordinary differential equations using Homotopy Analysis Method (HAM).
2. To determine exact analytical solution of that system of equations for limiting case.
3. Validation of HAM solution results with the exact analytical solution results for the limiting case.
4. To investigate and discuss the influence of dimensionless physical parameters on the fluid characteristics.

## **1.10 Significance of the Research**

The significance of the research:

1. The study of free convection incompressible fluid through vertical porous plate with Newtonian heating has generated many interests because in which heat transfer rate from the bounding surface is directly proportional to the local surface temperature and this study become more important in recent years due to its wide applications in science and engineering.
2. Boundary layer flow through porous surfaces in the presence of heat generation and thermal radiation has significant applications in industry such as water filtration, oil distillation, heat transfer from stored agricultural products, cooling of nuclear reactors, computer assemblies, automotive industry, textile industry and in a variety of other applications.
3. The study of Soret and Dufour effects on MHD flow can be useful in ionized fluids, chemical reactions, etc.

Thus, the study of the free convection flow due to heat and mass transfer along an impulsively started infinite vertical porous plate in the presence of heat generation, viscous dissipation, magnetic field, thermal radiation, chemical reaction, Soret and Dufour effects with Newtonian heating is important due to strong applications in science and engineering. Besides, this study will be helpful in order to solve the problems related to the heat and mass transfer boundary layer flow.

### **1.11 Scope of the Research**

This study will take into consideration of free convection boundary layer flow of viscous incompressible fluid past an impulsively started infinite vertical porous plate with Newtonian heating. The governing non-linear system of ordinary differential equations incorporated with different physical effects such as heat generation, viscous dissipation, thermal radiation, magnetic field, Soret and Dufour effects was solved by a semi-analytical method known as Homotopy Analysis Method (HAM) and HAM solution results are then compared with the analytical solution results in limiting case. In the literature, nobody has studied these effects on free convection flow past an impulsively started infinite vertical porous plate in the presence of Newtonian heating.

### **1.12 Chapter Summary**

This chapter not only highlights the breakthroughs in the literature for the heat and mass transfer models, but also describes three different problems of free convection boundary layer flow past an impulsively started infinite vertical porous plate with Newtonian heating. Moreover, critical literature review on free convection flow is elaborated with the emphasis on heat and mass transfer models, Newtonian heating, numerical, analytical and semi-analytical methods of solution and observed result, so as to identify the novelty of proposed studies.



## CHAPTER 2

### EFFECTS OF HEAT GENERATION AND VISCOUS DISSIPATION

#### 2.1 Introduction

Boundary layer flow through porous surface has many industrial applications such as water filtration in agricultural engineering, heat transfer from stored agriculture products, design of rocket nozzle and cooling of nuclear reactors. Kim [71] reported the heat transfer through moving vertical porous plate in a micropolar fluid. He found that by increasing the permeability parameter, velocity increases rapidly near the porous plate and then decreases to the relevant free stream velocity. Kim and Fedorov [7] examined the thermal radiation effects on unsteady mixed convection flow of a micropolar fluid along a vertical porous plate. They used Rosseland approximation to study the radiation effects for an optically thick fluid. Makinde [8] studied the free convection interaction with thermal radiation in a boundary layer flow past a moving vertical porous plate using shooting method. An analytical series solution for unsteady mixed convection stagnation point flow along a vertical surface in a porous medium was investigated by Liao et al. [9]. Seddeek and Salama [10] investigated the effects of variable viscosity and thermal conductivity on unsteady laminar flow past a semi-infinite vertical porous plate using shooting method.

Free convection flow with Newtonian heating, in which heat transfer rate from the bounding surface with a finite heat capacity is proportional to the local surface temperature, was extensively studied after Merkin's work [61]. Lesnic et al. [72] studied a free convection boundary layer flow along a vertical surface embedded in a

porous medium with Newtonian heating using finite difference method. They compared the full finite-difference solution and the small and large series solutions, and concluded that the full numerical solution is accurate. Chaudary and Jain [73] presented an exact solution of unsteady boundary layer flow past an infinite vertical plate with Newtonian heating using Laplace transform method. Mebine and Adigio [64] examined thermal radiation effects on unsteady free convection flow past a vertical porous plate with Newtonian heating. Salleh et al. [63] investigated the Prandtl number effects on boundary layer flow along an infinite plane wall with Newtonian heating using Keller box method. Narahari and Ishak [74] performed a theoretical investigation in the presence of thermal radiation, on unsteady free convection boundary layer flow near a vertical plate with Newtonian heating. The influence of thermal radiation on unsteady natural convection flow resulting from heat and mass transfer was analytically investigated by Narahari and Nayan [66] using Laplace transform technique. The unsteady free convection boundary layer flow over an infinite vertical plate with Newtonian heating was examined by Narahari and Dutta [69] for uniform mass diffusion and mass flux boundary conditions.

However, the effects of heat generation and viscous dissipation on the natural convection flow past an impulsively started infinite vertical porous plate with Newtonian heating have not been studied in the literature even though this study finds many engineering applications.

## 2.2 Problem Description

Consider the steady state free convection flow of a viscous incompressible fluid past a uniformly moving infinite vertical porous plate with Newtonian heating in the presence of heat generation and viscous dissipation. The  $x'$ -axis is chosen along the plate in the upward direction and  $y'$ -axis normal to it. Let  $u_0$  be the velocity of the moving plate as shown in Figure 2.1. The flow is being incompressible and all the fluid properties are taken to be constant except the density in the buoyancy-force term where the Boussinesq approximation is used. Then the free convection flow along the porous plate is governed by the following equations [75]:



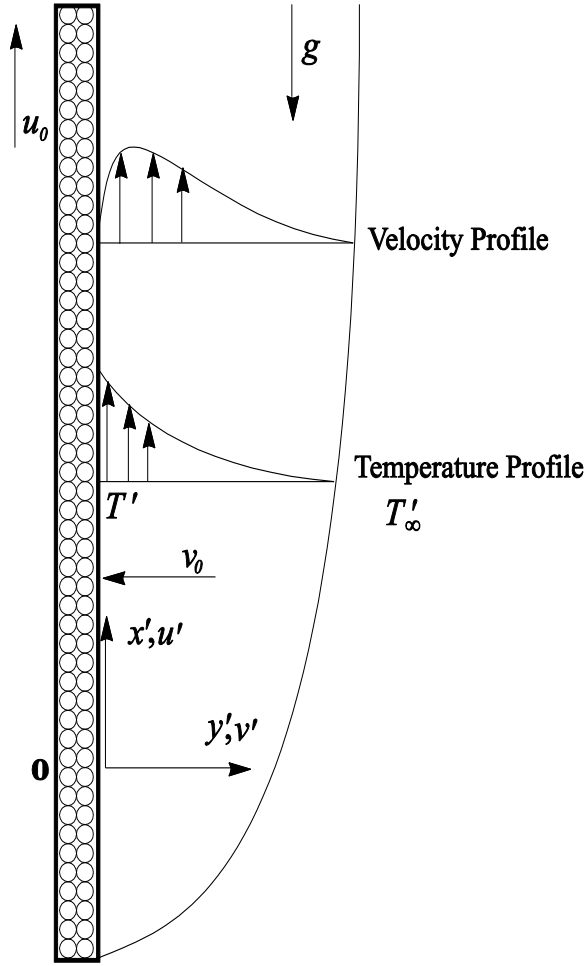


Figure 2.1: Physical Model

$$\frac{\partial u'}{\partial x'} + \frac{\partial v'}{\partial y'} = 0 \quad (2.01)$$

$$\rho \left( u' \frac{\partial u'}{\partial x'} + v' \frac{\partial u'}{\partial y'} \right) = -\frac{\partial P}{\partial x'} + \mu \left( \frac{\partial^2 u'}{\partial x'^2} + \frac{\partial^2 u'}{\partial y'^2} \right) - \rho g \quad (2.02)$$

$$\rho \left( u' \frac{\partial v'}{\partial x'} + v' \frac{\partial v'}{\partial y'} \right) = -\frac{\partial P}{\partial y'} + \mu \left( \frac{\partial^2 v'}{\partial x'^2} + \frac{\partial^2 v'}{\partial y'^2} \right) \quad (2.03)$$

$$u' \frac{\partial T'}{\partial x'} + v' \frac{\partial T'}{\partial y'} = \frac{k}{\rho c_p} \left( \frac{\partial^2 T'}{\partial x'^2} + \frac{\partial^2 T'}{\partial y'^2} \right) + \frac{\mu}{\rho c_p} \left( \frac{\partial u'}{\partial y'} \right)^2 + \frac{Q'}{\rho c_p} (T' - T'_\infty) \quad (2.04)$$

In the boundary layer analysis, the velocity and temperature gradients normal to the surface are much greater than those in the direction parallel to the surface [76], [77]; in

other words  $y' \sim \delta$ ,  $x' \sim L$ , and  $\delta \ll L$ , where  $\delta$  is the boundary layer thickness and  $L$  is the characteristic length, is considered. Therefore, fluid characteristics are independent of  $x'$  and only function of  $y'$ . Then by the usual Boussinesq approximation (see Appendix) above system of equations can be written as

$$\frac{\partial v'}{\partial y'} = 0 \quad (2.1)$$

$$v' \frac{\partial u'}{\partial y'} = \nu \frac{\partial^2 u'}{\partial y'^2} + g\beta(T' - T'_\infty) \quad (2.2)$$

$$v' \frac{\partial T'}{\partial y'} = \frac{k}{\rho c_p} \frac{\partial^2 T'}{\partial y'^2} + \frac{\nu}{c_p} \left( \frac{\partial u'}{\partial y'} \right)^2 + \frac{Q'}{\rho c_p} (T' - T'_\infty) \quad (2.3)$$

The boundary conditions are

$$\left. \begin{aligned} u' &= u_0, & \frac{\partial T'}{\partial y'} &= -\frac{h}{k} T' & \text{at } y' &= 0, \\ u' &\rightarrow 0, & T' &\rightarrow T'_\infty & \text{as } y' &\rightarrow \infty. \end{aligned} \right\} \quad (2.4)$$

Integrating equation (2.1) for constant suction, we get

$$v' = -v_0 \quad (2.5)$$

where  $v_0$  is the normal velocity of suction at the plate ( $v_0 > 0$ ) and  $v_0 = 0$  represents the case of non-permeable plate.

Equations (2.2) and (2.3) can now be written as

$$-v_0 \frac{\partial u'}{\partial y'} = \nu \frac{\partial^2 u'}{\partial y'^2} + g\beta(T' - T'_\infty) \quad (2.6)$$

$$-v_0 \frac{\partial T'}{\partial y'} = \frac{k}{\rho c_p} \frac{\partial^2 T'}{\partial y'^2} + \frac{\nu}{c_p} \left( \frac{\partial u'}{\partial y'} \right)^2 + \frac{Q'}{\rho c_p} (T' - T'_\infty) \quad (2.7)$$

Introducing the following non-dimensional quantities:

$$\left. \begin{aligned} y &= \frac{y'h}{k}, & u &= \frac{u'}{u_0}, & \theta &= \frac{T' - T'_\infty}{T'_\infty}, & s &= \frac{\nu_0 k}{h\nu}, \\ Gr &= \frac{g\beta T'_\infty k^2}{\nu u_0 h^2}, & Pr &= \frac{\mu c_p}{k}, & Ec &= \frac{u_0^2}{c_p T'_\infty}, & Q &= \frac{Q'k}{h^2}. \end{aligned} \right\} \quad (2.8)$$

Equations (2.6), (2.7) and (2.4) respectively take the following non-dimensional forms:

$$\frac{d^2 u}{dy^2} + s \frac{du}{dy} + Gr\theta = 0 \quad (2.9)$$

$$\frac{d^2 \theta}{dy^2} + Pr s \frac{d\theta}{dy} + Pr Ec \left( \frac{du}{dy} \right)^2 + Q\theta = 0 \quad (2.10)$$

with the dimensionless boundary conditions

$$\left. \begin{aligned} u &= 1, & \frac{d\theta}{dy} &= -(\theta + 1), & \text{at } y &= 0, \\ u &\rightarrow 0, & \theta &\rightarrow 0, & \text{as } y &\rightarrow \infty. \end{aligned} \right\} \quad (2.11)$$

### 2.3 Solution by HAM

The set of base functions for velocity  $u(y)$  and temperature  $\theta(y)$  can be written as

$$\left\{ y^k e^{-ny} \mid n \geq 0, k \geq 0 \right\} \quad (2.12)$$

It is assume that the solutions for  $u(y)$  and  $\theta(y)$  can be expressed as

$$u(y) = \sum_{n=0}^{\infty} a_n e^{-ny} \text{ and } \theta(y) = \sum_{n=0}^{\infty} b_n e^{-ny} \quad (2.13)$$

where  $a_n$  and  $b_n$  are co-efficients to be determined. Under the rule of solution expression and boundary conditions (2.11), it is easy to choose the initial approximations for the velocity and temperature as follow:

$$u_0(y) = e^{-y} \quad \text{and} \quad \theta_0(y) = e^{-2y} \quad (2.14)$$

A mapping is defined for velocity and temperature as

$$\{u(y), \theta(y)\} \rightarrow \{\phi(y; q), \psi(y; q)\}$$

where  $q$  is an embedding parameter that varies from 0 to 1, as a result  $\{\phi(y; q), \psi(y; q)\}$  varies from initial solution  $\{u_0(y), \theta_0(y)\}$  to exact solution  $\{u(y), \theta(y)\}$ .

Now, the auxiliary linear operators for equations (2.9) and (2.10) can be defined, respectively, as

$$\left. \begin{aligned} L_u[\phi(y; q)] &= \frac{d^2 \phi(y; q)}{dy^2} + \frac{d\phi(y; q)}{dy} \\ L_\theta[\psi(y; q)] &= \frac{1}{2} \frac{d^2 \psi(y; q)}{dy^2} + \frac{d\psi(y; q)}{dy} \end{aligned} \right\} \quad (2.15)$$

with the following properties,

$$\left. \begin{aligned} L_u(A_0 + A_1 e^{-y}) &= 0 \\ L_\theta(B_0 + B_1 e^{-2y}) &= 0 \end{aligned} \right\} \quad (2.16)$$

where  $A_0, A_1, B_0$  and  $B_1$  are coefficients. The non-linear operators can be defined from equations (2.9) and (2.10) as

$$N_u[\phi(y; q), \psi(y; q)] = \frac{d^2 \phi(y; q)}{dy^2} + s \frac{d\phi(y; q)}{dy} + Gr\psi(y; q) \quad (2.17)$$

$$N_\theta[\phi(y; q), \psi(y; q)] = \frac{d^2 \psi(y; q)}{dy^2} + Pr s \frac{d\psi(y; q)}{dy} + Pr Ec \left( \frac{d\phi(y; q)}{dy} \right)^2 + Q\psi(y; q) \quad (2.18)$$

Denoting  $\hbar_u$  and  $\hbar_\theta$  as the non-zero auxiliary parameters,  $H_u(y)$  and  $H_\theta(y)$  as the non-zero auxiliary functions, the zero-order deformations are

$$(1 - q)L_u[\phi(y; q) - u_0(y)] = q\hbar_u H_u(y) N_u[\phi(y; q), \psi(y; q)] \quad (2.19)$$

$$(1-q)L_\theta[\psi(y;q) - \theta_0(y)] = q\hbar_\theta H_\theta(y)N_\theta[\varphi(y;q), \psi(y;q)] \quad (2.20)$$

subject to the boundary conditions

$$\left. \begin{aligned} \varphi(0;q) &= 1, & \psi'(0;q) &= -\psi(0;q) - 1, \\ \varphi(\infty;q) &\rightarrow 0, & \psi(\infty;q) &\rightarrow 0. \end{aligned} \right\} \quad (2.21)$$

At  $q = 0$ , zero order deformation equations gives,

$$\left. \begin{aligned} \varphi(y;0) &= u_0(y) \\ \psi(y;0) &= \theta_0(y) \end{aligned} \right\} \quad (2.22)$$

and at  $q = 1$ , zero-order deformation equations gives,

$$\left. \begin{aligned} \varphi(y;1) &= u(y) \\ \psi(y;1) &= \theta(y) \end{aligned} \right\} \quad (2.23)$$

The auxiliary parameters  $(\hbar_u, \hbar_\theta)$  and auxiliary functions  $(H_u(y), H_\theta(y))$  are properly chosen, so that the  $n^{\text{th}}$  order deformation derivatives are

$$u_n(y) = \frac{1}{n!} \left. \frac{d^n \varphi(y;q)}{dq^n} \right|_{q=0} \quad (2.24)$$

$$\theta_n(y) = \frac{1}{n!} \left. \frac{d^n \psi(y;q)}{dq^n} \right|_{q=0} \quad (2.25)$$

with the help of equation (2.22) and Taylor's theorem, we expand  $\varphi(y;q)$  and  $\psi(y;q)$  in the power series of  $q$ ,

$$\varphi(y;q) = u_0(y) + \sum_{n=1}^{\infty} u_n(y) q^n \quad (2.26)$$

$$\psi(y;q) = \theta_0(y) + \sum_{n=1}^{\infty} \theta_n(y) q^n \quad (2.27)$$

It is assumed that the initial approximations, auxiliary linear operators, auxiliary parameters and auxiliary functions are properly chosen, so that the series in equations (2.26) and (2.27) are converge at  $q = 1$  and hence

$$u(y) = u_0(y) + \sum_{n=1}^{\infty} u_n(y) \quad (2.28)$$

$$\theta(y) = \theta_0(y) + \sum_{n=1}^{\infty} \theta_n(y) \quad (2.29)$$

By differentiating the zero-order deformation equations  $n$  times with respect to  $q$  then dividing by  $n!$ , and setting  $q = 0$ , we get the higher-order deformation equations as

$$\left. \begin{aligned} L_u[u_n(y) - \chi_n u_{n-1}(y)] &= \hbar_u H_u(y) R_n^u(u_{n-1}(y), \theta_{n-1}(y)) \\ L_\theta[\theta_n(y) - \chi_n \theta_{n-1}(y)] &= \hbar_\theta H_\theta(y) R_n^\theta(u_{n-1}(y), \theta_{n-1}(y)) \end{aligned} \right\} \quad (2.30)$$

subject to the boundary conditions

$$\left. \begin{aligned} u_n(0) &= 0, & \theta'_n(0) + \theta_n(0) &= 0, \\ u_n(\infty) &\rightarrow 0, & \theta_n(\infty) &\rightarrow 0. \end{aligned} \right\} \quad (2.31)$$

where

$$\chi_n = \begin{cases} 0 & n \leq 1 \\ 1 & n > 1 \end{cases}, \quad (2.32)$$

$$R_n^u(u_{n-1}(y), \theta_{n-1}(y)) = u''_{n-1}(y) + su'_{n-1}(y) + Gr\theta_{n-1}(y), \quad (2.33)$$

$$R_n^\theta(u_{n-1}(y), \theta_{n-1}(y)) = \theta''_{n-1}(y) + Pr s \theta'_{n-1}(y) + Pr Ec \left[ \sum_{j=0}^{n-1} u'_j(y) u'_{n-1-j}(y) \right] + Q\theta_{n-1}(y). \quad (2.34)$$

For simplicity [15], auxiliary functions and auxiliary parameters can be chosen as

$$H_u(y) = H_\theta(y) = 1 \text{ and } \hbar_u = \hbar_\theta = \hbar.$$

Let  $u_n^*(y)$  and  $\theta_n^*(y)$  denote the special solutions of the equations (2.30), respectively. Therefore,

$$\left. \begin{aligned} u_n^*(y) &= \chi_n u_{n-1}(y) + \hbar L_u^{-1} \left[ R_n^u(u_{n-1}(y), \theta_{n-1}(y)) \right] \\ \theta_n^*(y) &= \chi_n \theta_{n-1}(y) + \hbar L_\theta^{-1} \left[ R_n^\theta(u_{n-1}(y), \theta_{n-1}(y)) \right] \end{aligned} \right\} \quad (2.35)$$

where  $L_u^{-1}$  and  $L_\theta^{-1}$  are inverse linear operators. Therefore, the general solutions of equations (2.30) can be written as

$$\left. \begin{aligned} u_n(y) &= u_n^*(y) + A_0 + A_1 e^{-y} \\ \theta_n(y) &= \theta_n^*(y) + B_0 + B_1 e^{-2y} \end{aligned} \right\} \quad (2.36)$$

where the coefficients  $A_0, A_1, B_0$  and  $B_1$  are determined from the boundary conditions (2.31) as

$$\begin{aligned} A_0 &= -u_n^*(\infty), \quad A_1 = u_n^*(\infty) - u_n^*(0), \\ B_0 &= -\theta_n^*(\infty) \text{ and } B_1 = \theta_n^*(0) + \theta_n^*(0) - \theta_n^*(\infty). \end{aligned}$$

Now the skin friction ( $\tau$ ) at the surface of porous plate, which is given by the following formula

$$\tau = \frac{\tau'}{\rho G r u_0^2} = - \left. \frac{du}{dy} \right|_{y=0} = -u'(0) \quad (2.37)$$

and the heat transfer rate at the surface of the porous plate in terms of the Nusselt number ( $Nu$ ) is defined as

$$Nu = - \frac{v}{u_0(T' - T_\infty)} \left. \frac{dT'}{dy} \right|_{y=0} = 1 + \frac{1}{\theta(0)} \quad (2.38)$$

## 2.4 Exact Analytical Solution

In the absence of viscous dissipation ( $Ec = 0$ ), the non-linear system of equations (2.9) and (2.10) subject to the boundary conditions (2.11) reduces to

$$\frac{d^2 u}{dy^2} + s \frac{du}{dy} + Gr \theta = 0 \quad (2.39)$$

$$\frac{d^2 \theta}{dy^2} + Pr s \frac{d\theta}{dy} + Q \theta = 0 \quad (2.40)$$

with boundary conditions

$$\left. \begin{aligned} u = 1, \quad \frac{d\theta}{dy} = -(\theta + 1), \quad \text{at} \quad y = 0, \\ u \rightarrow 0, \quad \theta \rightarrow 0, \quad \text{as} \quad y \rightarrow \infty. \end{aligned} \right\} \quad (2.41)$$

Corresponding auxiliary linear equations of (2.39) and (2.40) are

$$m^2 u + s m u + Gr \theta = 0 \quad (2.42)$$

$$m^2 \theta + Pr s m \theta + Q \theta = 0 \quad (2.43)$$

where  $m = d/dy$ , solving equation (2.43)

$$(m^2 + Pr s m + Q)\theta = 0$$

$$m^2 + Pr s m + Q = 0$$

$$m = \frac{-Pr s \pm \sqrt{Pr^2 s^2 - 4Q}}{2}$$

Let,



$$m_1 = \frac{-\text{Pr } s + \sqrt{\text{Pr}^2 s^2 - 4Q}}{2}, \quad m_2 = \frac{-\text{Pr } s - \sqrt{\text{Pr}^2 s^2 - 4Q}}{2} \quad \text{or}$$

$$-m_2 = \left( \frac{\text{Pr } s + \sqrt{\text{Pr}^2 s^2 - 4Q}}{2} \right)$$

Now, the general solution for equation (2.43) will be

$$\theta(y) = c_1 e^{m_1 y} + c_2 e^{-m_2 y} \quad (2.44)$$

Since  $\theta \rightarrow 0$  as  $y \rightarrow \infty$ , therefore  $c_1 = 0$ .

$$\theta(y) = c_2 e^{-m_2 y} \quad \text{and} \quad \theta'(y) = -m_2 c_2 e^{-m_2 y}$$

Also, we have

$$\theta'(y) = -(\theta(y) + 1) \quad \text{at} \quad y = 0.$$

$$\text{Therefore, } c_2 = \frac{-1}{1 - m_2} \quad \text{or} \quad c_2 = \frac{1}{m_2 - 1}$$

Thus, equation (2.44) becomes

$$\theta(y) = \frac{1}{m_2 - 1} e^{-m_2 y} \quad (2.45)$$

Now, equation (2.42) can be written as

$$(m^2 + s m)u + \frac{Gr}{m_2 - 1} e^{-m_2 y} = 0$$

Its corresponding homogenous auxiliary equation is

$$(m^2 + s m)u = 0$$

$$m^2 + s m = 0$$

$$m = 0, m = -s$$

Complimentary solution will becomes

$$u_c(y) = c_3 + c_4 e^{-s y}$$

Now, particular integral can be written as

$$(m^2 + s m).u_p(y) = \frac{Gr}{1 - m_2} e^{-m_2 y}$$

$$u_p(y) = \frac{Gr}{1 - m_2} \frac{1}{(m^2 + s m)} e^{-m_2 y}$$

$$u_p(y) = \frac{Gr}{(1 - m_2)(m_2^2 - s m_2)} e^{-m_2 y}$$

Now,

$$u(y) = u_c(y) + u_p(y)$$

$$u(y) = c_3 + c_4 e^{-s y} + \frac{Gr e^{-m_2 y}}{(1 - m_2)(m_2^2 - s m_2)} \quad (2.46)$$

Applying boundary condition on (2.46), since  $u \rightarrow 0$  as  $y \rightarrow \infty$ , therefore  $c_3 = 0$

and  $u = 1$  at  $y = 0$ , so we have  $c_4 = 1 - \frac{Gr}{(1 - m_2)(m_2^2 - s m_2)}$ .

Thus, equation (2.46) will become as

$$u(y) = e^{-s y} + \frac{(e^{-m_2 y} - e^{-s y}) Gr}{(1 - m_2)(m_2^2 - s m_2)} \quad (2.47)$$

Hence, equations (2.45) and (2.47) represent the exact analytical solution of system of equations (2.39) and (2.40) for limiting case.

## 2.5 Result and Discussion

The auxiliary parameter  $\hbar \neq 0$  has significant role on the convergence of series solution obtained by the HAM. It is also called as convergence control parameter. A suitable value of auxiliary parameter  $\hbar$  can be chosen from the convergence region. The convergence regions for velocity and temperature fields are shown in Figures 2.2 and 2.3 using 20<sup>th</sup> order of HAM solution for fixed set of parameters  $Pr = 0.71, Gr = 0.2, Ec = 0.1, Q = 0.5$  and  $s = 4$ . The common convergence regions for both velocity and temperature fields are  $-0.6 \leq \hbar \leq -0.1$  and  $-0.6 \leq \hbar \leq -0.05$ , respectively. The coupled non-linear system of equations (2.9) and (2.10) subject to the boundary conditions (2.11) have been solved using homotopy analysis method (HAM). The HAM solution is validated by comparing with the exact solution in the absence of viscous dissipation ( $Ec = 0$ ). Comparison of the results for velocity and temperature fields is shown in Figures 2.4-2.8. From these figures it is clear that there is an excellent agreement between the HAM and exact solution results. This indicates that the HAM solution is accurate and giving promising results.

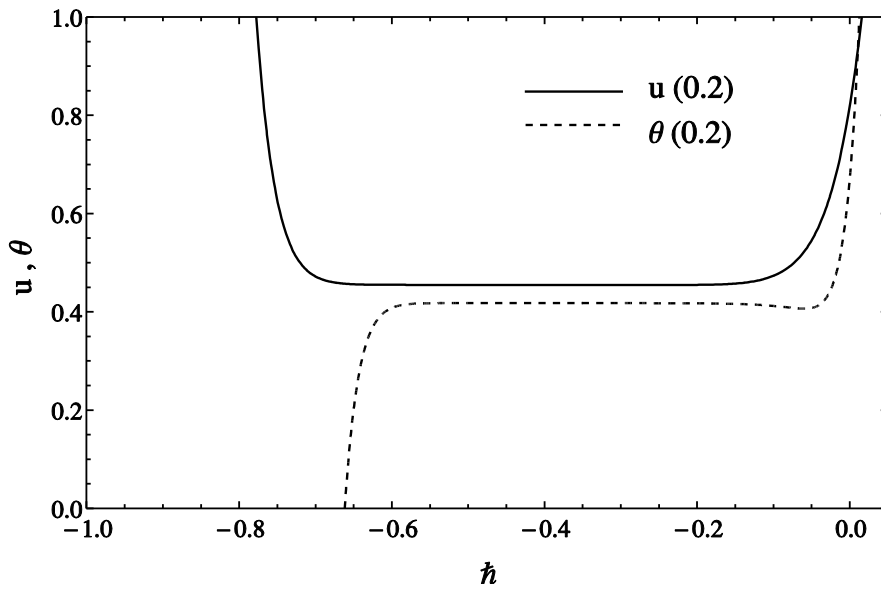


Figure 2.2:  $\hbar$  curves at 20<sup>th</sup> order of HAM

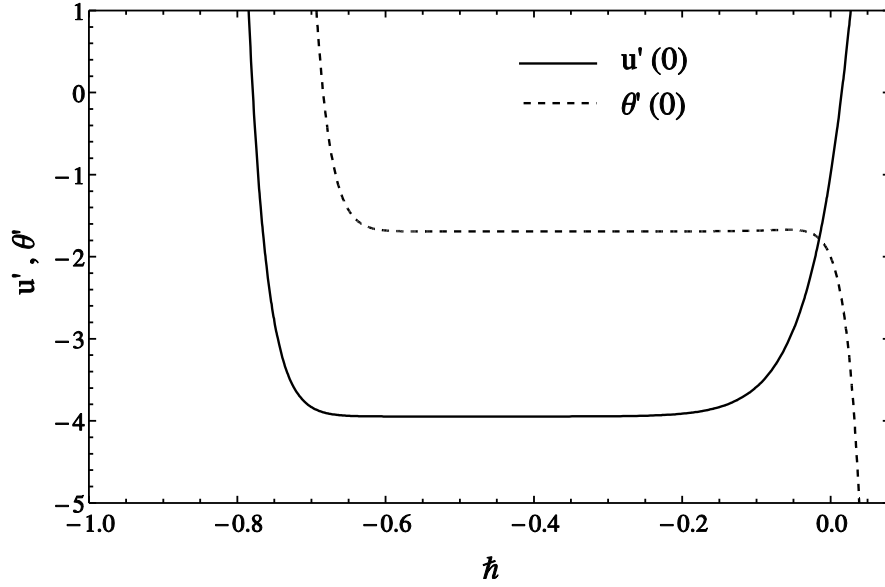


Figure 2.3:  $h$  curves at 20<sup>th</sup> order of HAM

The effects of different parameters on velocity and temperature fields have been investigated and the results are shown in Figures 2.9 to 2.15. Figure 2.9 shows the influence of suction parameter on the velocity field. It is observed that the fluid velocity decreases as the suction parameter increases. It has been observed that velocity boundary layer increases by increasing thermal Grashof number (as in Figure 2.10) whereas it decreases by increasing Prandtl number (as in Figure 2.11).

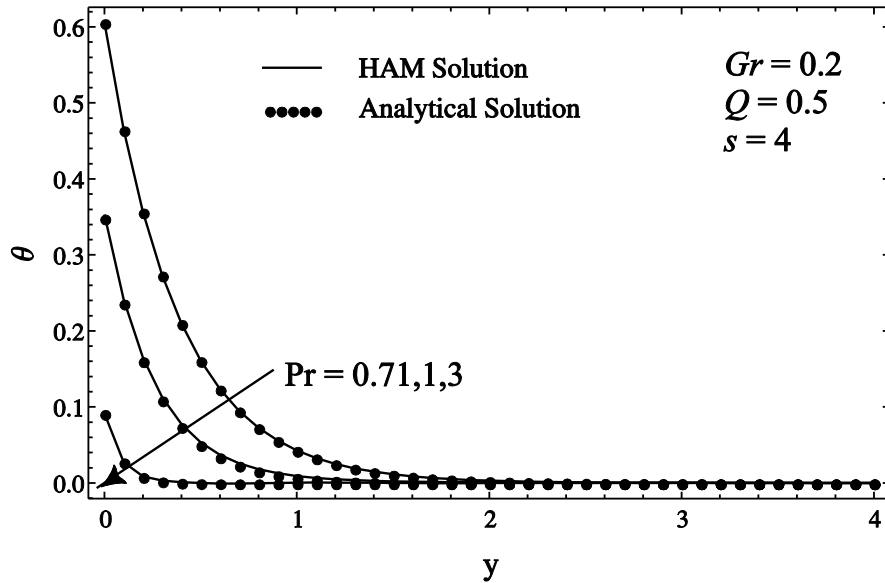


Figure 2.4: Comparison of temperature profiles for HAM and analytical solution at different  $Pr$  when  $Ec = 0$ .

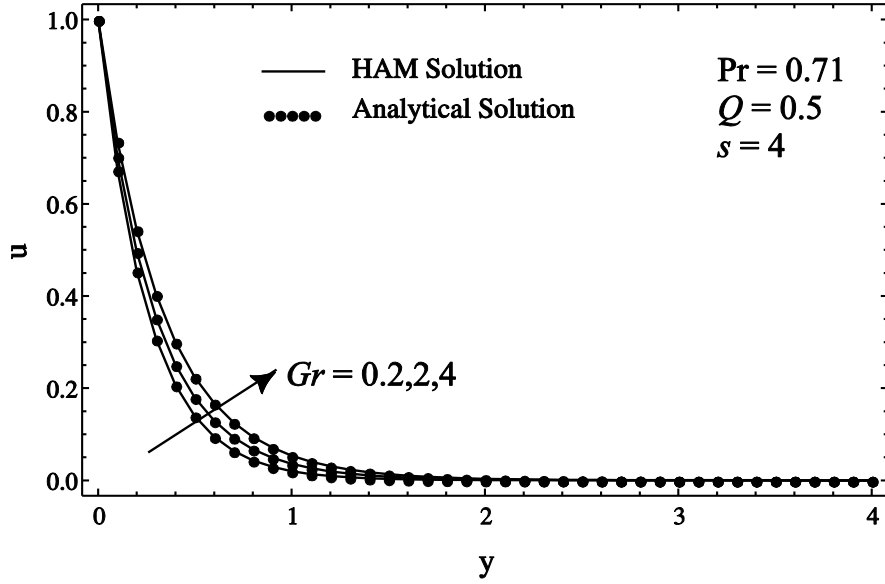


Figure 2.5: Comparison of velocity profiles for HAM and analytical solution at different  $Gr$  when  $Ec = 0$ .

Figures 2.12 to 2.15 have been plotted to observe the effects of  $s, Q, Pr$  and  $Ec$  on temperature profiles. It is noted that the fluid temperature decreases as the suction parameter increases in Figure 2.12. Also, thermal boundary layer thickness decreases rapidly by increasing the suction velocity of the vertical moving porous plate. Similar type of behavior is observed for thermal boundary layer variation with  $Pr$  from Figure 2.14.

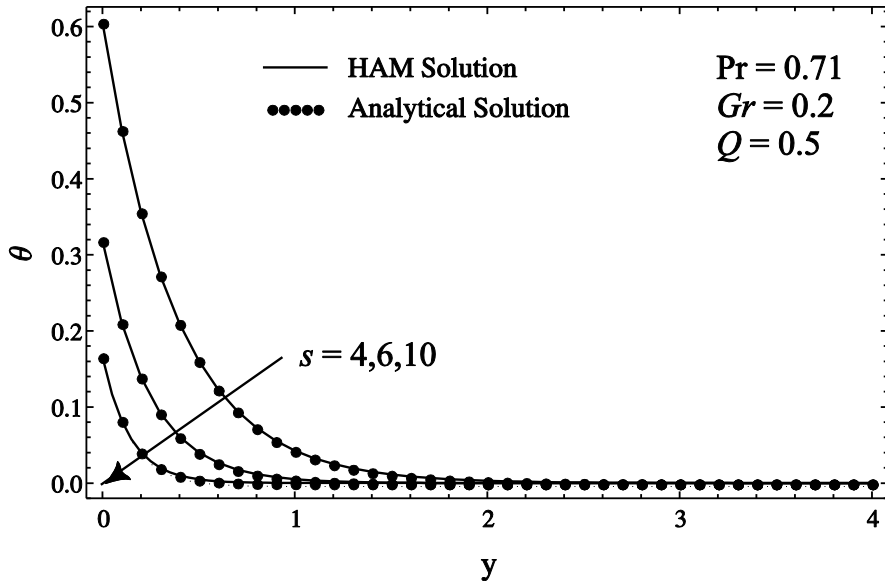


Figure 2.6: Comparison of temperature profiles for HAM and analytical solution at different  $s$  when  $Ec = 0$ .

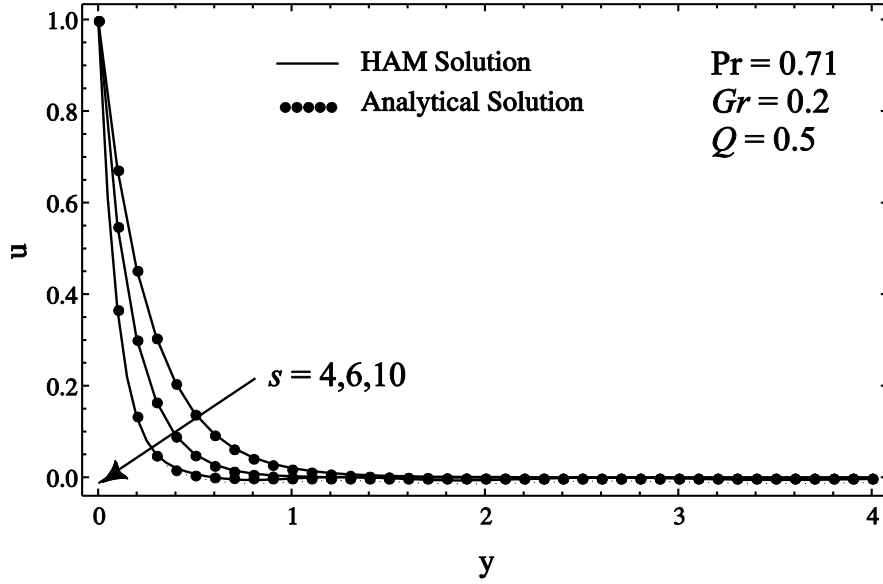


Figure 2.7: Comparison of velocity profiles for HAM and analytical solution at different  $s$  when  $Ec = 0$ .

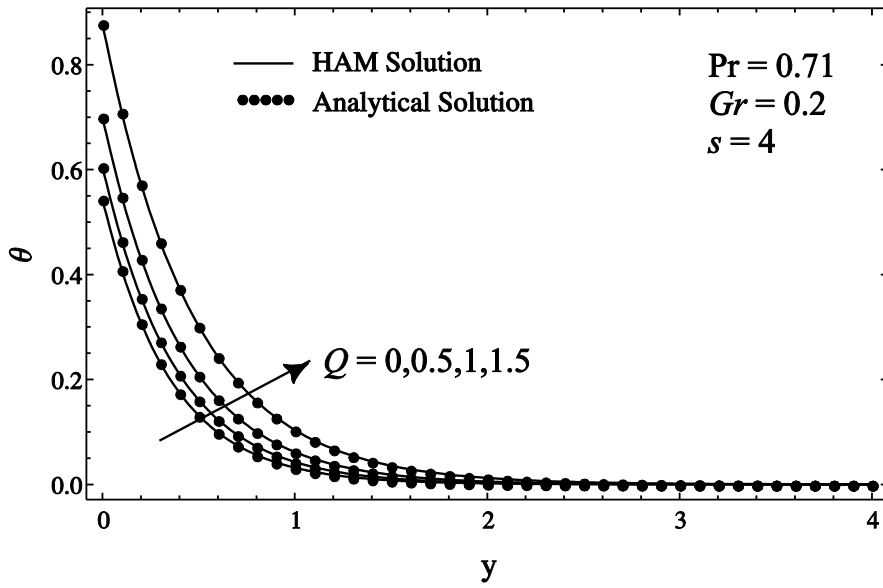


Figure 2.8: Comparison of temperature profiles for HAM and analytical solution at different  $Q$  when  $Ec = 0$ .

Figure 2.13 shows the influence of heat generation parameter on the temperature field. It is observed that the fluid temperature increasing with the increase of heat generation. Thus, the presence of heat source generates energy in the boundary layer that causes the increase in fluid temperature. The effect of Eckert number on the fluid temperature is shown in Figure 2.15. From this figure it can be seen that the temperature

increases with increasing Eckert number. This is because of the energy generated due to frictional heating in the boundary layer.

Effects of Eckert number and heat source parameter on the fluid velocity for a fixed set of parameters  $Pr = 0.71$ ,  $Gr = 0.2$  and  $s = 4$  are presented in the Table 2.1. It showed that velocity of the fluid increases with increasing Eckert number. Similar type of behavior is found with heat source parameter in Table 2.1. Thus, an increase in heat source parameter leads to an increase in the fluid velocity.

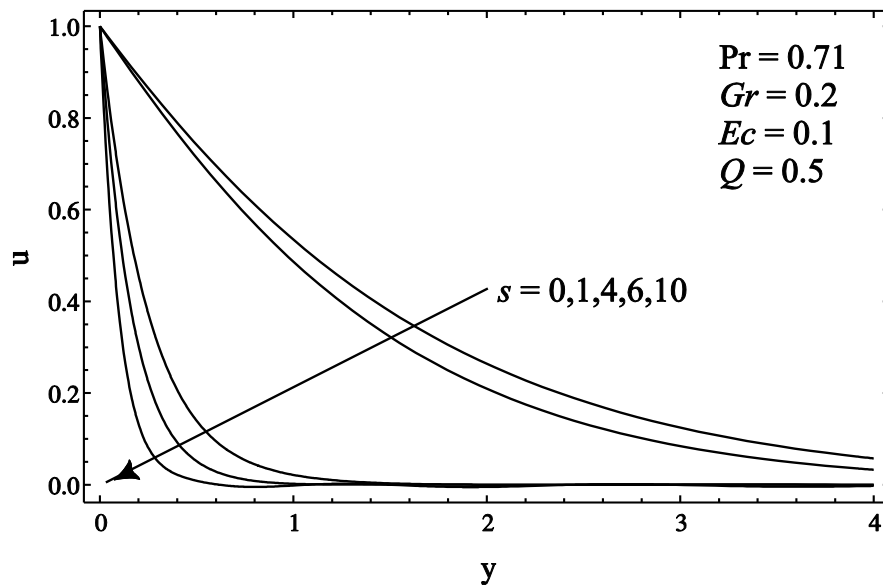


Figure 2.9: Influence of  $s$  on velocity profiles

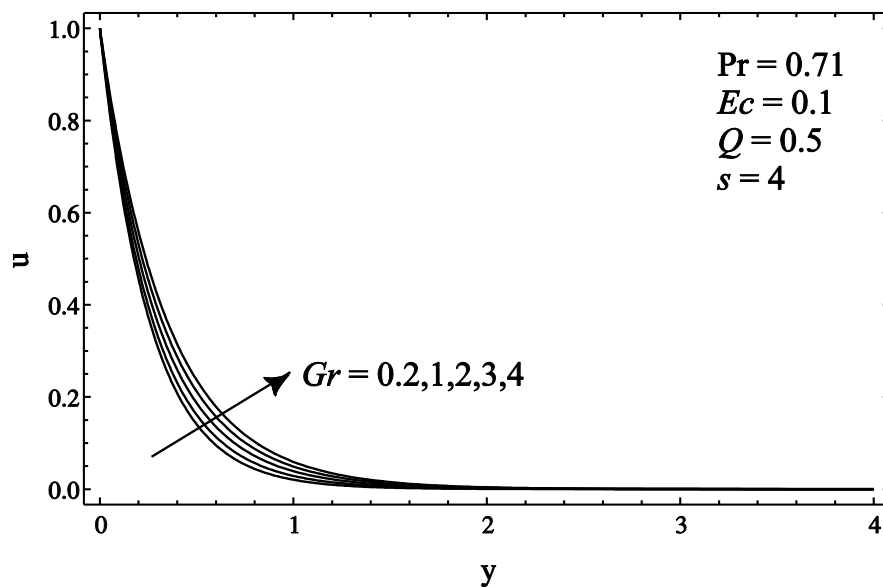


Figure 2.10: Influence of  $Gr$  on velocity profiles

The numerical results of skin friction and Nusselt number are calculated for different values of system parameters and displayed in the Table 2.2. It is observed that the skin friction increases with increasing Prandtl number and suction parameter whereas it decreases with increasing Grashof number, Eckert number and heat generation parameter. Also, from the Table 2.2, it can be seen that the Nusselt number increases with increasing Prandtl number and suction velocity whereas it decreases with increasing Grashof number, Eckert number and heat generation parameter.

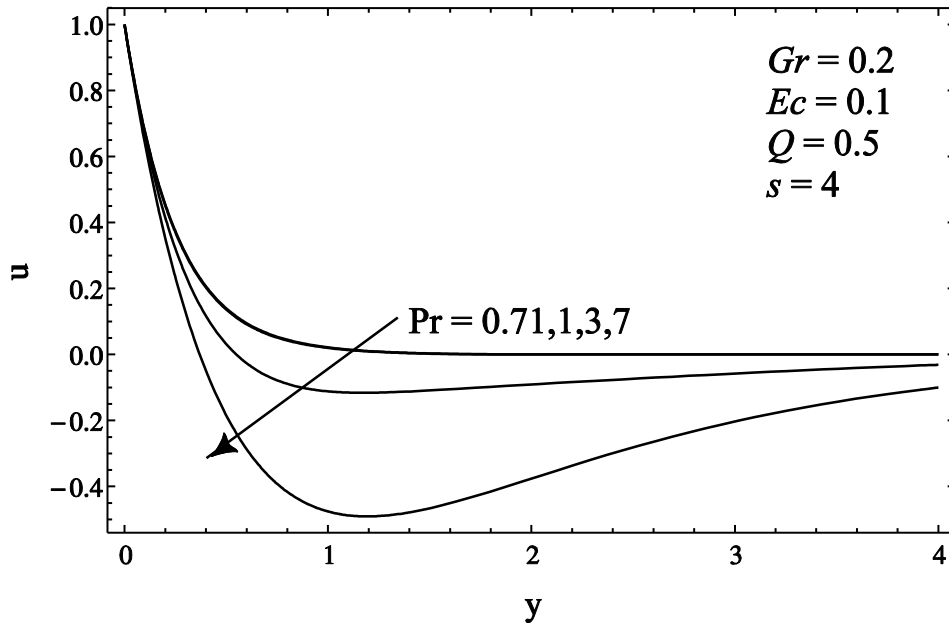


Figure 2.11: Influence of  $Pr$  on velocity profiles

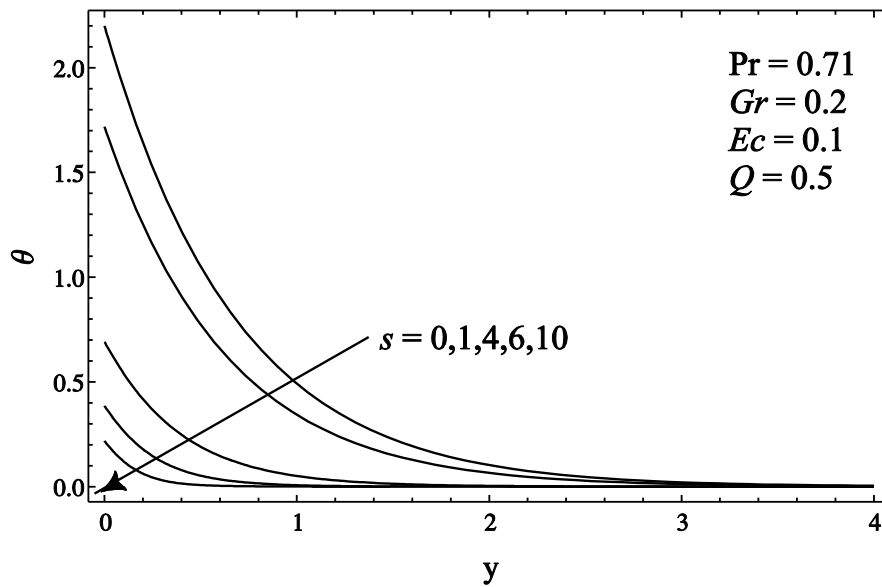


Figure 2.12: Influence of  $s$  on temperature profiles



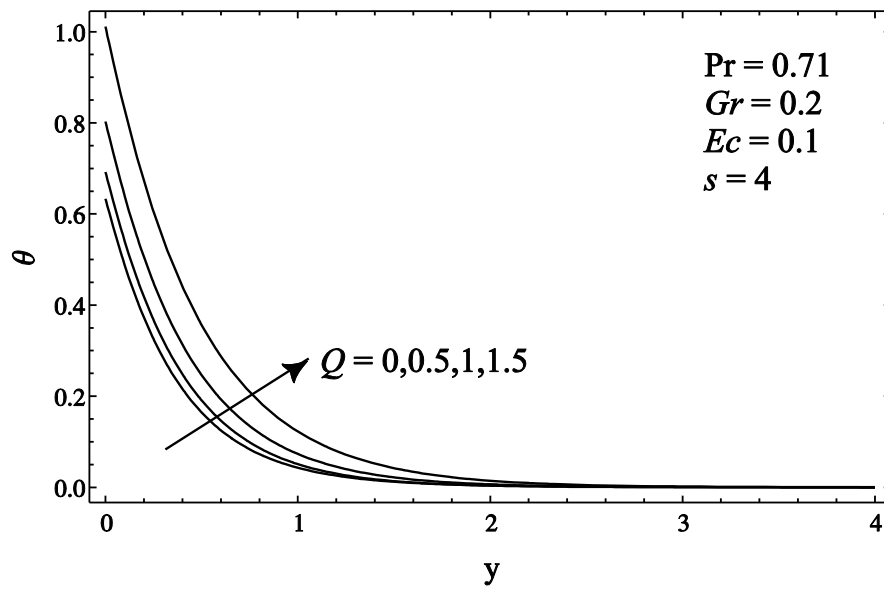


Figure 2.13: Influence of  $Q$  on temperature profiles

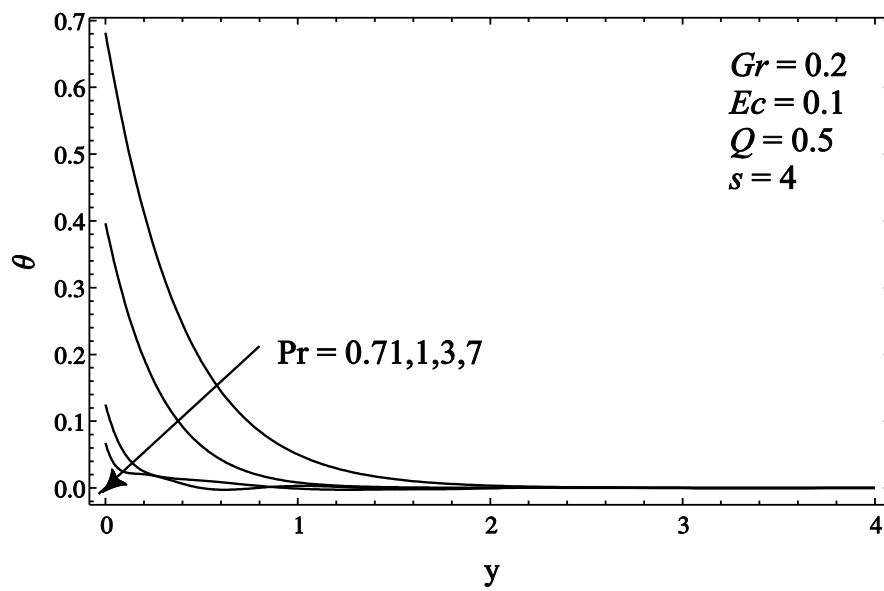


Figure 2.14: Influence of  $Pr$  on temperature profiles

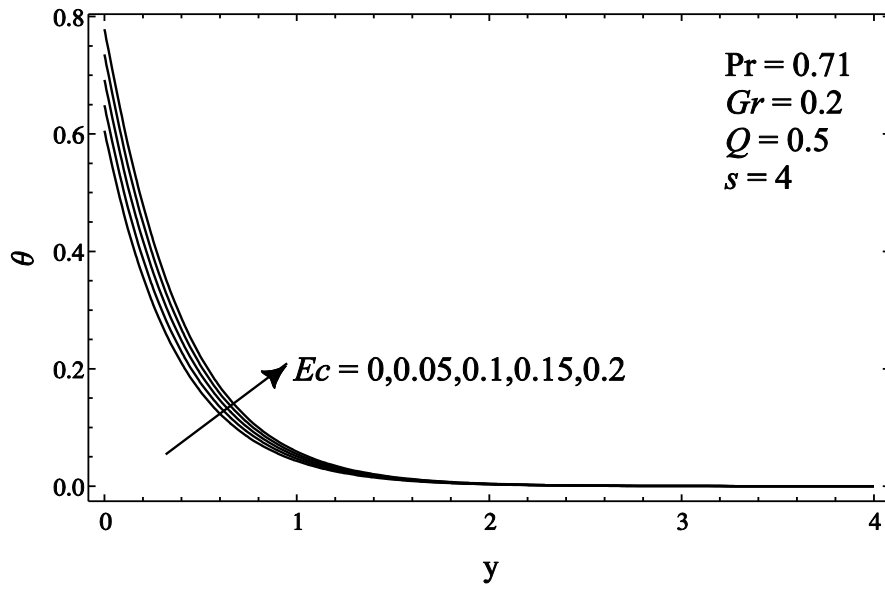


Figure 2.15: Influence of  $Ec$  on temperature profiles

Table 2.1: Effects of Eckert number ( $Ec$ ) and heat source parameter ( $Q$ ) on velocity profile

$Ec$	$Q$					
		$y = 0.1$	$y = 1$	$y = 2$	$y = 3$	$y = 4$
0	0.5	0.67359	0.02008	0.00049	0.000018	5.88E-7
0.05	0.5	0.67388	0.02025	0.00050	0.000019	1.53E-6
0.1	0.5	0.67417	0.02041	0.00052	0.00002	1.61E-6
0.15	0.5	0.67447	0.02057	0.00053	0.000021	1.68E-6
0.2	0.5	0.67475	0.02074	0.00055	0.000022	1.76E-6
0.1	0	0.67352	0.01986	0.00046	0.000015	1.900E-6
0.1	1	0.67525	0.02135	0.00065	0.000036	2.63E-6
0.1	1.5	0.67738	0.02348	0.00103	0.00009	7.892E-6

Table 2.2: Skin Friction ( $\tau$ ) and Nusselt number ( $Nu$ ) variation

Pr	$s$	$Gr$	$Ec$	$Q$	$\tau$	$Nu$
0.3	4	0.2	0.1	0.5	1.05984	1.12762
0.71	4	0.2	0.1	0.5	3.91252	2.46718
1	4	0.2	0.1	0.5	3.94273	3.52315
3	4	0.2	0.1	0.5	3.97018	9.01426
7	4	0.2	0.1	0.5	4.02631	15.8086
0.71	4	1	0.1	0.5	3.73415	2.45583
0.71	4	2	0.1	0.5	3.473	2.46894
0.71	4	3	0.1	0.5	3.21579	2.48113
0.71	4	4	0.1	0.5	2.96184	2.49237
0.71	4	0.2	0.1	0	3.95414	2.57897
0.71	4	0.2	0.1	1	3.93233	2.24546
0.71	4	0.2	0.1	1.5	3.90364	1.98915
0.71	0	0.2	0.1	0.5	0.56148	1.45462
0.71	1	0.2	0.1	0.5	0.62035	1.58208
0.71	6	0.2	0.1	0.5	5.95373	3.59575
0.71	10	0.2	0.1	0.5	9.77897	5.58857
0.71	4	0.2	0	0.5	3.95432	2.65142
0.71	4	0.2	0.05	0.5	3.95036	2.54101
0.71	4	0.2	0.15	0.5	3.94248	2.35983
0.71	4	0.2	0.2	0.5	3.93854	2.28459

## **2.6 Chapter Summary**

In this chapter, heat generation and viscous dissipation effects on free convection flow past an impulsively started infinite vertical porous plate in the presence of Newtonian heating have been studied by analytical technique known as Homotopy Analysis Method (HAM). There is an excellent agreement between exact analytical and HAM solution results in the absence of viscous dissipation. It can be seen from the results, an increase in the heat generation parameter and Eckert number lead to an increase in the fluid velocity and temperature. However, skin friction and heat transfer rate decrease with the increase in heat generation parameter and Eckert number.

## CHAPTER 3

### THERMAL RADIATION AND VISCOUS DISSIPATION EFFECTS IN THE PRESENCE OF MAGNETIC FIELD

#### **3.1 Introduction**

The effect of thermal radiation on natural convection heat transfer becomes very significant especially at high operating temperature. In many industrial processes, which occur at high temperature, the study of thermal radiation becomes more important for the design of apposite equipment. Nuclear reactors, gas turbines and the numerous propulsion devices for aircraft, missiles, satellites and space vehicles are examples of such industrial areas. Many researchers have been investigated the thermal radiation effect on porous plate by using analytical or approximate analytical methods. Laplace transformation, finite difference method, perturbation technique, shooting method and many other techniques have been applied to solve the heat and mass transfer problems. Hossain et al. [29] investigated the thermal radiation effect on free convection flow of a viscous incompressible fluid along a uniformly heated vertical porous plate with uniform suction and temperature depended viscosity. Kim and Fedorov [7] studied the thermal radiation effect on transient mixed convection flow of a micro-polar fluid past a moving semi-infinite vertical porous plate. They used Rosseland approximation to delineate the radiative heat flux with the constant velocity of porous plate. Makinde [8] carried out a numerical study to investigate the thermal radiation effect on free convection heat and mass transfer flow past a moving vertical porous plate. Makinde and Ogulu [33] investigated the thermal radiation effect on the heat and mass transfer flow past a vertical porous plate in the presence of transverse magnetic field with time dependent viscosity. They used shooting method to solve the

boundary layer equations with the consideration of first order homogenous chemical reaction. An analytical study for a first order homogenous chemical reaction and electrically conducting viscous fluid past a moving semi-infinite vertical porous plate in the presence of heat source and sink was reported by Ibrahim et al. [12].

The flow of heat transfer fluids near different types of boundaries can be controlled by magnetic field. This study has significant interests in the boundary layer flows subjected to an externally applied transverse magnetic field. Moreover, the study of magnetic field effects on the thermal transport process in the boundary layer flow with the inclusion of ohmic heating has gained considerable attention. Naby et al. [30] reported the thermal radiation effect on MHD unsteady free convection flow past a vertical porous plate by using a finite difference method in the presence of a uniform transverse magnetic field. Thermal radiation interaction with unsteady MHD flow past a vertical porous plate immersed in a porous medium in the presence of magnetic field was analyzed by Samad and Rehman [31]. They used the Nachtsheim-Swigert iteration technique to solve the governing equations with the time dependent suction velocity of the porous plate. Network simulation method was used to study the thermal radiation and viscous dissipation effects on MHD unsteady free convective flow over a vertical porous plate by Jordan [32]. In the presence of thermal radiation, effects of variable suction and thermophoresis on steady MHD combined free-forced convective heat and mass transfer flow over a semi-infinite inclined porous plate was examined by Aslam et al. [11]. Mohamed and Abo-Dahab [34] analyzed the effects of thermal radiation and chemical reaction on free convection MHD heat and mass transfer flow of a micro-polar fluid over a semi-infinite vertical moving porous plate in the presence of heat generation. They studied these effects with time-dependent variable suction velocity of the porous plate in the presence of a uniform transverse magnetic field. Pal and Talukdar [35] used a perturbation technique to investigate the thermal radiation and chemical reaction effects on unsteady mixed convection MHD heat and mass transfer boundary layer slip flow over a vertical porous plate in the presence of uniform transverse magnetic field. An interaction of thermal radiation and  $n^{\text{th}}$  order homogenous chemical reaction with MHD mixed convection heat and mass transfer flow of an incompressible Boussinesq fluid past a vertical porous plate embedded in a porous medium with constant heat flux and viscous dissipation was investigated by Makinde

[36]. The present work has been undertaken to study the effects of thermal radiation and viscous dissipation on free convection heat transfer flow of a viscous incompressible electrically conducting fluid over an impulsively started infinite vertical porous plate with Newtonian heating in the presence of transverse magnetic field.

### 3.2 Problem Description

In this chapter, the thermal radiation effect on free convection flow along an impulsively started infinite vertical porous plate permeated by a transverse magnetic field in the presence of Newtonian heating is examined. The  $x'$ -axis is taken along the plate in the upward direction and  $y'$ -axis normal to the plate as shown in Figure 3.1. The flow is being incompressible and it is assumed that the heat transfer rate from the surface with a finite heat capacity is proportional to the local surface temperature ( $T'$ ), i.e.

$$\frac{\partial T'}{\partial y'} = -\frac{h}{k} T' \quad \text{at } y' = 0$$

where  $T'$  is the temperature of the fluid,  $h$  is the heat transfer coefficient and  $k$  is the thermal conductivity of the plate. Since the plate is assumed to be infinite along the  $x'$ -axis direction, all the physical variables are independent from  $x'$  and are functions of  $y'$  only. Under the usual Boussinesq approximation [77], i.e., density changes with temperature, which gives rise to the buoyancy force, the governing boundary layer equations are simplified to the following form:

$$\frac{\partial v'}{\partial y'} = 0 \tag{3.1}$$

$$v' \frac{\partial u'}{\partial y'} = \nu \frac{\partial^2 u'}{\partial y'^2} + g\beta(T' - T'_\infty) - \frac{\sigma B_0^2}{\rho} u' \tag{3.2}$$

$$v' \frac{\partial T'}{\partial y'} = \frac{k}{\rho c_p} \frac{\partial^2 T'}{\partial y'^2} - \frac{1}{\rho c_p} \frac{\partial q_r}{\partial y'} + \frac{\mu}{\rho c_p} \left( \frac{\partial u'}{\partial y'} \right)^2 + \frac{\sigma B_0^2}{\rho c_p} u'^2 \tag{3.3}$$

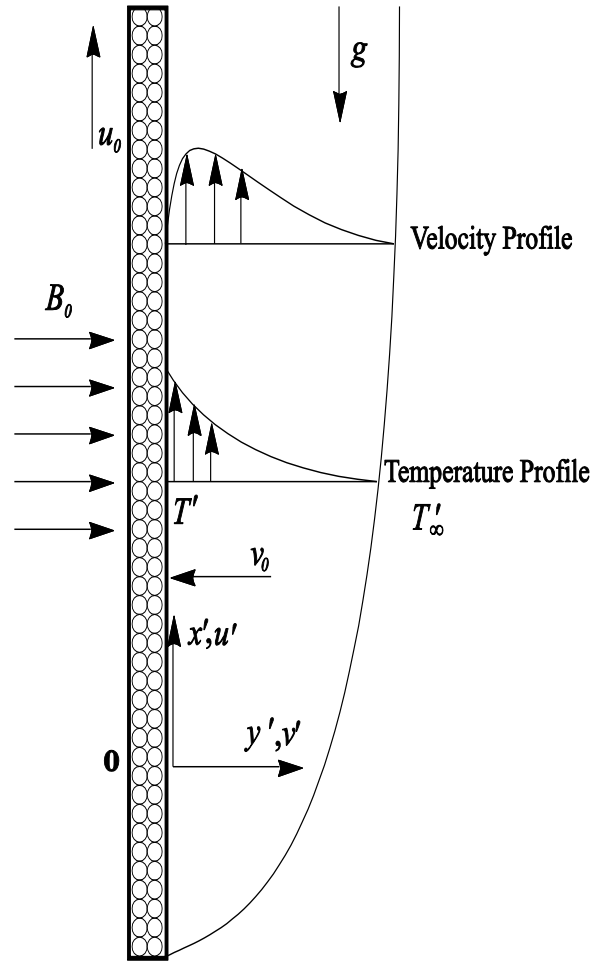


Figure 3.1: Physical Model

where  $u'$  is the fluid velocity in the  $x'$  direction,  $v'$  the suction velocity,  $\nu$  the kinematic viscosity,  $T_\infty'$  the free stream temperature,  $g$  the acceleration due to gravity,  $\beta$  the volumetric coefficient of thermal expansion,  $B_0$  the magnetic field component along  $y'$  axis,  $\sigma$  the electrical conductivity of the fluid,  $\rho$  the fluid density,  $c_p$  the specific heat at constant pressure,  $q_r$  the radiative heat flux; and  $\mu$  is the viscosity.

The boundary conditions are

$$\left. \begin{aligned} u' &= u_0, & \frac{\partial T'}{\partial y'} &= -\frac{h}{k}T', & \text{at } y' &= 0, \\ u' &\rightarrow 0, & T' &\rightarrow T_\infty', & \text{as } y' &\rightarrow \infty. \end{aligned} \right\} \quad (3.4)$$

Integrating equation (3.1) for constant suction, we get



$$v' = -v_0 \quad (3.5)$$

where  $v_0 > 0$  is the normal velocity of suction at the plate.

Equations (3.2) and (3.3) can now be written as

$$-v_0 \frac{\partial u'}{\partial y'} = v \frac{\partial^2 u'}{\partial y'^2} + g\beta(T' - T'_\infty) - \frac{\sigma B_0^2}{\rho} u' \quad (3.6)$$

$$-v_0 \frac{\partial T'}{\partial y'} = \frac{k}{\rho c_p} \frac{\partial^2 T'}{\partial y'^2} - \frac{1}{\rho c_p} \frac{\partial q_r}{\partial y'} + \frac{\mu}{\rho c_p} \left( \frac{\partial u'}{\partial y'} \right)^2 + \frac{\sigma B_0^2}{\rho c_p} u'^2 \quad (3.7)$$

For an optically thin gray gas, the radiation heat flux  $q_r$  in equation (3.7) satisfies the following non-linear differential equation:

$$\frac{\partial q_r}{\partial y'} = 4\alpha\sigma^*(T'^4 - T_\infty'^4) \quad (3.8)$$

where  $\alpha$  is the radiation absorption coefficient and  $\sigma^*$  is the Stefan-Boltzmann constant. Assuming that the temperature differences within the flow are sufficiently small such that  $T'^4$  can be expressed as a linear function of  $T'$  using the Taylor series expression, after neglecting higher-order terms, we get

$$T'^4 \cong 4T_\infty'^3 T' - 3T_\infty'^4 \quad (3.9)$$

In the view of equation (3.8) and (3.9), equation (3.7) becomes

$$-v_0 \frac{\partial T'}{\partial y'} = \frac{k}{\rho c_p} \frac{\partial^2 T'}{\partial y'^2} - \frac{16\alpha\sigma^* T_\infty'^3}{\rho c_p} (T' - T'_\infty) + \frac{\mu}{\rho c_p} \left( \frac{\partial u'}{\partial y'} \right)^2 + \frac{\sigma B_0^2}{\rho c_p} u'^2 \quad (3.10)$$

Introducing the following non-dimensional quantities:

$$\left. \begin{aligned} y &= \frac{y'h}{k}, \quad u = \frac{u'}{u_0}, \quad \theta = \frac{T' - T'_\infty}{T'_\infty}, \quad s = \frac{\nu_0 k}{h\nu}, \quad M = \frac{\sigma B_0^2 k^2}{\mu h^2}, \\ Gr &= \frac{g\beta T'_\infty k^2}{\nu u_0 h^2}, \quad Pr = \frac{\mu c_p}{k}, \quad Ec = \frac{\mu u_0^2}{k T'_\infty}, \quad R = \frac{16\alpha\sigma^* k T'^3_\infty}{h^2}. \end{aligned} \right\} \quad (3.11)$$

where  $u$  and  $\theta$  are the dimensionless velocity and temperature respectively,  $s$  is the suction parameter,  $M$  is the magnetic field parameter, i.e., square of the Hartmann number,  $Gr$  is the thermal Grashof number,  $Pr$  is the Prandtl number,  $Ec$  is the Eckert number and  $R$  is the radiation parameter.

In the view of equations (3.11), (3.6), (3.10) and (3.4) reduces to the following non-dimensional forms:

$$\frac{d^2 u}{dy^2} + s \frac{du}{dy} + Gr\theta - Mu = 0 \quad (3.12)$$

$$\frac{d^2 \theta}{dy^2} + Pr s \frac{d\theta}{dy} - R\theta + Ec \left( \frac{du}{dy} \right)^2 + Ec Mu^2 = 0 \quad (3.13)$$

The corresponding boundary conditions are

$$\left. \begin{aligned} u &= 1, \quad \frac{d\theta}{dy} = -(\theta + 1), \quad \text{at } y = 0, \\ u &\rightarrow 0, \quad \theta \rightarrow 0, \quad \text{as } y \rightarrow \infty. \end{aligned} \right\} \quad (3.14)$$

### 3.3 Solution by HAM

To solve the system of nonlinear equations (3.12) and (3.13) subject to the boundary conditions (3.14) by HAM, we assume the initial guesses and linear operators as defined in equations (2.14) and (2.15), respectively.

We then assume that the solutions of the form

$$u(y) = \sum_{n=0}^{\infty} a_n e^{-ny} \quad \text{and} \quad \theta(y) = \sum_{n=0}^{\infty} b_n e^{-ny} \quad (3.15)$$

with the non-linear operators

$$N_u[\varphi(y; q), \psi(y; q)] = \frac{d^2 \varphi(y; q)}{dy^2} + s \frac{d\varphi(y; q)}{dy} + Gr\psi(y; q) - M\varphi(y; q) \quad (3.16)$$

$$N_\theta[\varphi(y; q), \psi(y; q)] = \frac{d^2 \psi(y; q)}{dy^2} + Pr s \frac{d\psi(y; q)}{dy} - R\psi(y; q) + Ec \left( \frac{d\varphi(y; q)}{dy} \right)^2 + Ec M\varphi^2(y; q) \quad (3.17)$$

The generalized homotopies are then defined to be

$$(1-q)L_u[\varphi(y; q) - u_0(y)] = q\hbar_u H_u(y) N_u[\varphi(y; q), \psi(y; q)] \quad (3.18)$$

$$(1-q)L_\theta[\psi(y; q) - \theta_0(y)] = q\hbar_\theta H_\theta(y) N_\theta[\varphi(y; q), \psi(y; q)] \quad (3.19)$$

subject to the boundary conditions

$$\left. \begin{aligned} \phi(0; q) &= 1, & \psi'(0; q) &= -\psi(0; q) - 1, \\ \phi(\infty; q) &\rightarrow 0, & \psi(\infty; q) &\rightarrow 0. \end{aligned} \right\} \quad (3.20)$$

These generalized homotopies produce the  $n^{\text{th}}$  order deformation equations

$$\left. \begin{aligned} L_u[u_n(y) - \chi_n u_{n-1}(y)] &= \hbar_u H_u(y) R_n^u(u_{n-1}(y), \theta_{n-1}(y)) \\ L_\theta[\theta_n(y) - \chi_n \theta_{n-1}(y)] &= \hbar_\theta H_\theta(y) R_n^\theta(u_{n-1}(y), \theta_{n-1}(y)) \end{aligned} \right\} \quad (3.21)$$

subject to the boundary conditions

$$\left. \begin{aligned} u_n(0) &= 0, & \theta'_n(0) + \theta_n(0) &= 0, \\ u_n(\infty) &\rightarrow 0, & \theta_n(\infty) &\rightarrow 0. \end{aligned} \right\} \quad (3.22)$$

where

$$\chi_n = \begin{cases} 0 & n \leq 1 \\ 1 & n > 1, \end{cases}$$

$$R_n^u(u_{n-1}(y), \theta_{n-1}(y)) = u''_{n-1}(y) + s u'_{n-1}(y) + Gr\theta_{n-1}(y) - M u_{n-1}(y) \quad (3.23)$$

$$R_n^\theta(u_{n-1}(y), \theta_{n-1}(y)) = \theta_{n-1}''(y) + \text{Pr } s \theta_{n-1}'(y) - R \theta_{n-1}(y) + Ec \left[ \sum_{j=0}^{n-1} u_j'(y) u_{n-1-j}'(y) \right] + Ec M \left[ \sum_{j=0}^{n-1} u_j(y) u_{n-1-j}(y) \right] \quad (3.24)$$

For simplicity [15], again we chose auxiliary functions and auxiliary parameters as

$$H_u(y) = H_\theta(y) = 1 \text{ and } \hbar_u = \hbar_\theta = \hbar$$

For each  $n$  we can get the required solutions from the  $n^{\text{th}}$  order deformation equations, subject to the boundary conditions (3.22).

The skin friction and Nusselt number formulae are used as mentioned in (2.37) and (2.38).

### 3.4 Exact Analytical Solution

Exact analytical solution of the prescribed system of equations (3.12), (3.13) with boundary conditions (3.14) can be find in the absence of viscous dissipation and ohmic heating, i.e., ( $Ec = 0$ ). For this purpose, the system of equations (3.12), (3.13) subject to the boundary conditions (3.14) can be written as

$$\frac{d^2 u}{dy^2} + s \frac{du}{dy} + Gr \theta - M u = 0 \quad (3.25)$$

$$\frac{d^2 \theta}{dy^2} + \text{Pr } s \frac{d\theta}{dy} - R \theta = 0 \quad (3.26)$$

subject to the boundary conditions

$$\left. \begin{aligned} u = 1, \quad \frac{d\theta}{dy} = -(\theta + 1), \quad \text{at} \quad y = 0, \\ u \rightarrow 0, \quad \theta \rightarrow 0, \quad \text{as} \quad y \rightarrow \infty. \end{aligned} \right\} \quad (3.27)$$

Corresponding auxiliary linear equations of (3.25) and (3.26) are

$$m^2 u + s m u + Gr \theta - M u = 0 \quad (3.28)$$

$$m^2 \theta + \text{Pr} s m \theta - R \theta = 0 \quad (3.29)$$

where  $m = d/dy$ , solving equation (3.29)

$$(m^2 + \text{Pr} s m - R) \theta = 0$$

$$m = \frac{-\text{Pr} s \pm \sqrt{\text{Pr}^2 s^2 + 4R}}{2}$$

Let,

$$m_1 = \frac{-\text{Pr} s + \sqrt{\text{Pr}^2 s^2 + 4R}}{2}, \quad m_2 = \frac{-\text{Pr} s - \sqrt{\text{Pr}^2 s^2 + 4R}}{2} \quad \text{or}$$

$$-m_2 = \left( \frac{\text{Pr} s + \sqrt{\text{Pr}^2 s^2 + 4R}}{2} \right)$$

Now, the general solution for equation (3.29) will be

$$\theta(y) = c_1 e^{m_1 y} + c_2 e^{-m_2 y} \quad (3.30)$$

$$\theta'(y) = m_1 c_1 e^{m_1 y} - m_2 c_2 e^{-m_2 y}$$

Now applying boundary conditions

$$\theta'(y) = -(\theta(y) + 1) \quad \text{at} \quad y = 0$$

$$m_1 c_1 - m_2 c_2 = -c_1 - c_2 - 1$$

$$(m_1 + 1)c_1 + (1 - m_2)c_2 + 1 = 0$$

and as  $y \rightarrow \infty$  equation (3.30) becomes

$$\theta(\infty) = c_1 e^{m_1(\infty)} + c_2 e^{-m_2(\infty)}$$

$$\text{Here } c_1 \text{ must be zero. Therefore, } c_2 = \frac{-1}{1 - m_2} \quad \text{or} \quad c_2 = \frac{1}{m_2 - 1}$$

Thus, equation (3.30) becomes as

$$\theta(y) = \frac{1}{m_2 - 1} e^{-m_2 y} \quad (3.31)$$

Now (3.28) can be written as

$$(m^2 + s m - M)u + \frac{Gr}{m_2 - 1} e^{-m_2 y} = 0 \quad (3.32)$$

Its corresponding homogenous auxiliary equation is

$$(m^2 + s m - M)u = 0$$

$$m^2 + s m - M = 0$$

$$m = \frac{-s \pm \sqrt{s^2 + 4M}}{2}$$

Let,

$$m_3 = \frac{-s + \sqrt{s^2 + 4M}}{2} \quad \text{and} \quad m_4 = \frac{-s - \sqrt{s^2 + 4M}}{2} \quad \text{or}$$

$$-m_4 = \left( \frac{s + \sqrt{s^2 + 4M}}{2} \right)$$

Complimentary solution of (3.32) will be

$$u_c(y) = c_3 e^{m_3 y} + c_4 e^{-m_4 y}$$

Now, particular integral can be written as

$$(m^2 + s m - M)u_p(y) = \frac{Gr}{1 - m_2} e^{-m_2 y}$$

$$u_p(y) = \frac{Gr}{1 - m_2} \frac{1}{(m^2 + s m - M)} e^{-m_2 y}$$

$$u_p(y) = \frac{Gr}{(1 - m_2)} \frac{e^{-m_2 y}}{(m^2 - s m - M)}$$

Now,

$$u(y) = u_c(y) + u_p(y)$$

$$u(y) = c_3 e^{m_3 y} + c_4 e^{-m_4 y} + \frac{Gr e^{-m_2 y}}{(1 - m_2)(m_2^2 - s m_2 - M)} \quad (3.33)$$

Since  $u \rightarrow 0$  as  $y \rightarrow \infty$ , therefore  $c_3 = 0$ . Also  $u = 1$  at  $y = 0$ , we have

$$c_4 = 1 - \frac{Gr}{(1 - m_2)(m_2^2 - s m_2 - M)}.$$

Thus, equation (3.33) will become as

$$u(y) = \left[ 1 - \frac{Gr}{(1 - m_2)(m_2^2 - s m_2 - M)} \right] e^{-m_4 y} + \frac{Gr e^{-m_2 y}}{(1 - m_2)(m_2^2 - s m_2 - M)} \quad (3.34)$$

Hence, equations (3.31) and (3.34) represent the exact analytical solution of system of equations (3.25) and (3.26) for limiting case.

### 3.5 Result and Discussion

In the solution of HAM, auxiliary parameter  $\hbar \neq 0$  effectively controls the convergence of series solution. To ensure the convergence of series solution so called  $\hbar$  curves for velocity and temperature profiles are plotted at 20<sup>th</sup> order of HAM in Figures 3.2 and 3.3 for fixed set of parameters  $R = 5, M = 2, s = 2, Ec = 0.1, Pr = 0.71, Gr = 2$ . The common convergence regions for both velocity and temperature profiles are  $-0.19 \leq \hbar \leq -0.05$  and  $-0.18 \leq \hbar \leq -0.03$ , respectively.

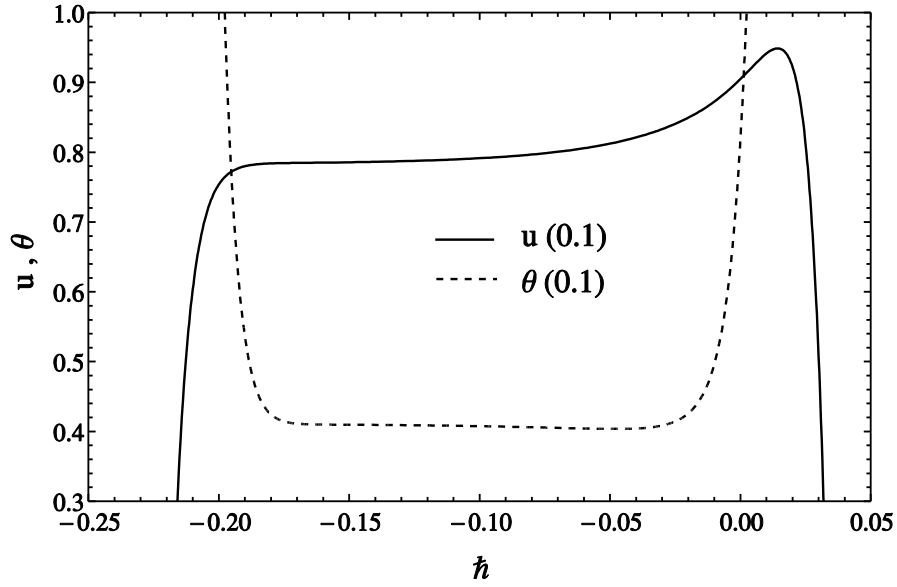


Figure 3.2:  $\hbar$  curves at 20<sup>th</sup> order of HAM

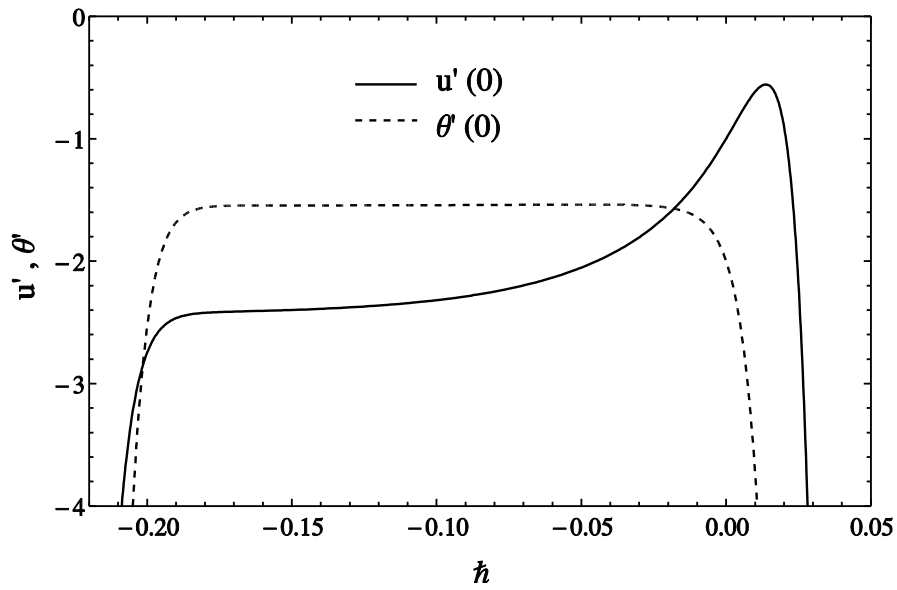


Figure 3.3:  $\hbar$  curves at 20<sup>th</sup> order of HAM

Homotopy Analysis Method (HAM) has been applied to solve a coupled non-linear system of equations (3.12) and (3.13) subject to the boundary conditions (3.14). The results obtained by the HAM have been compared with the exact solution results in the absence of viscous dissipation and ohmic heating. An excellent agreement is found between the results, which can be seen from figures 3.4 to 3.9.



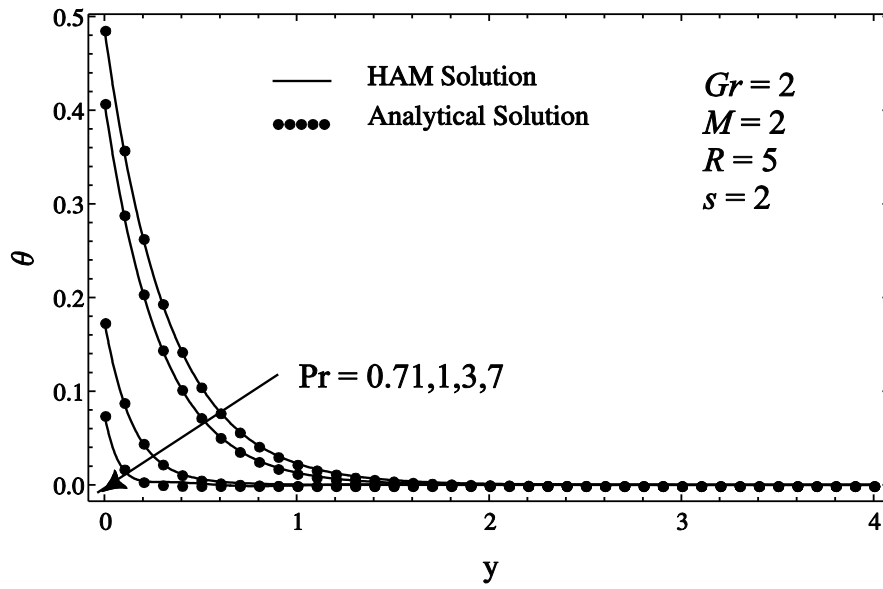


Figure 3.4: Comparison of temperature profiles for HAM and analytical solution at different  $Pr$  when  $Ec = 0$ .

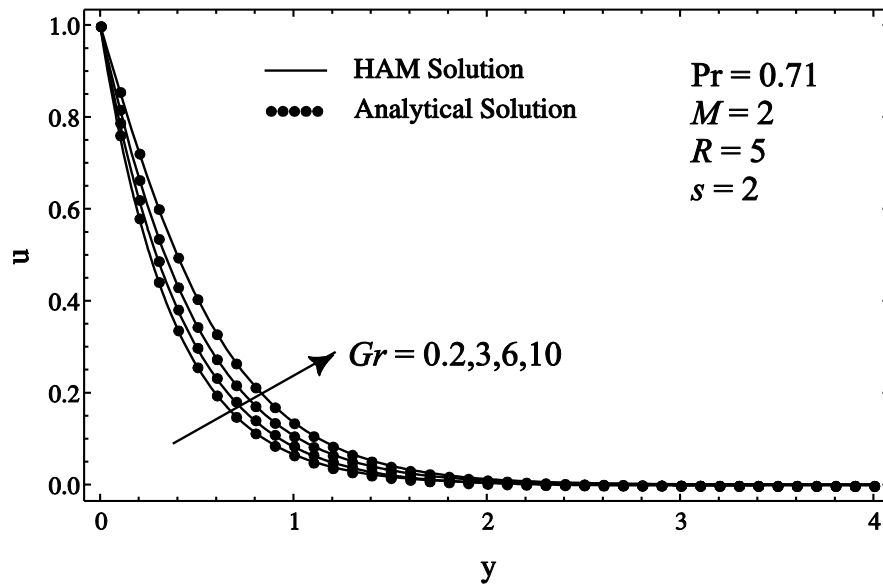


Figure 3.5: Comparison of velocity profiles for HAM and analytical solution at different  $Gr$  when  $Ec = 0$ .

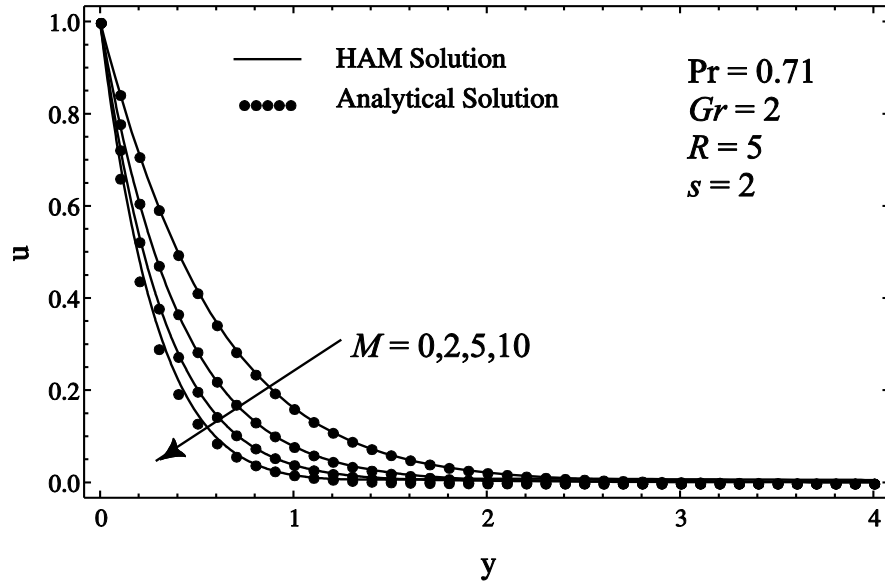


Figure 3.6: Comparison of velocity profiles for HAM and analytical solution at different  $M$  when  $Ec = 0$ .

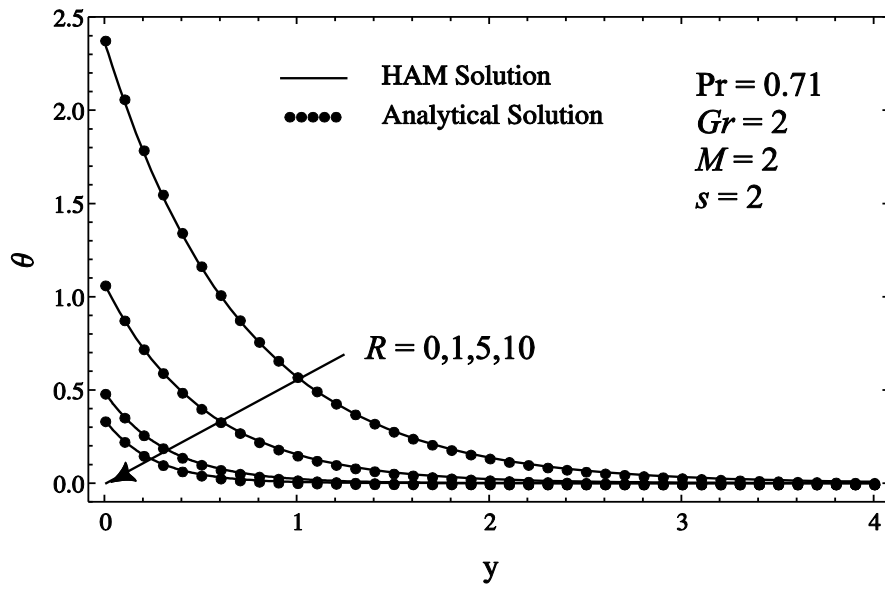


Figure 3.7: Comparison of temperature profiles for HAM and analytical solution at different  $R$  when  $Ec = 0$ .

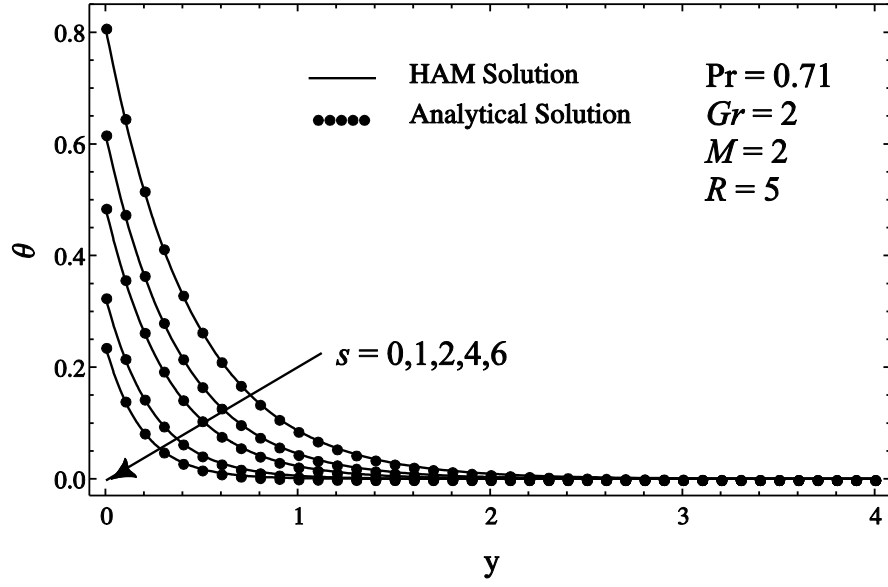


Figure 3.8: Comparison of temperature profiles for HAM and analytical solution at different  $s$  when  $Ec = 0$ .

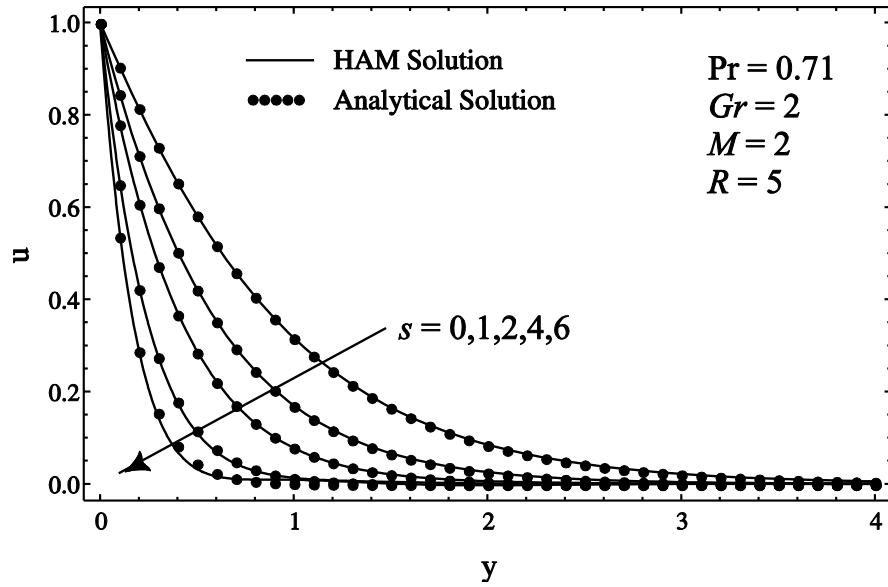


Figure 3.9: Comparison of velocity profiles for HAM and analytical solution at different  $s$  when  $Ec = 0$ .

Figures 3.10 to 3.19 depict the effects of Prandtl number ( $Pr$ ), thermal Grashof number ( $Gr$ ), magnetic field parameter ( $M$ ), radiation parameter ( $R$ ), suction parameter ( $s$ ) and Eckert number ( $Ec$ ) on velocity and temperature fields, respectively. The velocity profiles for various values of Prandtl number are plotted in Figure 3.10.

It is observed that an increase in the value of prandtl number decreases the fluid velocity. This is may be due to the fact that the fluids with high Prandtl number have greater viscosity, which makes the fluid thick and hence, it moves slowly. Similar type of behavior is observed for thermal boundary layer variation with Prandtl number from Figure 3.11. The effects of thermal Grashof number on velocity profile are presented in Figure 3.12. It is noticed that an increase in Grashof number increases the fluid velocity. This would happen because with an increase in  $Gr$  the effect of viscous force decreases, and thus the velocity boundary layer thickness increases.

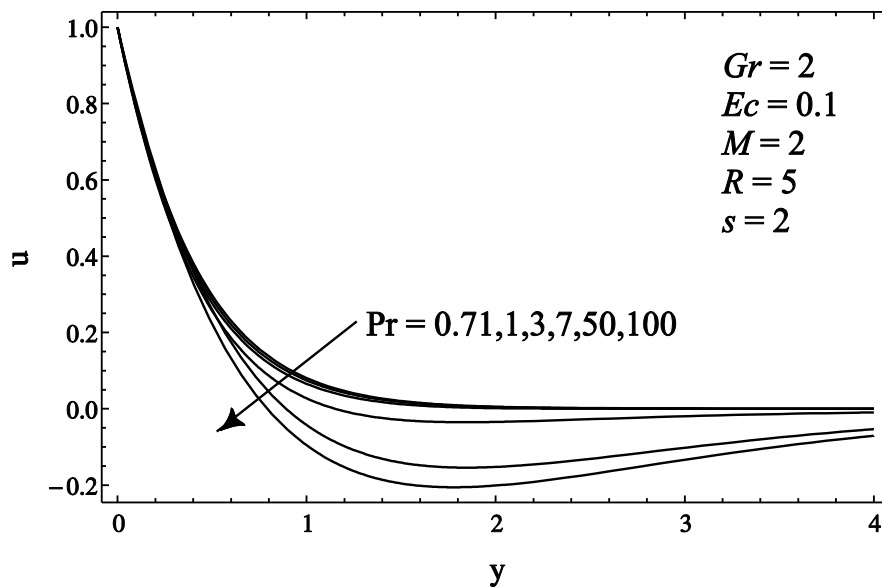


Figure 3.10: Influence of  $Pr$  on velocity profiles.

Figures 3.13 and 3.14 show the influence of magnetic field parameter on velocity and temperature profiles. In Figure 3.13, it is observed that with an increase in magnetic field parameter velocity of the fluid decreases. This is may be due to the fact that the Lorentz force which, is produced by the application of a transverse magnetic field, causes to decelerate the fluid velocity in the boundary layer. Physically, the higher value of magnetic field parameter results in the higher Lorentz force. Similar type of trend was observed by Makinde and Ogulu [33].

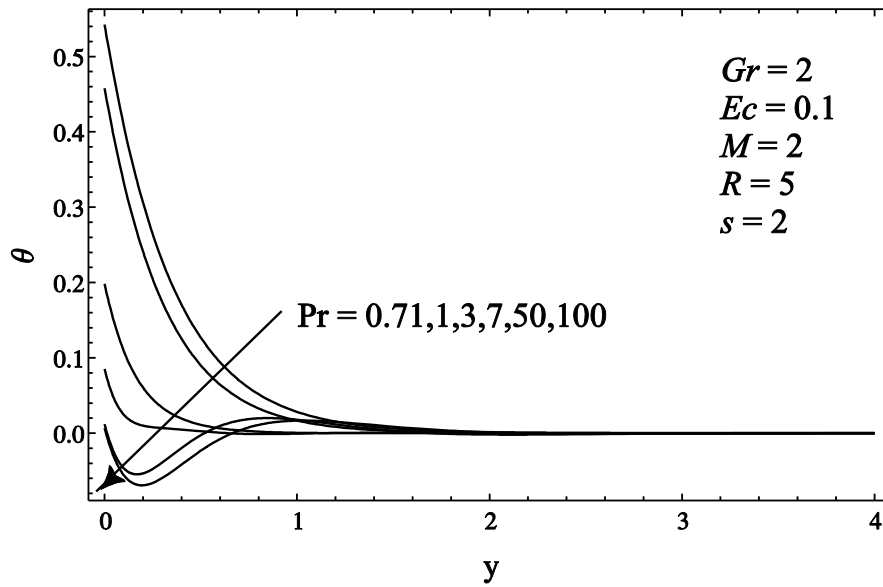


Figure 3.11: Influence of  $Pr$  on temperature profiles.

Figure 3.14 reveals that an increase in the magnetic field parameter causes to rise the thermal boundary layer thickness. This is may be due to the fact that extra work is done to drag the fluid against the magnetic field which causes to increase the thermal energy of the fluid in the thermal boundary layer region and consequently temperature profile rises. The influence of thermal radiation parameter on velocity and temperature fields is plotted in Figures 3.15 and 3.16. It has a significant reducing effect on both the velocity and temperature fields.

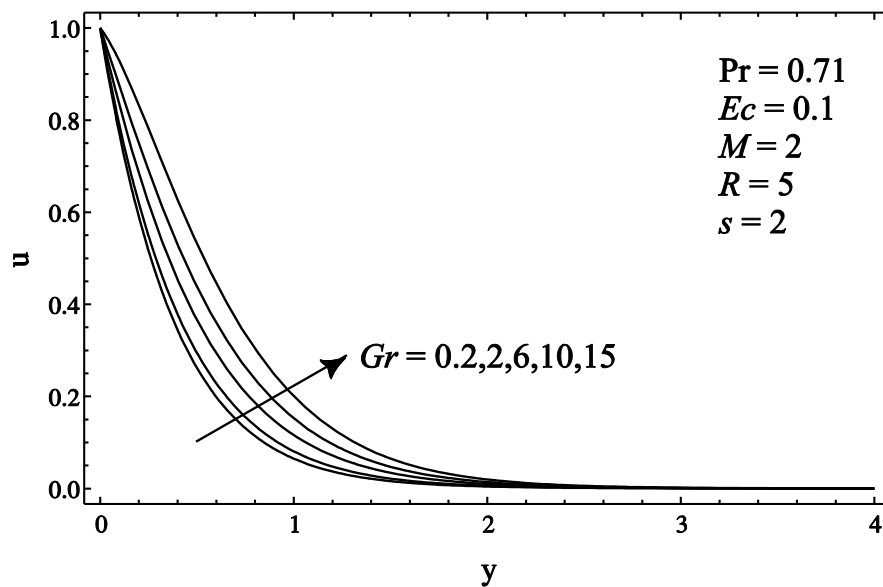


Figure 3.12: Influence of  $Gr$  on velocity profiles.

It is observed that an increase in the thermal radiation parameter causes to decrease in the velocity as well as temperature distributions in the boundary layer. This is because rises in the thermal radiation parameter have tendency to dominant the conduction effects over radiation absorption. Therefore, higher value of radiation parameter causes to decrease in the momentum as well as thermal boundary layer thickness.

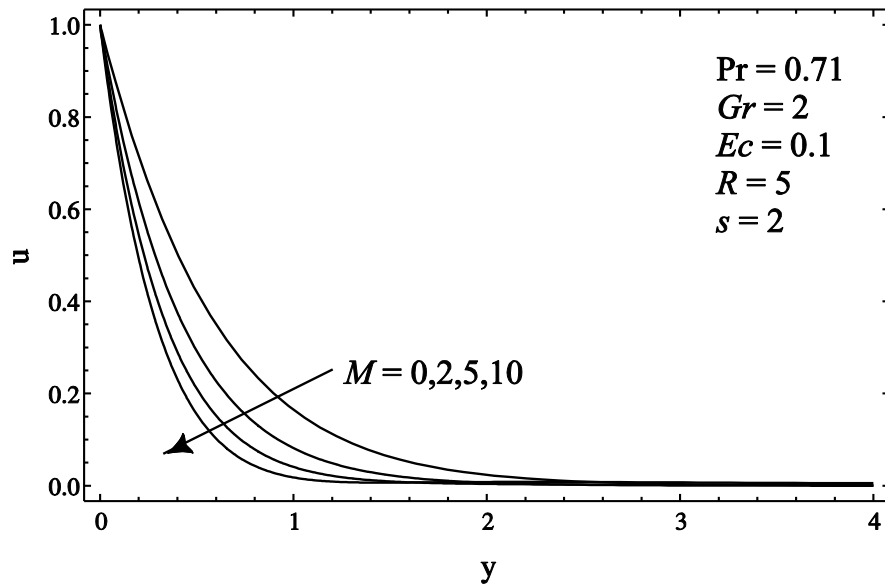


Figure 3.13: Influence of  $M$  on velocity profiles.

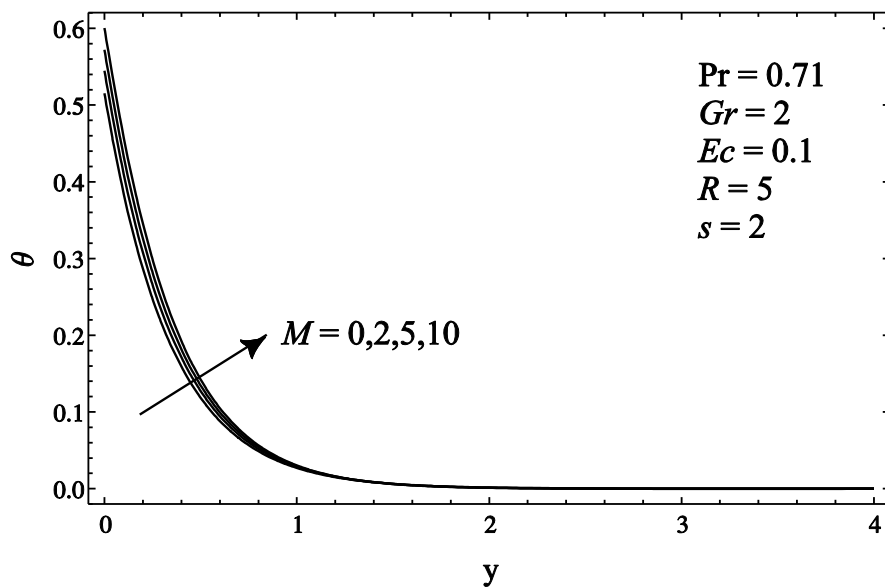


Figure 3.14: Influence of  $M$  on temperature profiles.

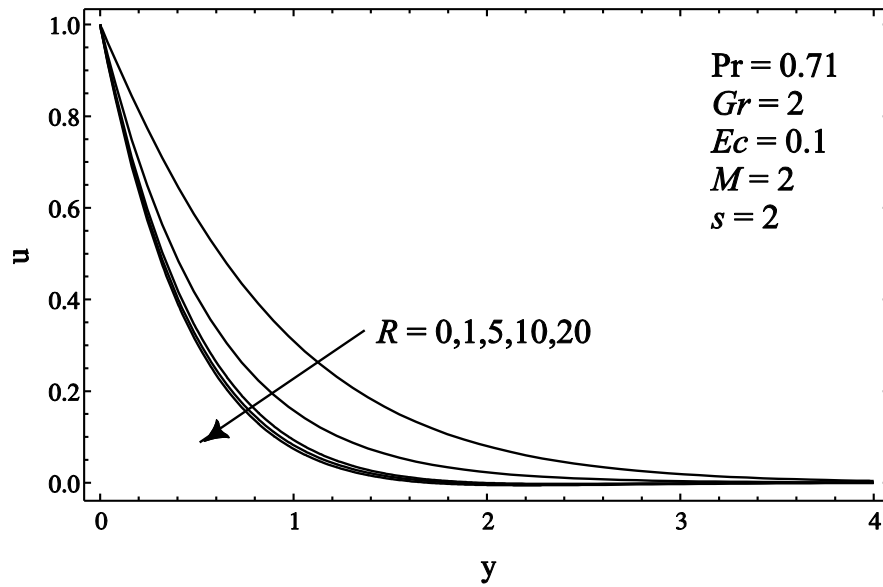


Figure 3.15: Influence of  $R$  on velocity profiles.

The influence of suction parameter on velocity and temperature fields is plotted in Figures 3.17 and 3.18. It is noted that fluid velocity decreases as suction parameter increases. Similar type of behavior is observed for thermal boundary layer variation with suction parameter from Figure 3.18. Also, it has been observed that thermal boundary layer thickness decreases rapidly by increasing the suction velocity of the vertical moving porous plate.

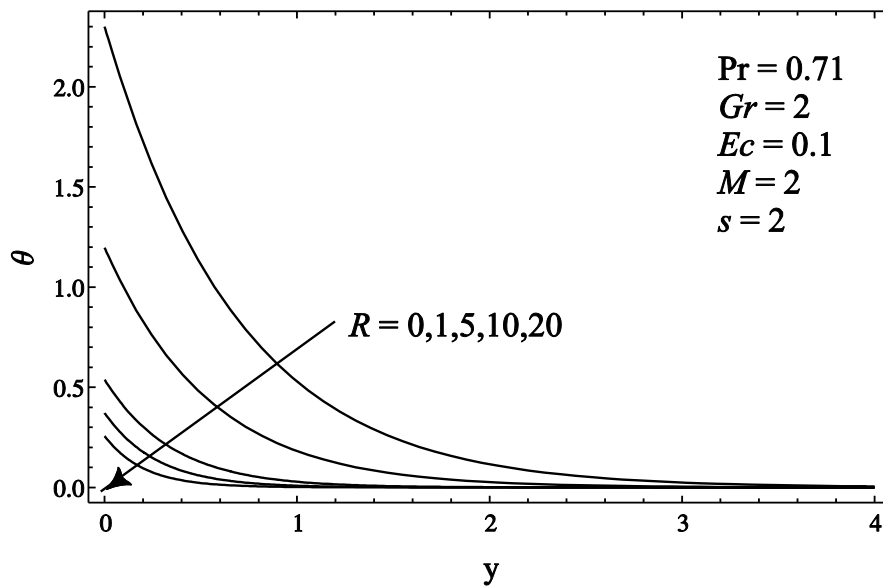


Figure 3.16: Influence of  $R$  on temperature profiles.

The effect of Eckert number on fluid temperature can be seen in Figure 3.19. This Figure shows that temperature profile increases with an increase in Eckert number. This is may be due to energy generated by work done against the viscous fluid stresses. Greater viscous dissipative heat causes a rise in the temperature of the moving fluid.

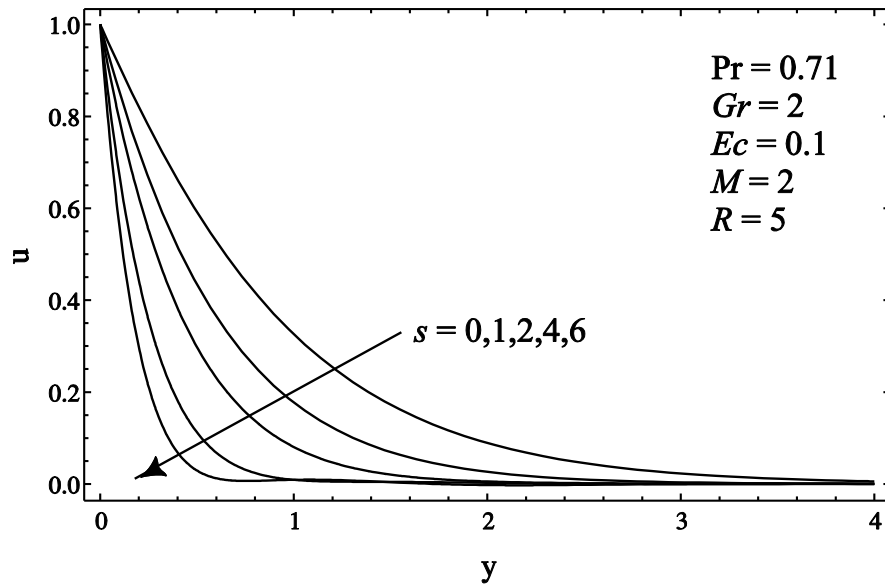


Figure 3.17: Influence of  $s$  on velocity profiles.

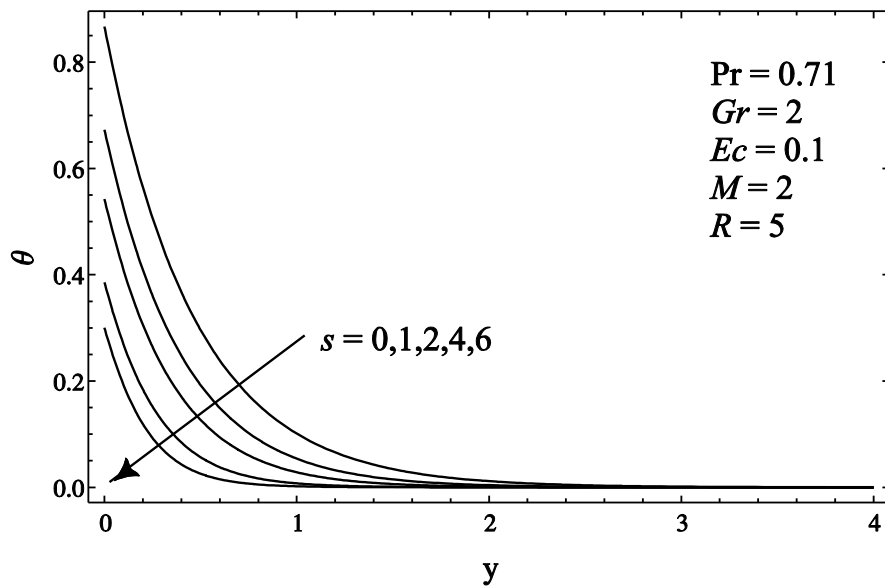


Figure 3.18: Influence of  $s$  on temperature profiles.



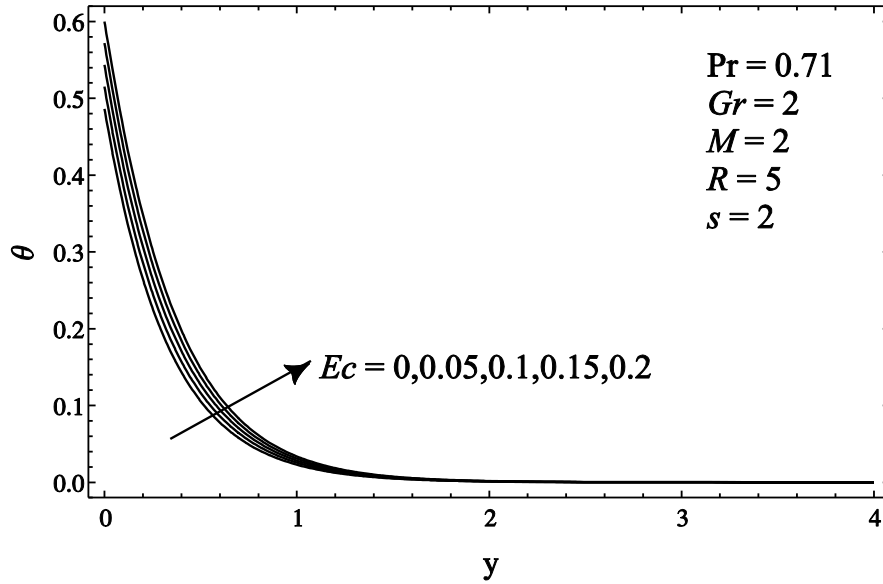


Figure 3.19: Influence of  $Ec$  on temperature profiles.

The influence of Eckert number and thermal Grashof number on velocity and temperature fields is presented in Table 3.1 and Table 3.2, respectively. In Table 3.1 it can be observed that the fluid velocity increases gradually by increasing Eckert number. This is may be due to increase in average translation kinetic energy of the fluid particles. The influence of thermal Grashof number on temperature profile is presented in Table 3.2. It is noticed that the fluid temperature increases near the porous plate by increasing thermal Grashof number. However, as distance ( $y$ ) increases from the plate; the fluid temperature decreases to zero.

The variation of skin friction and Nusselt number at the vertical porous plate is calculated and presented in Table 3.3. It is observed that the skin friction increases by increasing Prandtl number, suction velocity of the porous plate, magnetic field parameter and radiation parameter while skin friction decreases with thermal Grashof number and Eckert number. From Table 3.3 it is also found that the Nusselt number increases with increasing Prandtl number, thermal Grashof number, radiation parameter and suction velocity whereas it decreases with Eckert number and magnetic field parameter.

Table 3.1: Influence of Eckert number ( $Ec$ ) on fluid velocity

$y \backslash Ec$	0	0.05	0.1	0.15	0.2
0	1	1	1	1	1
0.5	0.288429	0.291298	0.294159	0.297014	0.299863
1	0.07767	0.079227	0.080783	0.082339	0.083896
1.5	0.020443	0.021024	0.021606	0.022188	0.022772
2	0.005700	0.005881	0.006063	0.006244	0.006426
2.5	0.001802	0.001853	0.001905	0.001955	0.002007
3	0.000612	0.000627	0.000641	0.000656	0.000670
3.5	0.000185	0.000189	0.000193	0.000198	0.000203
4	0.000028	0.000031	0.000032	0.000034	0.000036

Table 3.2: Influence of thermal Grashof number ( $Gr$ ) on fluid temperature

$y \backslash Gr$	0.2	2	6	10	15
0	0.54771	0.543714	0.536585	0.531793	0.529116
0.5	0.127486	0.1269	0.126207	0.12635	0.127762
1	0.028227	0.028273	0.028596	0.029236	0.030529
1.5	0.006161	0.006189	0.006318	0.006545	0.006984
2	0.001343	0.001351	0.001384	0.001442	0.001554
2.5	0.000292	0.000294	0.000302	0.000316	0.000342
3	0.000063	0.000064	0.000065	0.000069	0.000075
3.5	0.000013	0.000013	0.000014	0.000014	0.000016
4	2.959E-6	2.973E-6	3.043E-6	3.172E-6	3.434E-6

Table 3.3: Skin Friction ( $\tau$ ) and Nusselt number ( $Nu$ ) variation

Pr	$Gr$	$Ec$	$s$	$M$	$R$	$\tau$	$Nu$
0.3	2	0.1	2	2	5	2.187823	2.408550
0.71	2	0.1	2	2	5	2.318805	2.843596
1	2	0.1	2	2	5	2.380207	3.184474
3	2	0.1	2	2	5	2.432189	6.043606
7	2	0.1	2	2	5	2.445486	12.70957
0.71	0.2	0.1	2	2	5	2.616490	2.825782
0.71	6	0.1	2	2	5	1.803467	2.863637
0.71	10	0.1	2	2	5	1.246268	2.880430
0.71	15	0.1	2	2	5	0.539239	2.889943
0.71	2	0	2	2	5	2.399372	3.055982
0.71	2	0.05	2	2	5	2.380807	2.941027
0.71	2	0.1	2	2	5	2.362325	2.839202
0.71	2	0.15	2	2	5	2.343924	2.748379
0.71	2	0.2	2	2	5	2.325601	2.666867
0.71	2	0.1	0	2	5	0.938857	2.153464
0.71	2	0.1	1	2	5	1.588374	2.486149
0.71	2	0.1	4	2	5	3.918558	3.591152
0.71	2	0.1	6	2	5	5.602275	4.331709
0.71	2	0.1	2	0	5	1.635060	2.940836
0.71	2	0.1	2	5	5	2.998375	2.748319
0.71	2	0.1	2	10	5	3.439559	2.665627
0.71	2	0.1	2	2	0	0.997461	1.434802
0.71	2	0.1	2	2	1	1.747897	1.835384
0.71	2	0.1	2	2	5	2.052392	2.859875
0.71	2	0.1	2	2	10	2.148354	3.693427
0.71	2	0.1	2	2	20	2.215011	4.904925

### 3.6 Chapter Summary

This chapter highlights the thermal radiation and viscous dissipation effects on free convection boundary layer flow past an impulsively started infinite vertical porous plate with Newtonian heating in the presence of transverse magnetic field. Homotopy Analysis Method is used to solve a system of coupled non-linear ordinary differential equations. The present results are compared with the exact analytical solution results in the absence of viscous dissipation and an excellent agreement is found between them. The study revealed that the fluid velocity decreases by increasing magnetic field and thermal radiation parameter whereas it increases with increasing Eckert number. On the other hand, a rise in the thermal boundary layer thickness causes due to increase in the magnetic field parameter and Eckert number however, it decreases with increasing radiation parameter. Moreover, the skin friction increases by increasing magnetic field and radiation parameter while it decreases with an increase in the Eckert number, and the Nusselt number increases with increasing radiation parameter whereas it decreases with an increase in the Eckert number and magnetic field parameter.

## CHAPTER 4

### SORET AND DUFOUR EFFECTS IN THE PRESENCE OF THERMAL RADIATION, VISCOUS DISSIPATION AND CHEMICAL REACTION

#### 4.1 Introduction

The study of boundary layer flow in heat and mass transfer problems has attracted considerable attention of researchers during last few decades due to its numerous applications in nature and technology. Magneto hydrodynamics (MHD) viscous flows are important in astrophysics, geophysics such as high temperature plasma, radiation propagation through ionosphere, aeronautics, missile aerodynamics, magneto hydrodynamics pumps and generators. Effects of magnetic field in free convection flow play an important role in ionized fluids, chemical reactions, etc. In engineering, heat and mass transfer through porous surfaces has many applications such as oil extraction, fossil fuels, distillation and drying of solid particles from the mixture.

When heat and mass transfer takes place simultaneously in a moving fluid, the relations between fluxes and driving potentials are more complex in nature. An energy flux generated by composition gradient is termed the Dufour or diffusion-thermo effect. On the other hand, mass flux generated by temperature gradient is termed the Soret or thermal-diffusion effect. Generally, Soret and Dufour effects in heat and mass transfer process are neglected due to smaller order of magnitude than the effects described by Fourier's and Fick's laws. However, when the density difference occurs Soret and Dufour effects play an important role in the flow regimes. These effects are considered as second order phenomena and may become important in the engineering areas such as nuclear waste disposal, hydrology and geothermal energy. Due to the significance of

Soret and Dufour effects for the fluids many researchers have been studied and reported results for such type of flows. Postelnicu [38] investigated the Soret and Dufour effects on free convection heat and mass transfer flow past a vertical surface in porous medium in the presence of chemical reaction using finite difference technique. Thermophoresis particle deposition in free convection flow over a vertical plate embedded in a saturated non-Darcy porous medium under the influence of Soret and Dufour effects was analyzed by Partha [41] using similarity solution technique. He found that increasing concentration distribution Soret effect has significant influence not only in aiding, but also in opposing buoyancies. Mahdy [44] presented a study of non-similar boundary layer non-Darcian mixed convection heat and mass transfer flow of a non-Newtonian fluid past a vertical isothermal plate embedded in a porous medium with the Soret and Dufour effects using Newton-Raphson shooting technique. Kumar and Murthy [45] analyzed the Soret and Dufour effects on heat and mass transfer double-diffusive free convection boundary layer flow past a corrugated vertical surface embedded in a non-Darcy porous medium using finite difference scheme. A numerical study of Soret and Dufour effects on the combined laminar free convection flow of non-Newtonian fluids along a vertical plate embedded in a porous medium with thermal radiations was studied by Tai and Char [46]. Using Runge Kutta Gill integration scheme with shooting technique, Kandasamy et al. [49] examined the Soret and Dufour effects with thermophoresis and chemical reaction on free convection heat and mass transfer flow past a porous stretching surface in the presence of heat source and sink. Arasu et al. [50] studied the lie group analysis for Soret and Dufour effects on free convection heat and mass transfer flow over a vertical porous stretching surface with time depended fluid viscosity embedded in a porous medium in the presence of thermophoresis particle deposition. Cheng [51] investigated, making use of the cubic spline collocation method, the Soret and Dufour effects on the free convection boundary layer flow past a vertical plate embedded in a porous medium saturated with a non-Newtonian power law fluid. Makinde and Olanrewaju [53] employed a shooting iteration technique with the forth order Runge-Kutta integration scheme to examine the Soret and Dufour effects on unsteady mixed convection flow over a vertical porous flat plate moving through a binary mixture of chemically reacting radiative fluid.

The study of heat and mass transfer with magnetohydrodynamic viscous flows through porous medium has been made a fundamental importance due to its applications in many devices, like the MHD power generators, MHD heat exchangers and cooling of the nuclear reactors. Raptis and Soundalgekar [79] investigated the MHD free convection flow past a steadily moving infinite vertical porous plate with constant heat flux and constant suction. Raptis et al. [80] examined the free convection flow of an electrically conducting viscous incompressible rarefied gas past an infinite vertical porous plate in the presence of transvers magnetic field. Mansour et al. [39] studied the effects of chemical reaction and thermal stratification on MHD free convection heat and mass transfer flow over a vertical stretching surface embedded in a porous medium in the presence of Soret and Dufour effects by shooting method. Chamkha and Nakhi [40] reported the MHD mixed convection radiation interaction along a permeable surface immersed in a porous medium in the presence of Soret and Dufour effects. A numerical study of free convection MHD heat and mass transfer flow past a stretching surface embedded in a saturated porous medium with Soret and Dufour effects was studied by Beg et al. [42]. Vempati and Gari [47] used the finite element method to investigate the Soret and Dufour effects on unsteady MHD flow past an infinite vertical porous plate with thermal radiation and oscillatory suction velocity. For electrically conducting fluid, a free convective chemically reacting MHD boundary layer heat and mass transfer flow along a vertical plate in the presence of suction and injection with Soret and Dufour effects was reported by Olanrewaju and Makinde [53]. Prasad et al. [52] carried out an implicit numerical study of Soret and Dufour effects on MHD free convection heat and mass transfer flow past a vertical porous plate embedded in a non-Darcian porous medium in the presence of uniform magnetic field. A numerical study of Soret and Dufour effects on unsteady MHD free convective flow of an electrically conducting fluid over a vertical plate embedded in a non-Darcy porous medium was studied by Odat and Ghamdi [54]. They employed an implicit finite difference scheme of a Crank Nicolson type and found that the skin friction and Sherwood number decreases either by increasing Dufour number or by decreasing Soret number. Prakash et al. [57] accounted for the Dufour and radiation effects on unsteady MHD free convection flow past an impulsively started an infinite vertical plate embedded in a porous medium with variable temperature and uniform mass diffusion

in the presence of transverse magnetic field, employing the Laplace transform method. Turkyilmazoglu [60] carried out an analytical and numerical study of Soret and Dufour effects on MHD mixed convection flow of an electrically conducting, viscoelastic fluid over a stretching vertical porous surface embedded in a porous medium in the presence of uniform magnetic field. However, Soret and Dufour effects on MHD natural convection flow along an infinite vertical porous plate with Newtonian heating in the presence of thermal radiation and chemical reaction have not been addressed in the literature. Hence the motivation.

## 4.2 Problem Description

In this chapter, we analyze the Soret and Dufour effects on the heat and mass transfer MHD flow past an impulsively started infinite vertical porous plate with Newtonian heating in the presence of thermal radiation, viscous dissipation and first order chemical reaction. Viscous dissipation effects are adopted in the energy equation. Here we consider the steady state free convection magneto hydro-dynamic (MHD) boundary layer flow of a viscous, incompressible and electrically conducting fluid past an impulsively started infinite vertical porous plate with Newtonian heating. The  $x'$ -axis is taken along the porous plate in the upward direction and  $y'$ -axis is perpendicular to the plate as shown in Figure 4.1. A uniform magnetic field of strength  $B_0$  is applied normal to the plate in the  $y'$ -axis direction. A first order homogenous chemical reaction is also considered with constant rate  $k_c$  between the diffusing species and the fluid. Under the usual Boussinesq approximation [76], [77], [81]; the governing equations for the balances of mass, energy, momentum and concentration species can be written as follows:

$$\frac{\partial v'}{\partial y'} = 0 \quad (4.1)$$

$$v' \frac{\partial u'}{\partial y'} = \nu \frac{\partial^2 u'}{\partial y'^2} + g\beta(T' - T'_\infty) + g\beta^*(C' - C'_\infty) - \frac{\sigma B_0^2}{\rho} u' \quad (4.2)$$



$$v' \frac{\partial T'}{\partial y'} = \frac{k}{\rho c_p} \frac{\partial^2 T'}{\partial y'^2} - \frac{1}{\rho c_p} \frac{\partial q_r}{\partial y'} + \frac{\mu}{\rho c_p} \left( \frac{\partial u'}{\partial y'} \right)^2 + \frac{\sigma B_0^2}{\rho c_p} u'^2 + \frac{D_m k_T}{c_s c_p} \frac{\partial^2 C'}{\partial y'^2} \quad (4.3)$$

$$v' \frac{\partial C'}{\partial y'} = D_m \frac{\partial^2 C'}{\partial y'^2} - k_c (C' - C'_\infty) + \frac{D_m k_T}{T_m} \frac{\partial^2 T'}{\partial y'^2} \quad (4.4)$$

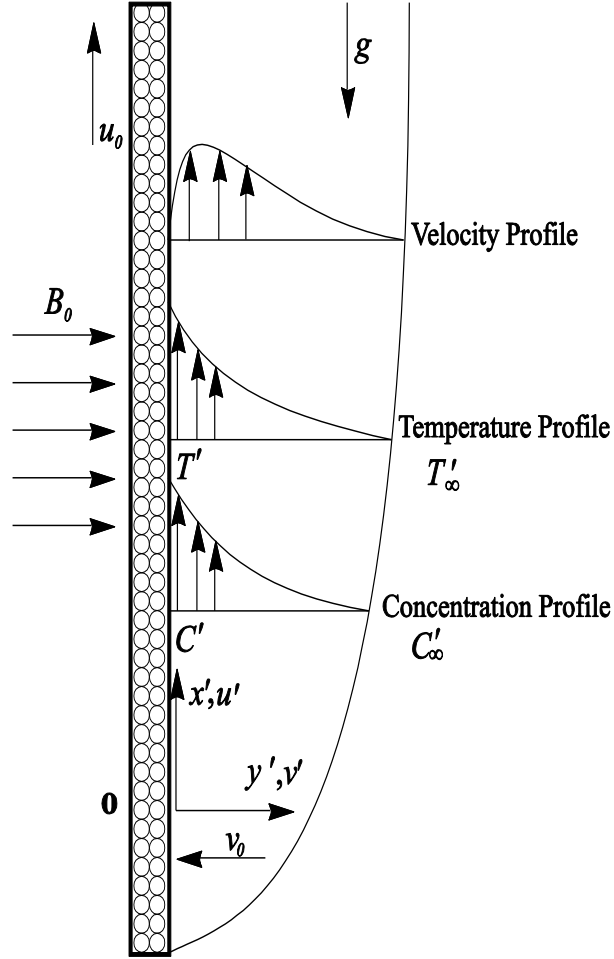


Figure 4.1: Physical Model

The appropriate boundary conditions can be written as

$$\left. \begin{aligned} u' &= u_0, \quad \frac{\partial T'}{\partial y'} = -\frac{h}{k} T', \quad C' = C'_w, \quad \text{at } y' = 0, \\ u' &\rightarrow 0, \quad T' \rightarrow T'_\infty, \quad C' \rightarrow C'_\infty, \quad \text{as } y' \rightarrow \infty. \end{aligned} \right\} \quad (4.5)$$

where  $x'$  and  $y'$  are the coordinate axis along and normal to the vertical porous plate, respectively.  $v'$  is the suction velocity of porous plate and  $u'$  is the component of fluid velocity.  $\nu$ ,  $g$ ,  $\sigma$  and  $\rho$  are the kinematic viscosity, acceleration due to gravity, electrical conductivity and fluid density, respectively.  $T'$  is the temperature of the fluid near the plate,  $T'_\infty$  is the free stream temperature,  $C'$  is the dimensional concentration and  $C'_\infty$  is the free stream dimensional concentration.  $c_p$ ,  $c_s$ ,  $\mu$ ,  $k$  and  $h$  are the specific heat at constant pressure, concentration susceptibility, viscosity, thermal conductivity of the porous plate and convective heat transfer coefficient, respectively.  $\beta$  and  $\beta^*$  are the thermal and concentration expansion coefficients, respectively.  $D_m$ ,  $T_m$ ,  $q_r$ ,  $k_T$  and  $k_c$  are the mass diffusivity, mean fluid temperature, radiative heat flux, thermal diffusion ratio and rate of chemical reaction, respectively.

Integrating equation (4.1) for constant suction, we get

$$v' = -v_0 \quad (4.6)$$

where  $v_0 > 0$  is the normal velocity of suction at the plate.

Equations (4.2) to (4.4) can now be written as

$$-v_0 \frac{\partial u'}{\partial y'} = \nu \frac{\partial^2 u'}{\partial y'^2} + g\beta(T' - T'_\infty) + g\beta^*(C' - C'_\infty) - \frac{\sigma B_0^2}{\rho} u' \quad (4.7)$$

$$-v_0 \frac{\partial T'}{\partial y'} = \frac{k}{\rho c_p} \frac{\partial^2 T'}{\partial y'^2} - \frac{1}{\rho c_p} \frac{\partial q_r}{\partial y'} + \frac{\mu}{\rho c_p} \left( \frac{\partial u'}{\partial y'} \right)^2 + \frac{\sigma B_0^2}{\rho c_p} u'^2 + \frac{D_m k_T}{c_s c_p} \frac{\partial^2 C'}{\partial y'^2} \quad (4.8)$$

$$-v_0 \frac{\partial C'}{\partial y'} = D_m \frac{\partial^2 C'}{\partial y'^2} - k_c (C' - C'_\infty) + \frac{D_m k_T}{T_m} \frac{\partial^2 T'}{\partial y'^2} \quad (4.9)$$

For an optically thin gray gas, absorbing/emitting radiation but a non-scattering medium, the radiation heat flux  $q_r$  in equation (4.8) satisfies the following non-linear differential equation:

$$\frac{\partial q_r}{\partial y'} = 4\alpha\sigma^*(T'^4 - T_\infty'^4) \quad (4.10)$$

where  $\alpha$  is radiation absorption coefficient and  $\sigma^*$  is the Stefan-Boltzmann constant.

It is assumed that the difference between fluid temperature  $T'$  and free stream temperature  $T_\infty'$  is sufficiently small such that  $T'^4$  can be expressed as a linear function of  $T'$  using the Taylor series expression, after neglecting higher-order terms, we get

$$T'^4 \cong 4T_\infty'^3 T' - 3T_\infty'^4 \quad (4.11)$$

In the view of equations (4.10) and (4.11), equation (4.8) yield

$$-v_0 \frac{\partial T'}{\partial y'} = \frac{k}{\rho c_p} \frac{\partial^2 T'}{\partial y'^2} - \frac{16\alpha\sigma^* T_\infty'^3}{\rho c_p} (T' - T_\infty') + \frac{\mu}{\rho c_p} \left( \frac{\partial u'}{\partial y'} \right)^2 + \frac{\sigma B_0^2}{\rho c_p} u'^2 + \frac{D_m k_T}{c_s c_p} \frac{\partial^2 C'}{\partial y'^2} \quad (4.12)$$

Introducing the following non-dimensional quantities:

$$\left. \begin{aligned} y &= \frac{y'h}{k}, \quad u = \frac{u'}{u_0}, \quad \theta = \frac{T' - T_\infty'}{T_\infty'}, \quad C = \frac{C' - C_\infty'}{C_w' - C_\infty'}, \quad \gamma = \frac{k_c k^2}{v h^2}, \\ s &= \frac{v_0 k}{h v}, \quad Gr = \frac{g \beta T_\infty' k^2}{v u_0 h^2}, \quad Gm = \frac{g \beta^* (C_w' - C_\infty') k^2}{v u_0 h^2}, \\ M &= \frac{\sigma B_0^2 k^2}{\mu h^2}, \quad Pr = \frac{\mu c_p}{k}, \quad R = \frac{16\alpha\sigma^* k T_\infty'^3}{h^2}, \quad Ec = \frac{\mu u_0^2}{k T_\infty'}, \\ Sc &= \frac{v}{D_m}, \quad Du = \frac{D_m k_T (C_w' - C_\infty')}{v c_s c_p T_\infty'}, \quad Sr = \frac{D_m k_T T_\infty'}{v T_m (C_w' - C_\infty')}. \end{aligned} \right\} \quad (4.13)$$

where  $u$ ,  $\theta$  and  $C$  are the dimensionless velocity, temperature and concentration respectively,  $s$  is the suction parameter,  $M$  is the magnetic field parameter, i.e., square of the Hartmann number,  $Gr$  is the thermal Grashof number,  $Gm$  is the mass Grashof number,  $Pr$  is the Prandtl number,  $Ec$  is the Eckert number,  $Sc$  is the Schmidt number,  $Du$  is the Dufour number,  $Sr$  is the Soret number,  $\gamma$  is the chemical reaction parameter and  $R$  is the radiation parameter.

In the view of equations (4.13) equations (4.7), (4.12) and (4.9) reduces to the following non-dimensional forms, respectively, as

$$\frac{d^2 u}{dy^2} + s \frac{du}{dy} + Gr \theta + Gm C - M u = 0 \quad (4.14)$$

$$\frac{d^2 \theta}{dy^2} + Pr s \frac{d\theta}{dy} - R \theta + Ec \left( \frac{du}{dy} \right)^2 + Ec M u^2 + Pr D u \frac{d^2 C}{dy^2} = 0 \quad (4.15)$$

$$\frac{d^2 C}{dy^2} + s Sc \frac{dC}{dy} - \gamma C + Sr Sc \frac{d^2 \theta}{dy^2} = 0 \quad (4.16)$$

The corresponding boundary conditions are

$$\left. \begin{aligned} u = 1, \quad \frac{d\theta}{dy} = -(\theta + 1), \quad C = 1, \quad \text{at } y = 0, \\ u \rightarrow 0, \quad \theta \rightarrow 0, \quad C \rightarrow 0, \quad \text{as } y \rightarrow \infty. \end{aligned} \right\} \quad (4.17)$$

### 4.3 Solution by HAM

Under the rule of solution expression and boundary conditions (4.17), it is easy to choose the initial guesses and auxiliary linear operators for system of equations (4.14), (4.15) and (4.16), respectively, as follows;

$$u_0(y) = e^{-y}, \quad \theta_0(y) = e^{-2y} \quad \text{and} \quad C_0(y) = e^{-y} \quad (4.18)$$

$$\left. \begin{aligned} L_u[\varphi(y; q)] &= \frac{d^2 \varphi(y; q)}{dy^2} + \frac{d\varphi(y; q)}{dy} \\ L_\theta[\psi(y; q)] &= \frac{1}{2} \frac{d^2 \psi(y; q)}{dy^2} + \frac{d\psi(y; q)}{dy} \\ L_C[\zeta(y; q)] &= \frac{d^2 \zeta(y; q)}{dy^2} + \frac{d\zeta(y; q)}{dy} \end{aligned} \right\} \quad (4.19)$$

with the following non-linear operators,

$$N_u[\varphi(y; q), \psi(y; q), \zeta(y; q)] = \frac{d^2 \varphi(y; q)}{dy^2} + s \frac{d\varphi(y; q)}{dy} + Gr\psi(y; q) + Gm\zeta(y; q) - M\varphi(y; q) \quad (4.20)$$

$$N_\theta[\varphi(y; q), \psi(y; q), \zeta(y; q)] = \frac{d^2 \psi(y; q)}{dy^2} + Pr.s \frac{d\psi(y; q)}{dy} - R\psi(y; q) + Ec \left( \frac{d\varphi(y; q)}{dy} \right)^2 + Ec M\varphi^2(y; q) + Pr.Du \frac{d^2 \zeta(y; q)}{dy^2} \quad (4.21)$$

$$N_c[\varphi(y; q), \psi(y; q), \zeta(y; q)] = \frac{d^2 \zeta(y; q)}{dy^2} + s.Sc \frac{d\zeta(y; q)}{dy} - \gamma\zeta(y; q) + Sr.Sc \frac{d^2 \psi(y; q)}{dy^2} \quad (4.22)$$

The generalized homotopies are then defined to be

$$(1-q)L_u[\varphi(y; q) - u_0(y)] = q\hbar_u H_u(y) N_u[\varphi(y; q), \psi(y; q), \zeta(y; q)] \quad (4.23)$$

$$(1-q)L_\theta[\psi(y; q) - \theta_0(y)] = q\hbar_\theta H_\theta(y) N_\theta[\varphi(y; q), \psi(y; q), \zeta(y; q)] \quad (4.24)$$

$$(1-q)L_c[\zeta(y; q) - C_0(y)] = q\hbar_c H_c(y) N_c[\varphi(y; q), \psi(y; q), \zeta(y; q)] \quad (4.25)$$

subject to the boundary conditions

$$\left. \begin{aligned} \phi(0; q) = 1, \quad \psi'(0; q) = -\psi(0; q) - 1, \quad \zeta(0; q) = 1, \\ \phi(\infty; q) \rightarrow 0, \quad \psi(\infty; q) \rightarrow 0, \quad \zeta(\infty; q) = 0. \end{aligned} \right\} \quad (4.26)$$

These generalized homotopies produce the  $n^{\text{th}}$  order deformation equations as

$$\left. \begin{aligned} L_u[u_n(y) - \chi_n u_{n-1}(y)] &= \hbar_u H_u(y) R_n^u(u_{n-1}(y), \theta_{n-1}(y), C_{n-1}(y)) \\ L_\theta[\theta_n(y) - \chi_n \theta_{n-1}(y)] &= \hbar_\theta H_\theta(y) R_n^\theta(u_{n-1}(y), \theta_{n-1}(y), C_{n-1}(y)) \\ L_c[C_n(y) - \chi_n C_{n-1}(y)] &= \hbar_c H_c(y) R_n^C(u_{n-1}(y), \theta_{n-1}(y), C_{n-1}(y)) \end{aligned} \right\} \quad (4.27)$$

subject to the boundary conditions

$$\left. \begin{aligned} u_n(0) = 0, \quad \theta'_n(0) + \theta_n(0) = 0, \quad C_n(0) = 0, \\ u_n(\infty) \rightarrow 0, \quad \theta_n(\infty) \rightarrow 0, \quad C_n(\infty) \rightarrow 0. \end{aligned} \right\} \quad (4.28)$$

where

$$\chi_n = \begin{cases} 0 & n \leq 1 \\ 1 & n > 1, \end{cases}$$

$$R_n^u(u_{n-1}(y), \theta_{n-1}(y), C_{n-1}(y)) = u_{n-1}''(y) + s.u_{n-1}'(y) + Gr.\theta_{n-1}(y) + Gm.C_{n-1}(y) - M.u_{n-1}(y) ,$$

$$R_n^\theta(u_{n-1}(y), \theta_{n-1}(y), C_{n-1}(y)) = \theta_{n-1}''(y) + Pr.s.\theta_{n-1}'(y) - R\theta_{n-1}(y) + Ec.\left[\sum_{j=0}^{n-1} u_j'(y)u_{n-1-j}'(y)\right] + Ec.M.\left[\sum_{j=0}^{n-1} u_j(y)u_{n-1-j}(y)\right] + Pr.Du.C_{n-1}''(y)$$

and

$$R_n^C(u_{n-1}(y), \theta_{n-1}(y), C_{n-1}(y)) = C_{n-1}''(y) + s.Sc.C_{n-1}'(y) - \gamma.C_{n-1}(y) + Sr.Sc.\theta_{n-1}''(y)$$

For simplicity [15], auxiliary functions and auxiliary parameters can be chosen as

$$H_u(y) = H_\theta(y) = H_C(y) = 1 \text{ and } \hbar_u = \hbar_\theta = \hbar_C = \hbar$$

For each  $n$  we can get the required solutions from the  $n^{\text{th}}$  order deformation equations, subject to the boundary conditions (4.28).

Skin friction and Nusselt number formulae are used as mentioned in (2.37) and (2.38), and the mass transfer at the surface of porous plate in terms of the Sherwood number ( $Sh$ ) is defined as

$$Sh = -\frac{\nu}{u_0(C_w' - C_\infty')} \frac{dC'}{dy'} \Big|_{y=0} = -\frac{\partial C}{\partial y} \Big|_{y=0} \quad (4.29)$$

#### 4.4 Exact Analytical Solution

In the absence of viscous dissipation and Dufour effect, i.e.,  $Ec = Du = 0$  the system of equations (4.14), (4.15) and (4.16) subject to the boundary conditions (4.17) can be written as

$$\frac{d^2 u}{dy^2} + s \frac{du}{dy} + Gr\theta + GmC - Mu = 0 \quad (4.30)$$

$$\frac{d^2 \theta}{dy^2} + Pr s \frac{d\theta}{dy} - R\theta = 0 \quad (4.31)$$

$$\frac{d^2 C}{dy^2} + s Sc \frac{dC}{dy} - \gamma C + Sr Sc \frac{d^2 \theta}{dy^2} = 0 \quad (4.32)$$

subject to the Boundary Conditions

$$\left. \begin{aligned} u = 1, \quad \frac{d\theta}{dy} = -(\theta + 1), \quad C = 1, \quad \text{at} \quad y = 0, \\ u \rightarrow 0, \quad \theta \rightarrow 0, \quad C \rightarrow 0, \quad \text{as} \quad y \rightarrow \infty. \end{aligned} \right\} \quad (4.33)$$

Corresponding auxiliary equation for (4.31)

$$(m^2 + Pr s m - R)\theta = 0$$

where  $m = d/dy$

$$m^2 + Pr s m - R = 0$$

$$m = \frac{-Pr s \pm \sqrt{Pr^2 s^2 + 4R}}{2}$$

Let,

$$\begin{aligned} m_1 &= \frac{-Pr s + \sqrt{Pr^2 s^2 + 4R}}{2}, \quad m_2 = \frac{-Pr s - \sqrt{Pr^2 s^2 + 4R}}{2} \quad \text{or} \\ -m_2 &= \left( \frac{Pr s + \sqrt{Pr^2 s^2 + 4R}}{2} \right) \end{aligned}$$

Now, the general solution for equation (4.31) will becomes

$$\theta(y) = a_1 e^{m_1 y} + a_2 e^{-m_2 y} \quad (4.34)$$

$$\theta'(y) = m_1 a_1 e^{m_1 y} - m_2 a_2 e^{-m_2 y}$$

Now applying boundary conditions

$$\theta'(y) = -(\theta(y) + 1) \quad \text{at } y = 0$$

$$m_1 a_1 - m_2 a_2 = -a_1 - a_2 - 1$$

$$(m_1 + 1)a_1 + (1 - m_2)a_2 + 1 = 0$$

as  $y \rightarrow \infty$ , equation (4.34) becomes

$$\theta(\infty) = a_1 e^{m_1(\infty)} + a_2 e^{-m_2(\infty)}$$

Here  $a_1$  must be zero. Therefore,  $a_2 = \frac{-1}{1 - m_2}$  or  $a_2 = \frac{1}{m_2 - 1}$ .

Thus (4.34) becomes as

$$\theta(y) = \frac{1}{m_2 - 1} e^{-m_2 y} \quad (4.35)$$

Now (4.32) can be written as

$$\frac{d^2 C}{dy^2} + s Sc \frac{dC}{dy} - \gamma C + Sr Sc \frac{d^2}{dy^2} \left( \frac{1}{m_2 - 1} e^{-m_2 y} \right) = 0 \quad (4.36)$$

$$\frac{d^2 C}{dy^2} + s Sc \frac{dC}{dy} - \gamma C + Sr Sc \left( \frac{m_2^2}{m_2 - 1} \right) e^{-m_2 y} = 0$$

Its corresponding homogenous auxiliary equation is

$$(m^2 + s Sc m - \gamma) C = 0$$

$$m^2 + s Sc m - \gamma = 0$$



$$m = \frac{-sSc \pm \sqrt{s^2 Sc^2 + 4\gamma}}{2}$$

Let,

$$m_3 = \frac{-sSc + \sqrt{s^2 Sc^2 + 4\gamma}}{2} \quad \text{and} \quad m_4 = \frac{-sSc - \sqrt{s^2 Sc^2 + 4\gamma}}{2} \quad \text{or}$$

$$-m_4 = \left( \frac{sSc + \sqrt{s^2 Sc^2 + 4\gamma}}{2} \right)$$

Complimentary solution of (4.36) will becomes

$$C_c(y) = a_3 e^{m_3 y} + a_4 e^{-m_4 y}$$

Particular solution for (4.36) will be

$$(m^2 + sScm - \gamma)C_p(y) = SrSc \left( \frac{m_2^2}{1 - m_2} \right) e^{-m_2 y}$$

$$C_p(y) = \left( \frac{SrScm_2^2}{1 - m_2} \right) \left( \frac{1}{m^2 + sScm - \gamma} \right) e^{-m_2 y}$$

$$C_p(y) = \frac{SrScm_2^2 e^{-m_2 y}}{(1 - m_2)(m_2^2 - sScm_2 - \gamma)}$$

Now,

$$C(y) = C_c(y) + C_p(y)$$

$$u(y) = a_3 e^{m_3 y} + a_4 e^{-m_4 y} + \frac{SrScm_2^2 e^{-m_2 y}}{(1 - m_2)(m_2^2 - sScm_2 - \gamma)} \quad (4.37)$$

Since  $u \rightarrow 0$  as  $y \rightarrow \infty$ , therefore,  $a_3 = 0$ . Also,  $u = 1$  at  $y = 0$ , we have

$$a_4 = 1 - \frac{SrScm_2^2}{(1 - m_2)(m_2^2 - sScm_2 - \gamma)}$$

Thus (4.37) will becomes

$$C(y) = \left[ 1 - \frac{Sr Sc m_2^2}{(1-m_2)(m_2^2 - s Sc m_2 - \gamma)} \right] e^{-m_4 y} + \frac{Sr Sc m_2^2 e^{-m_2 y}}{(1-m_2)(m_2^2 - s Sc m_2 - \gamma)}$$

$$C(y) = e^{-m_4 y} + \frac{Sr Sc m_2^2 (e^{-m_2 y} - e^{-m_4 y})}{(1-m_2)(m_2^2 - s Sc m_2 - \gamma)} \quad (4.38)$$

Now, equation (4.30) can be written as

$$\frac{d^2 u}{dy^2} + s \frac{du}{dy} + Gr \left( \frac{1}{m_2 - 1} e^{-m_2 y} \right) + Gm \left( e^{-m_4 y} + \frac{Sr Sc m_2^2 (e^{-m_2 y} - e^{-m_4 y})}{(1-m_2)(m_2^2 - s Sc m_2 - \gamma)} \right) - Mu = 0$$

$$\frac{d^2 u}{dy^2} + s \frac{du}{dy} - Mu = Gr \left( \frac{1}{1-m_2} e^{-m_2 y} \right) - Gm \left( e^{-m_4 y} + \frac{Sr Sc m_2^2 (e^{-m_2 y} - e^{-m_4 y})}{(1-m_2)(m_2^2 - s Sc m_2 - \gamma)} \right) \quad (4.39)$$

Corresponding homogenous equation of (4.39) will be,

$$(m^2 + s m - M)u = 0$$

$$m^2 + s m - M = 0$$

$$m = \frac{-s \pm \sqrt{s^2 + 4M}}{2}$$

Let,

$$m_5 = \frac{-s + \sqrt{s^2 + 4M}}{2} \quad \text{and} \quad m_6 = \frac{-s - \sqrt{s^2 + 4M}}{2} \quad \text{or} \quad -m_6 = \left( \frac{s + \sqrt{s^2 + 4M}}{2} \right)$$

Complimentary solution of (4.39) will becomes

$$u_c(y) = a_5 e^{m_5 y} + a_6 e^{-m_6 y}$$

Particular solution for (4.39) will be

$$(m^2 + s m - M)u_p(y) = Gr \left( \frac{1}{1 - m_2} e^{-m_2 y} \right) - Gm \left( e^{-m_4 y} + \frac{Sr Sc m_2^2 (e^{-m_2 y} - e^{-m_4 y})}{(1 - m_2)(m_2^2 - s Sc m_2 - \gamma)} \right)$$

$$u_p(y) = Gr \left( \frac{1}{(1 - m_2)(m^2 + s m - M)} \right) e^{-m_2 y} - Gm \left( \frac{e^{-m_4 y}}{(m^2 + s m - M)} + \frac{Sr Sc m_2^2 (e^{-m_2 y} - e^{-m_4 y})}{(1 - m_2)(m_2^2 - s Sc m_2 - \gamma)(m^2 + s m - M)} \right)$$

$$u_p(y) = \frac{Gr e^{-m_2 y}}{(1 - m_2)(m_2^2 - s m_2 - M)} - \frac{Gm e^{-m_4 y}}{(m_2^2 - s m_2 - M)} - \frac{Gm Sr Sc m_2^2}{(1 - m_2)(m_2^2 - s Sc m_2 - \gamma)} \left( \frac{e^{-m_2 y}}{m_2^2 - s m_2 - M} - \frac{e^{-m_4 y}}{m_4^2 - s m_4 - M} \right)$$

Now,

$$u(y) = u_c(y) + u_p(y)$$

$$u(y) = a_5 e^{m_5 y} + a_6 e^{-m_6 y} + \frac{Gr e^{-m_2 y}}{(1 - m_2)(m_2^2 - s m_2 - M)} - \frac{Gm e^{-m_4 y}}{(m_2^2 - s m_2 - M)} - \frac{Gm Sr Sc m_2^2}{(1 - m_2)(m_2^2 - s Sc m_2 - \gamma)} \left( \frac{e^{-m_2 y}}{m_2^2 - s m_2 - M} - \frac{e^{-m_4 y}}{m_4^2 - s m_4 - M} \right)$$

Now applying boundary conditions. Since  $u \rightarrow 0$  as  $y \rightarrow \infty$ , therefore  $a_5 = 0$  and  $u = 1$  at  $y = 0$ , so we have

$$a_6 = 1 - \frac{Gr}{(1 - m_2)(m_2^2 - s m_2 - M)} + \frac{Gm}{(m_2^2 - s m_2 - M)} + \frac{Gm Sr Sc m_2^2}{(1 - m_2)(m_2^2 - s Sc m_2 - \gamma)} \left( \frac{1}{m_2^2 - s m_2 - M} - \frac{1}{m_4^2 - s m_4 - M} \right)$$

Thus,

$$\begin{aligned}
u(y) = & \left[ 1 - \frac{Gr}{(1-m_2)(m_2^2 - s m_2 - M)} + \frac{Gm}{(m_2^2 - s m_2 - M)} + \right. \\
& \left. \frac{Gm Sr Sc m_2^2}{(1-m_2)(m_2^2 - s Sc m_2 - \gamma)} \left( \frac{1}{m_2^2 - s m_2 - M} - \frac{1}{m_4^2 - s m_4 - M} \right) \right] e^{-m_6 y} + \\
& \frac{Gr e^{-m_2 y}}{(1-m_2)(m_2^2 - s m_2 - M)} - \frac{Gm e^{-m_4 y}}{(m_2^2 - s m_2 - M)} - \\
& \frac{Gm Sr Sc m_2^2}{(1-m_2)(m_2^2 - s Sc m_2 - \gamma)} \left( \frac{e^{-m_2 y}}{m_2^2 - s m_2 - M} - \frac{e^{-m_4 y}}{m_4^2 - s m_4 - M} \right) \\
u(y) = & \left[ 1 - \frac{Gr}{(1-m_2)(m_2^2 - s m_2 - M)} + \frac{Gm}{(m_2^2 - s m_2 - M)} + \right. \\
& \left. \frac{Gm Sr Sc m_2^2}{(1-m_2)(m_2^2 - s Sc m_2 - \gamma)} \left( \frac{1}{m_2^2 - s m_2 - M} - \frac{1}{m_4^2 - s m_4 - M} \right) \right] e^{-m_6 y} \\
& + \frac{Gr e^{-m_2 y}}{(1-m_2)(m_2^2 - s m_2 - M)} - \frac{Gm e^{-m_4 y}}{(m_2^2 - s m_2 - M)} - \\
& \frac{Gm Sr Sc m_2^2}{(1-m_2)(m_2^2 - s Sc m_2 - \gamma)} \left( \frac{e^{-m_2 y}}{m_2^2 - s m_2 - M} - \frac{e^{-m_4 y}}{m_4^2 - s m_4 - M} \right) \\
u(y) = & e^{-m_6 y} + \frac{Gr(e^{-m_2 y} - e^{-m_6 y})}{(1-m_2)(m_2^2 - s m_2 - M)} + \frac{Gm(e^{-m_6 y} - e^{-m_4 y})}{m_4^2 - s m_4 - M} + \\
& \frac{m_2^2 Gm Sr Sc}{(1-m_2)(m_2^2 - s Sc m_2 - \gamma)} \cdot \left( \frac{(e^{-m_6 y} - e^{-m_2 y})}{m_2^2 - s m_2 - M} + \frac{(e^{-m_4 y} - e^{-m_6 y})}{m_4^2 - s m_4 - M} \right)
\end{aligned} \tag{4.40}$$

Hence, equations (4.35), (4.38) and (4.40) represent the exact analytical solution of system of equations (4.30), (4.31) and (4.32) subject to the boundary conditions (4.33) for the special case.

## 4.5 Result and Discussion

Convergence of series solutions, obtained by HAM, depends upon the auxiliary parameter  $\hbar$ . Liao [15] explained the admissible range for auxiliary parameter is determined by the horizontal portion of so called  $\hbar$  curves. To illustrate this concept,  $\hbar$  curves for velocity, temperature and concentration profiles are plotted at 20<sup>th</sup> order of HAM in Figure 4.2 and their derivatives at  $y = 0$  are plotted in Figure 4.3 for fixed set

of parameters  $Pr = 0.71$ ,  $Gr = 2$ ,  $Ec = 0.1$ ,  $M = 2$ ,  $s = 2$ ,  $R = 5$ ,  $Gm = 1$ ,  $Sc = 0.6$ ,  $\gamma = 1$ ,  $Sr = 0.5$ , and  $Du = 0.2$ . The admissible convergence regions for velocity, temperature and concentration profiles are  $-0.18 \leq \hbar \leq -0.05$ ,  $-0.18 \leq \hbar \leq -0.03$  &  $-0.2 \leq \hbar \leq -0.02$ , respectively.

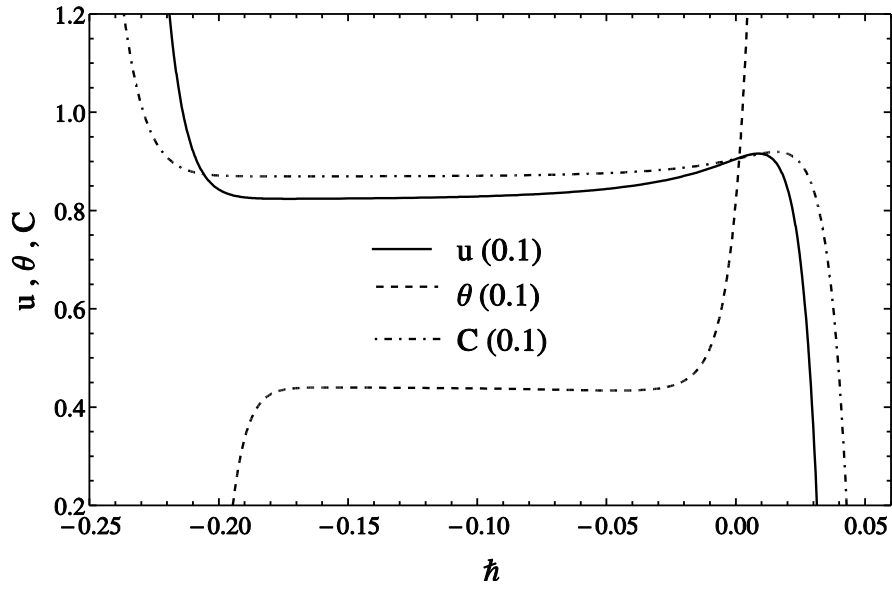


Figure 4.2:  $\hbar$  curves at 20<sup>th</sup> order of HAM

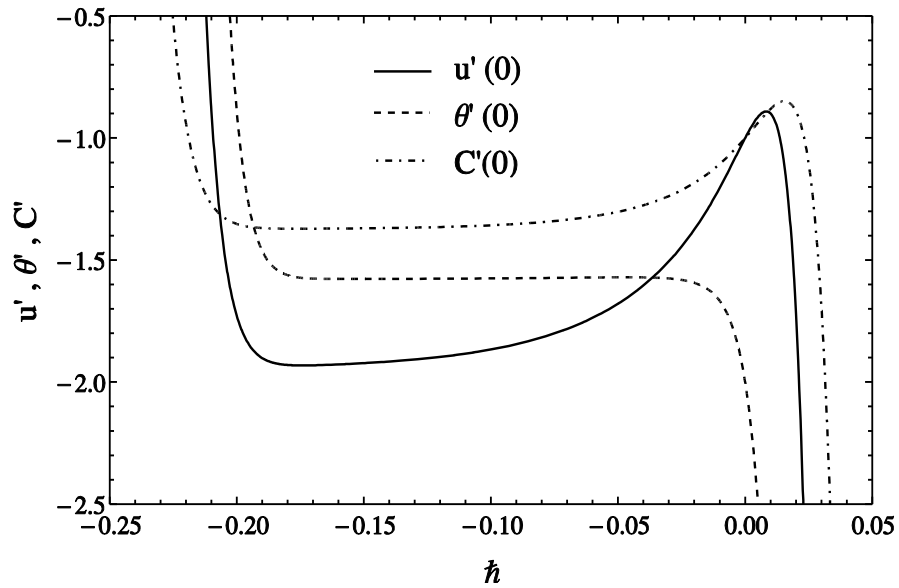


Figure 4.3:  $\hbar$  curves at 20<sup>th</sup> order of HAM

In this study, homotopy solutions of a coupled non-linear system of equations (4.14), (4.15) and (4.16) with boundary condition (4.17) have been compared with the exact analytical solution results in the absence of viscous dissipation and Dufour effects for different values of system parameters. An excellent agreement has been found between HAM and exact analytical results that is presented from Figures 4.4 to 4.14.

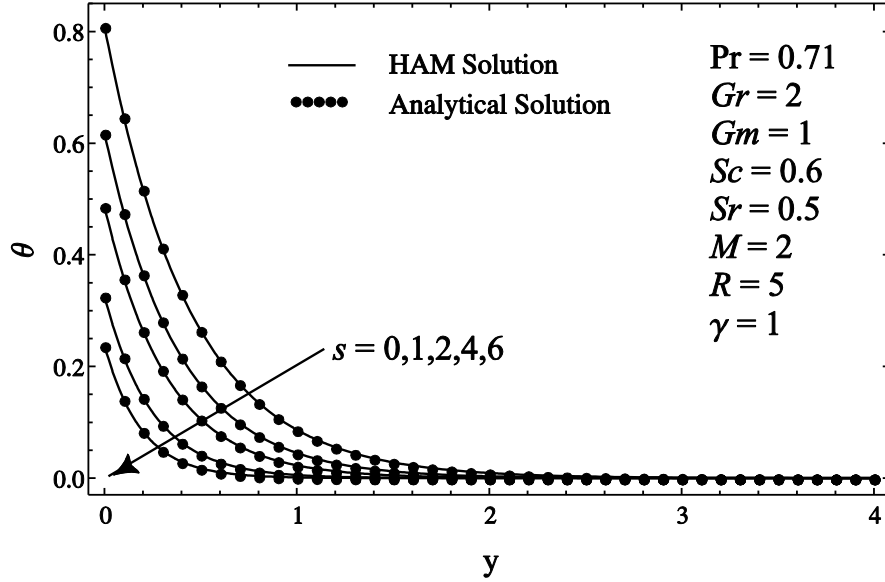


Figure 4.4: Comparison of temperature profiles for HAM and analytical solution at different  $s$  when  $Ec = Du = 0$ .

Figures 4.15 to 4.32 are plotted to understand the effects of flow parameters on the velocity, temperature and concentration profiles. Figure 4.15 has been presented in order to see the suction parameter effects on the dimensionless velocity profile. It can be seen that increasing the suction parameter decreases the velocity of moving fluid near the vertical plate.

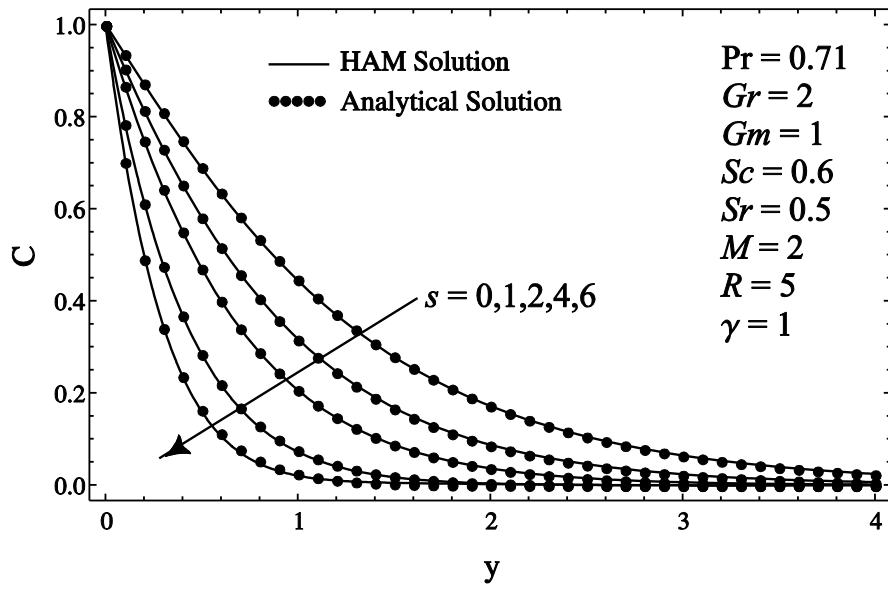


Figure 4.5: Comparison of Concentration profiles for HAM and analytical solution at different  $s$  when  $Ec = Du = 0$ .

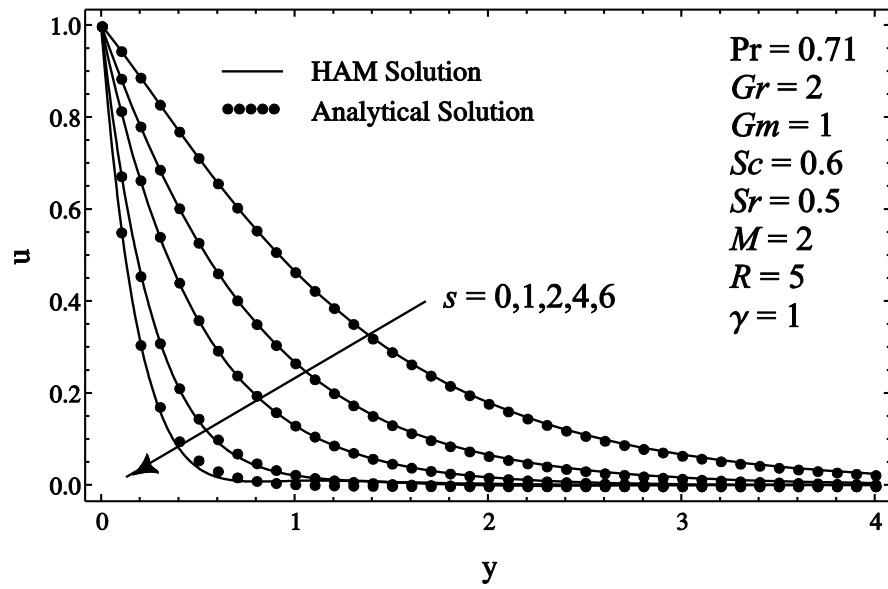


Figure 4.6: Comparison of velocity profiles for HAM and analytical solution at different  $s$  when  $Ec = Du = 0$ .

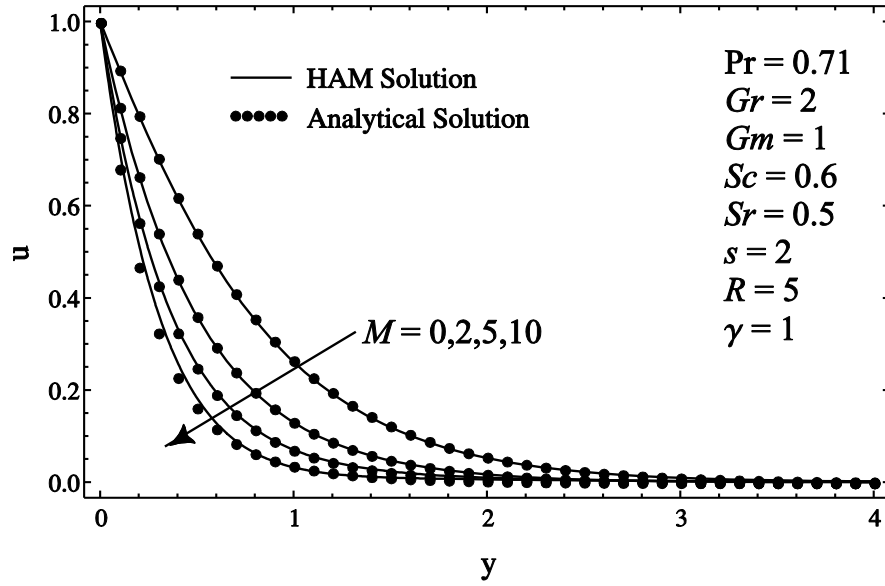


Figure 4.7: Comparison of velocity profiles for HAM and analytical solution at different  $M$  when  $Ec = Du = 0$ .

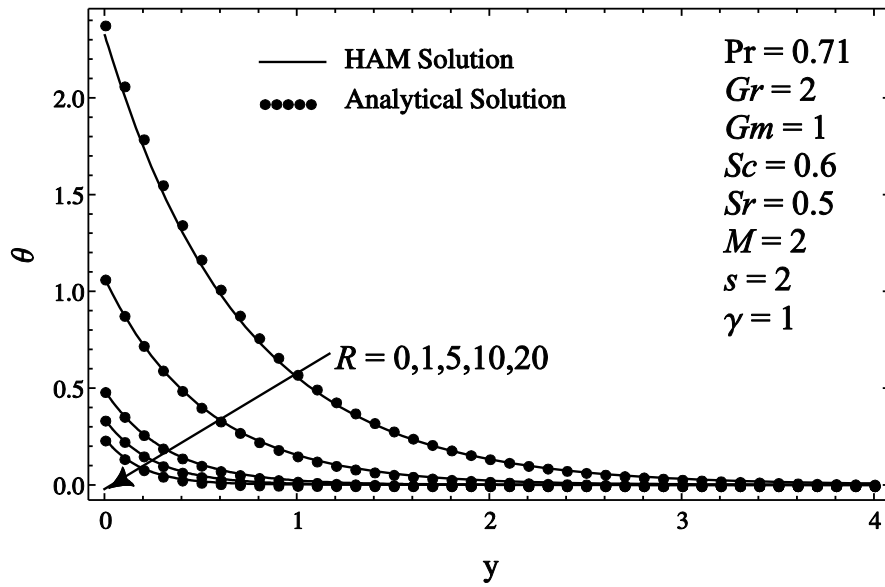


Figure 4.8: Comparison of temperature profiles for HAM and analytical solution at different  $R$  when  $Ec = Du = 0$ .



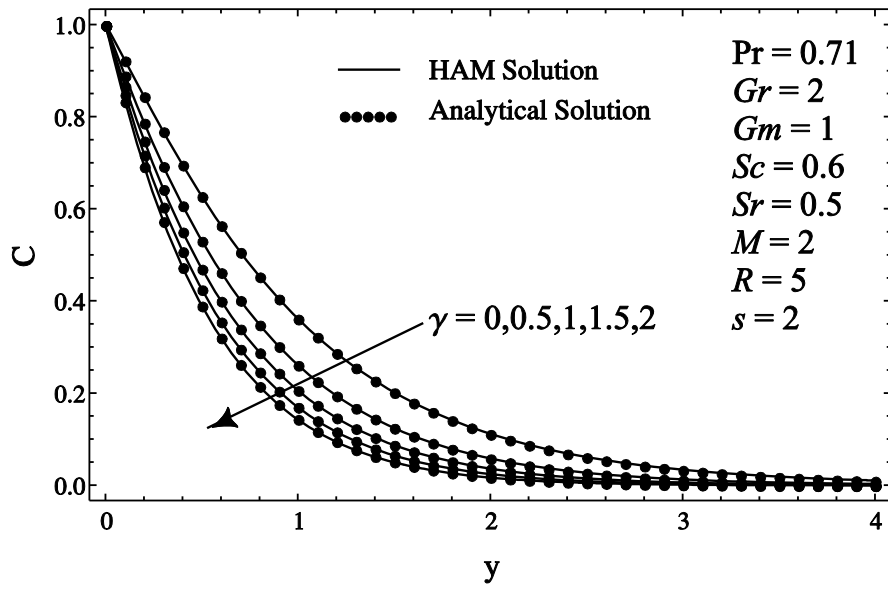


Figure 4.9: Comparison of concentration profiles for HAM and analytical solution at different  $\gamma$  when  $Ec = Du = 0$ .

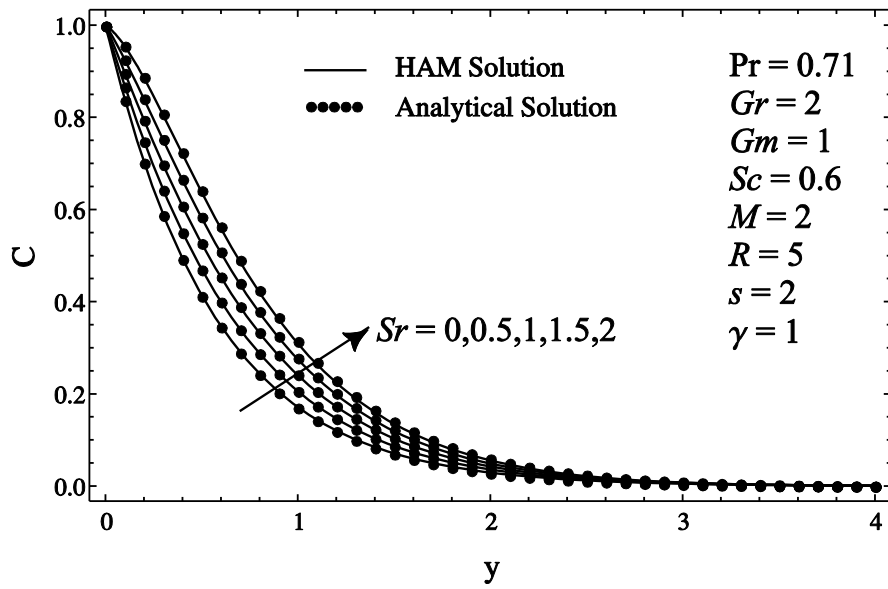


Figure 4.10: Comparison of concentration profiles for HAM and analytical solution at different  $Sr$  when  $Ec = Du = 0$ .

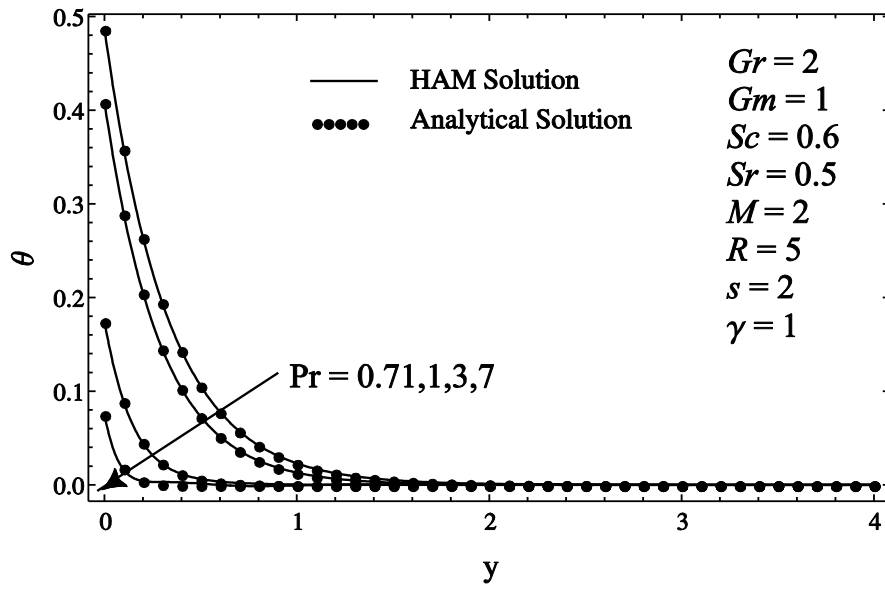


Figure 4.11: Comparison of temperature profiles for HAM and analytical solution at different  $Pr$  when  $Ec = Du = 0$ .

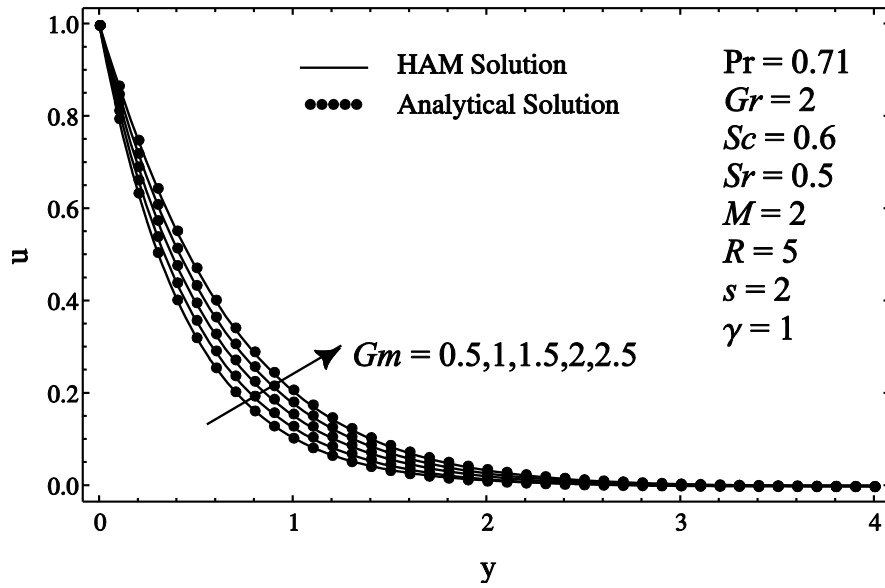


Figure 4.12: Comparison of velocity profiles for HAM and analytical solution at different  $Gm$  when  $Ec = Du = 0$ .

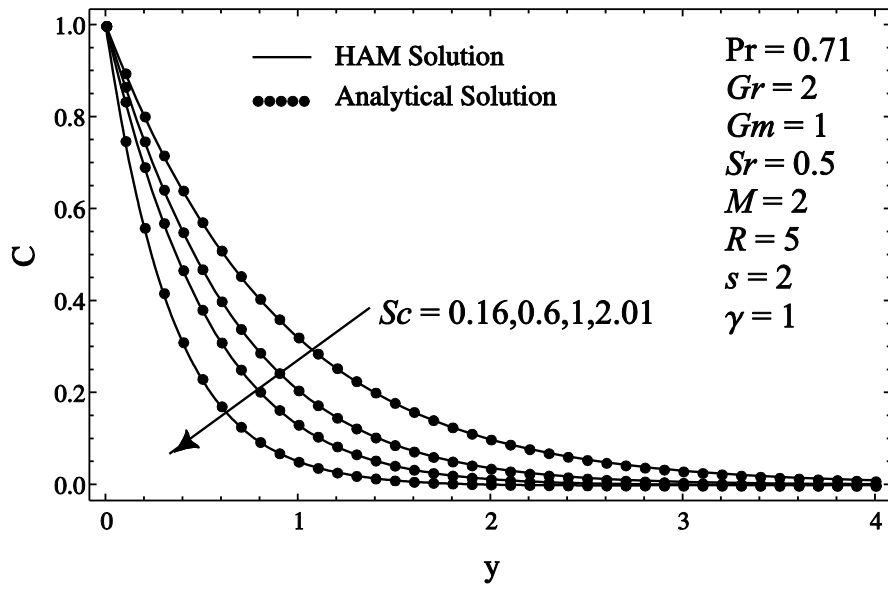


Figure 4.13: Comparison of concentration profiles for HAM and analytical solution at different  $Sc$  when  $Ec = Du = 0$ .

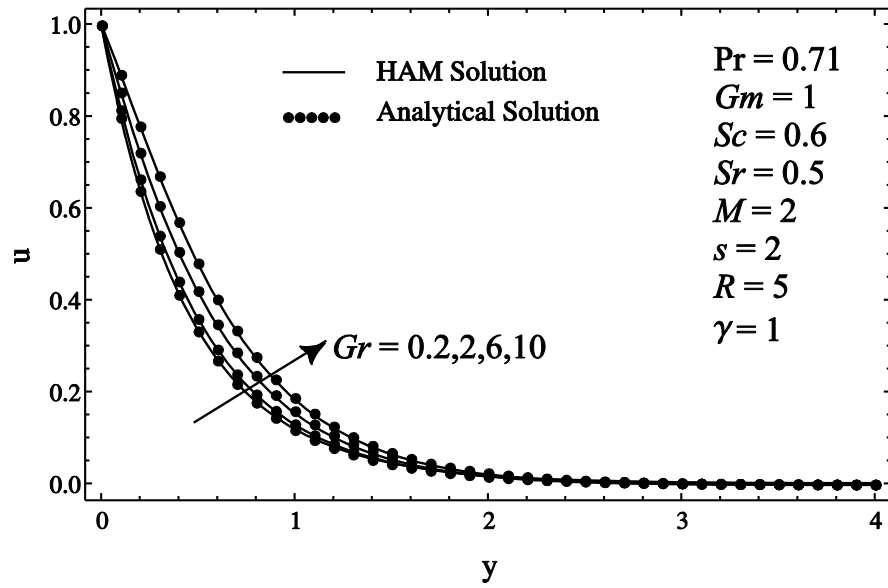


Figure 4.14: Comparison of velocity profiles for HAM and analytical solution at different  $Gr$  when  $Ec = Du = 0$ .

Figure 4.16 and Figure 4.20 depict the Soret and Dufour number effects on the velocity profile. It is interesting to note that the velocity profile increases by increasing Soret and Dufour number. This is may be due to the fact that either a decrease in concentration difference or an increase in temperature difference in the momentum equation. The similar trend is observed in Figure 4.17 for different values of radiation parameter on velocity field. This is because an increased dominance of absorption radiation in the porous plate over convection, thereby increasing the buoyancy force and momentum boundary layer thickness. Figure 4.18 shows the variation of magnetic field parameter on the velocity. As expected, the velocity field decreases when  $M$  increases. This is because the application of transverse magnetic field in an electrically conducting fluid causes to produce the Lorentz force, which resists the fluid flow. Hence, the velocity boundary layer thickness decreases with increasing values of the magnetic field parameter. The behavior of the chemical reaction parameter on velocity profile is shown in the Figure 4.19. By increasing chemical reaction parameter velocity field decreases. Figures 4.21 to 4.22 display the influence of various thermal Grashof number and mass Grashof number on the velocity profile. It is obvious from these figures that the momentum boundary layer thickness increases as thermal Grashof number and mass Grashof number increases.

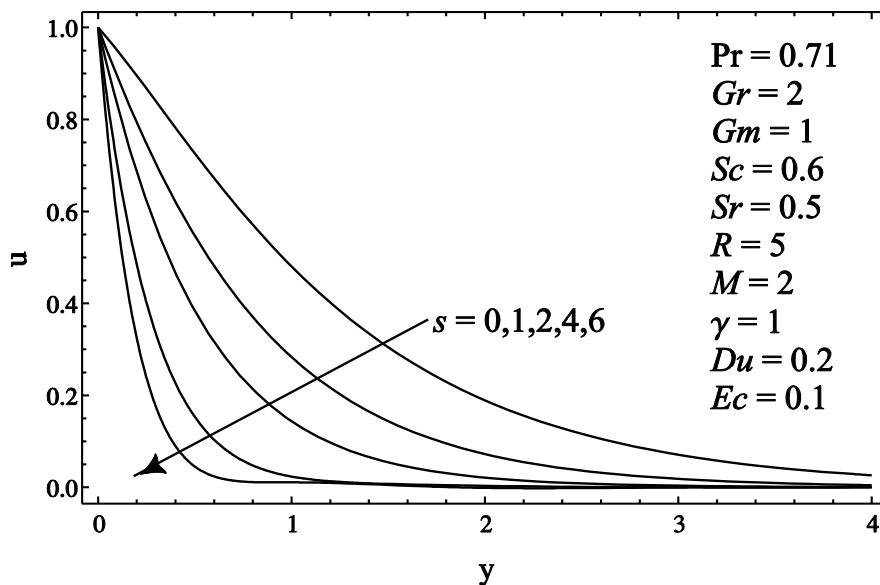


Figure 4.15: Influence of  $s$  on the dimensionless velocity profile.

Figures 4.23 to 4.28 indicate the influence of  $s, M, Sr, R, Du$  and  $Ec$  on the temperature profile. Figure 4.23 exhibits the suction parameter effect on the temperature profile. As expected, an increase in the  $s$  decreases the thermal boundary layer thickness.

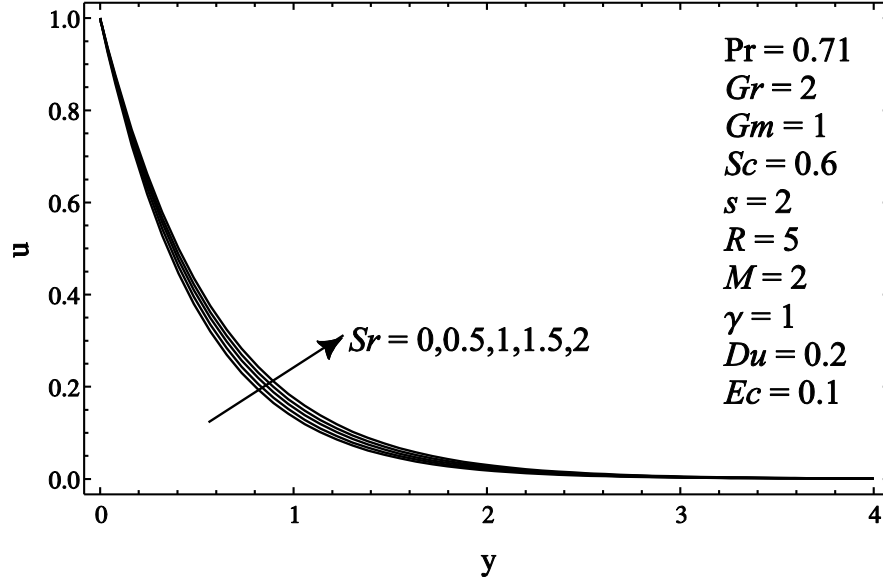


Figure 4.16: Influence of  $Sr$  on the dimensionless velocity profile.

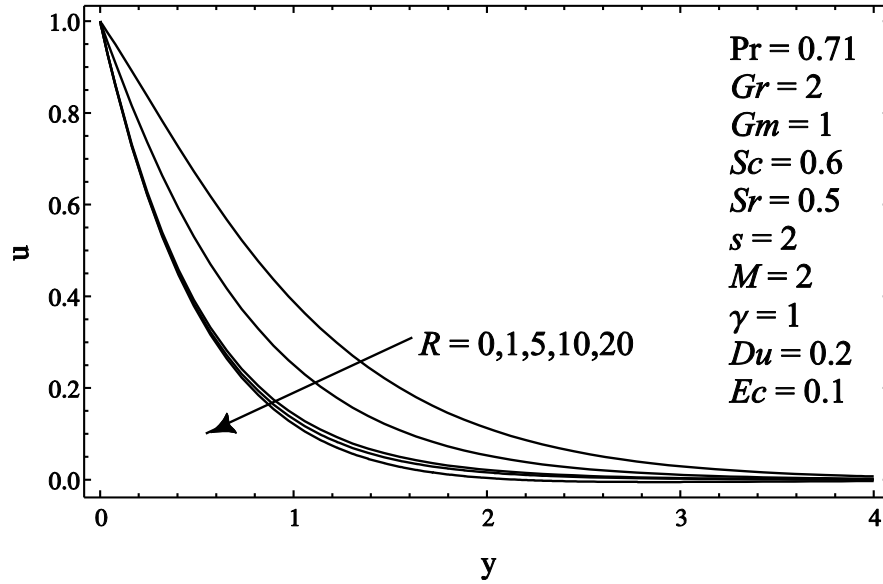


Figure 4.17: Influence of  $R$  on the dimensionless velocity profile.

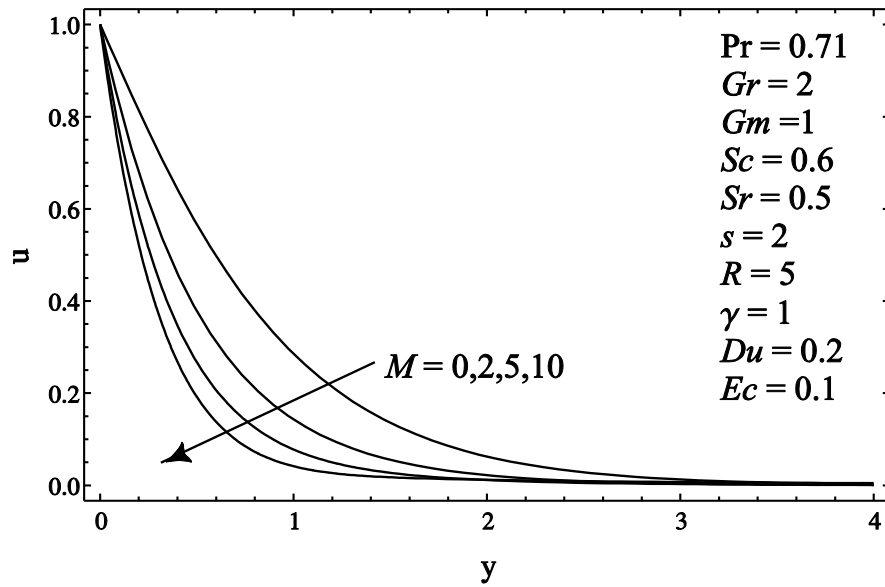


Figure 4.18: Influence of  $M$  on the dimensionless velocity profile.

Figure 4.24 reveals that an increase in the magnetic field parameter causes to rise the thermal boundary layer thickness. This is may be due to the fact that extra work is done to drag the fluid against the magnetic field which causes to increase the thermal energy of the fluid in the thermal boundary layer region and consequently temperature profile rises. There is a decrease in the temperature when  $Sr$  increase as illustrated in Figure 4.25.

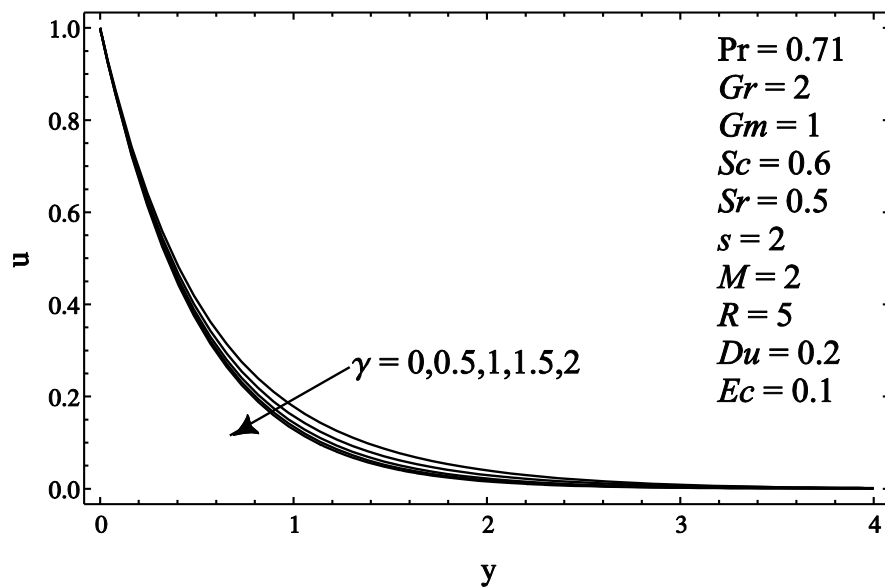


Figure 4.19: Influence of  $\gamma$  on the dimensionless velocity profile.

The influence of thermal radiation on temperature profile can be seen in Figure 4.26. It is observed that an increase in the thermal radiation parameter causes to decrease in the temperature distribution in the boundary layer. Therefore, higher value of radiation parameter causes to decrease the thermal boundary layer thickness.

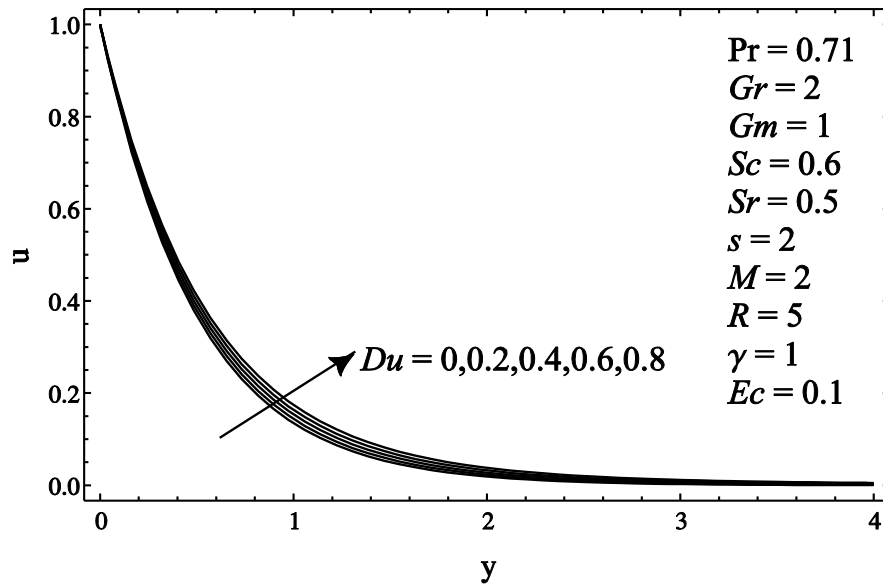


Figure 4.20: Influence of  $Du$  on the dimensionless velocity profile.

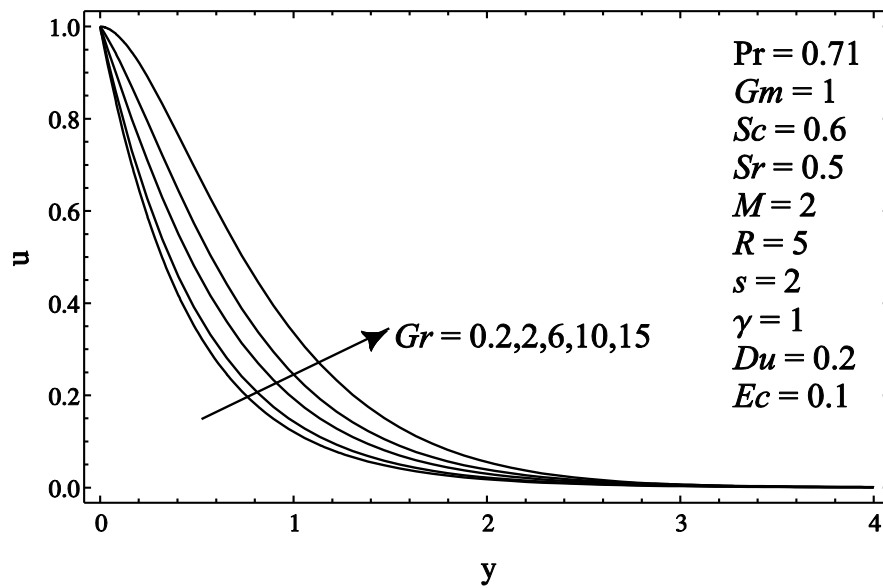


Figure 4.21: Influence of  $Gr$  on the dimensionless velocity profile.

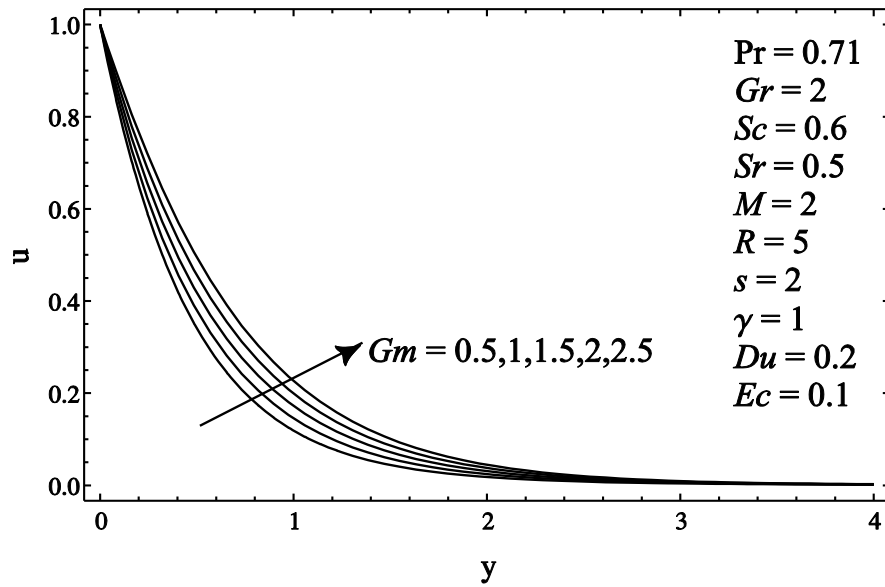


Figure 4.22: Influence of  $Gm$  on the dimensionless velocity profile.

Figure 4.27 reveals an increase in the Dufour number causes to increase the thermal boundary layer thickness. Physically, Dufour term that involves in the energy equation measures the contribution of concentration gradient to energy flux in the flow regime. Hence, it has a significant role on the boundary layer flow and it leads to an increase in the temperature profile. It can also be seen from Figure 4.28, an increase in the Eckert number leads to rise the fluid temperature. The rise in temperature may be due to increase in energy generated by work done against the viscous fluid stresses.

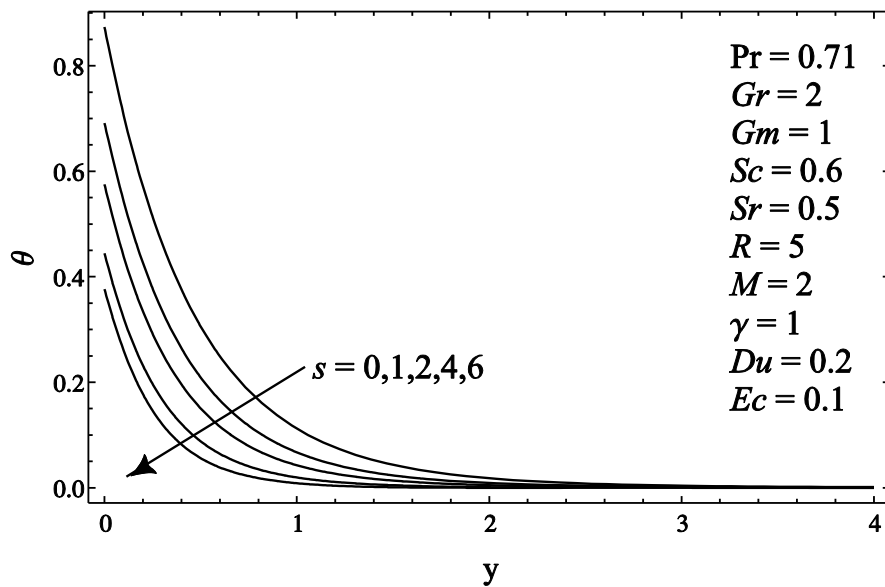


Figure 4.23: Influence of  $s$  on the dimensionless temperature profile.



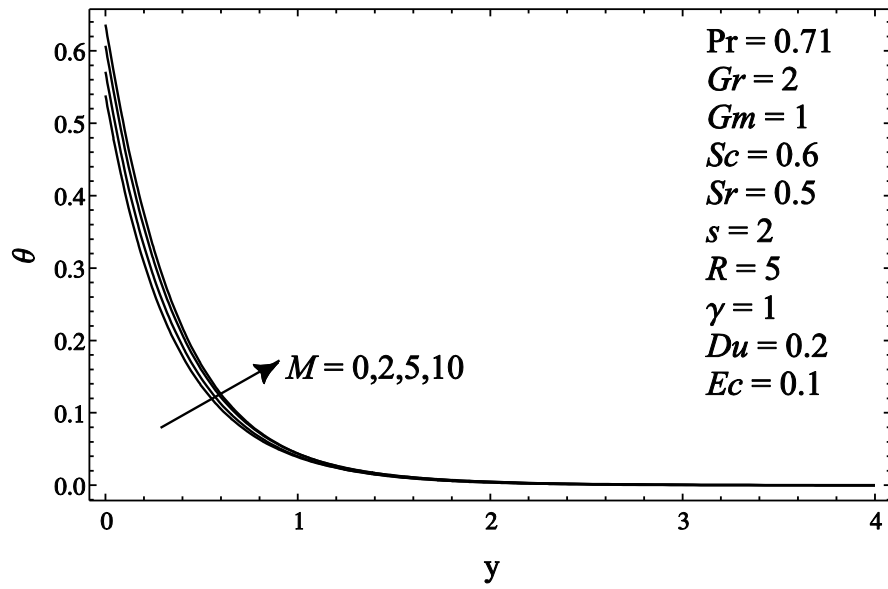


Figure 4.24: Influence of  $M$  on the dimensionless temperature profile.

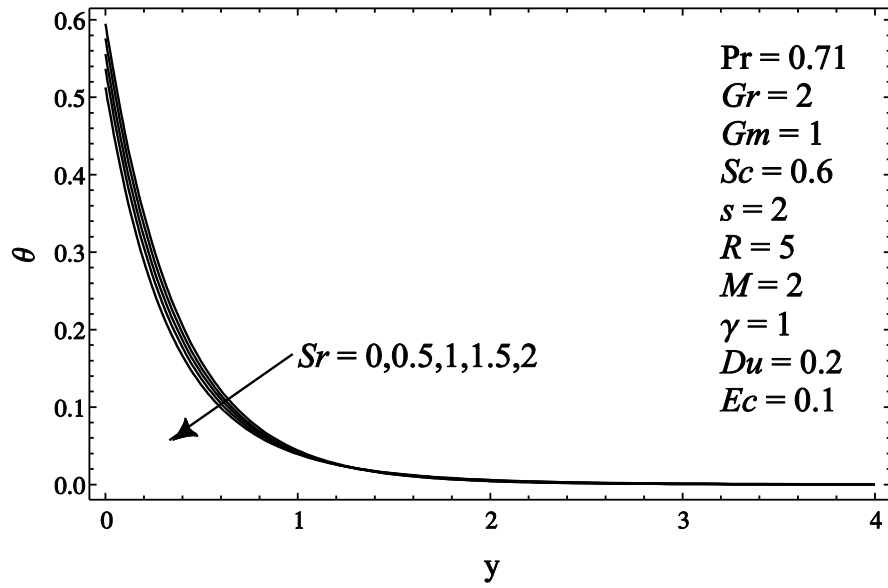


Figure 4.25: Influence of  $Sr$  on the dimensionless temperature profile.

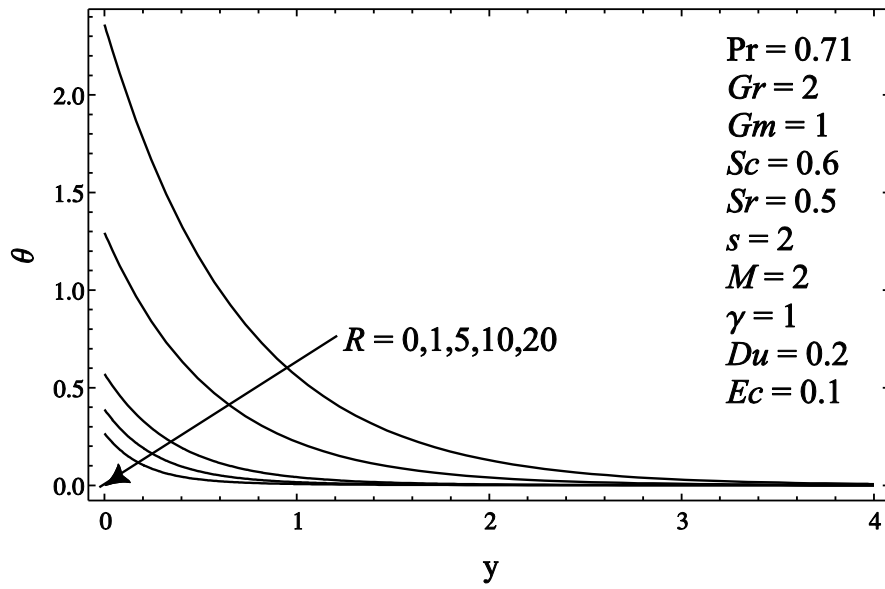


Figure 4.26: Influence of  $R$  on the dimensionless temperature profile.

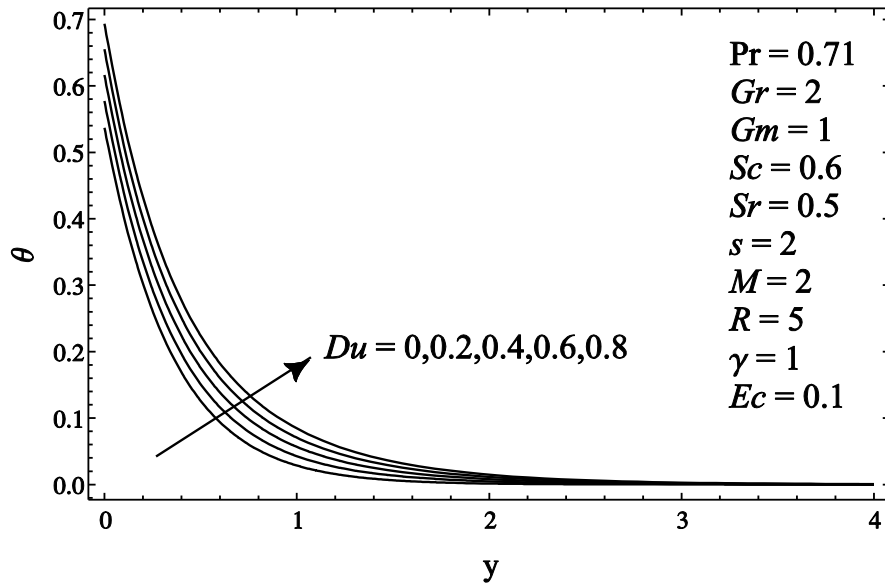


Figure 4.27: Influence of  $Du$  on the dimensionless temperature profile.

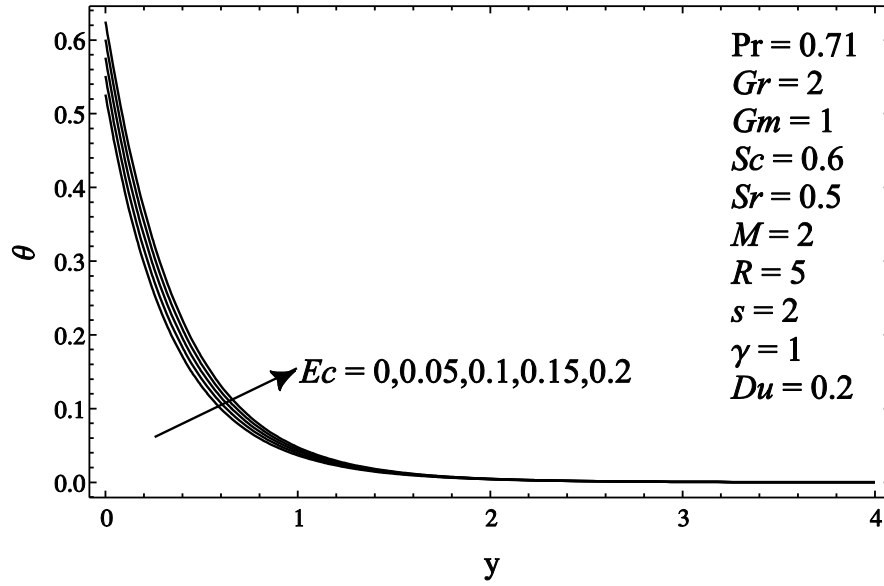


Figure 4.28: Influence of  $Ec$  on the dimensionless temperature profile.

The behaviors of  $s$ ,  $Sr$ ,  $R$  and  $\gamma$  on the concentration profile are shown in Figures 4.29 to 4.32. It can be observe in Figure 4.29, the concentration profile decreases with an increase in  $s$ . Moreover, the effect of Soret number on concentration profile is displayed in Figure 4.30. Physically, Soret number that appears in the concentration equation measures the contribution of temperature gradient to species diffusion and consequently, enhances the concentration profile. However, concentration profile decreases when both  $R$  and  $\gamma$  increase as shown in Figures 4.31 and 4.32.

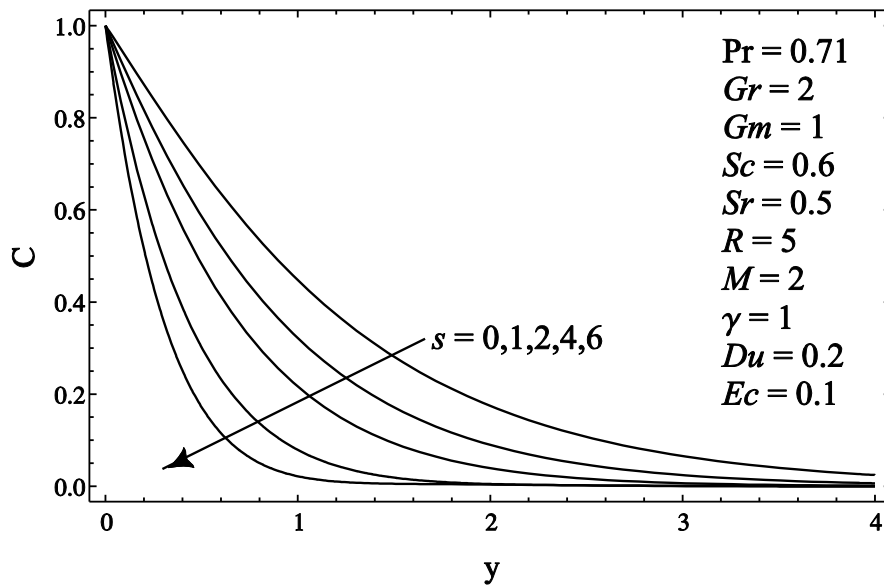


Figure 4.29: Influence of  $s$  on the dimensionless concentration profile.

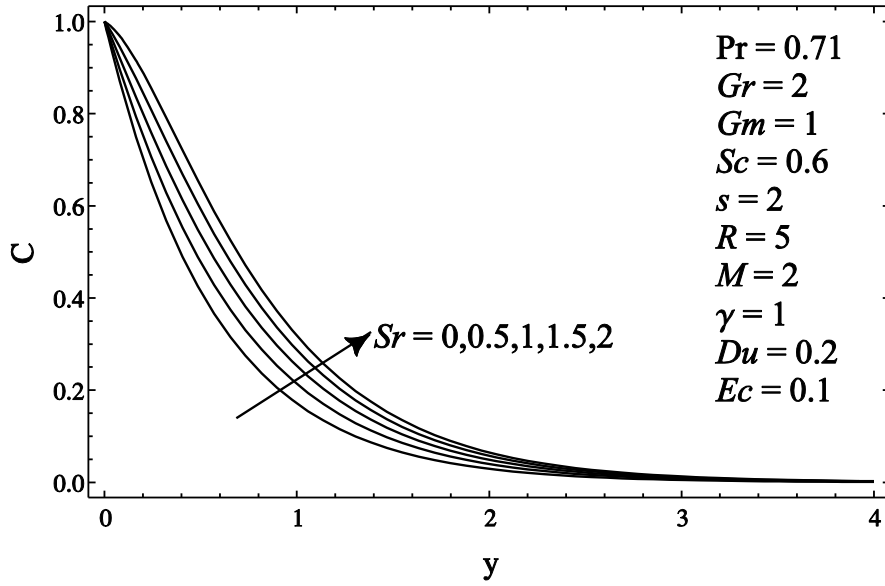


Figure 4.30: Influence of  $Sr$  on the dimensionless concentration profile.

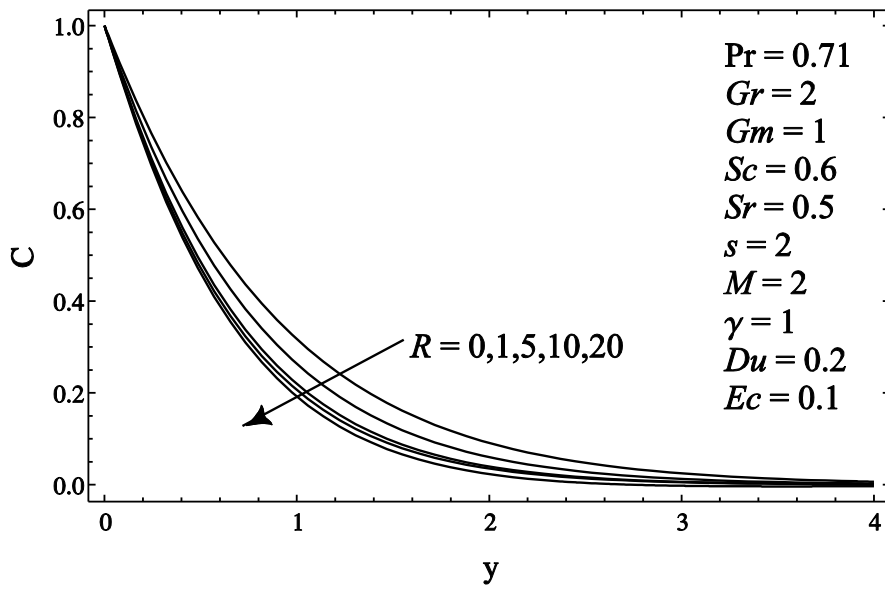


Figure 4.31: Influence of  $R$  on the dimensionless concentration profile.

Influence of magnetic field parameter and Dufour number on concentration profile is numerically presented in Tables 4.1 and 4.2, respectively. It has been observed that concentration profile increases when magnetic field parameter increases. On the other hand, by increasing Dufour number, concentration profile increases. Table 4.3 displays the influence of chemical reaction parameter on the temperature profile. Near the plate, temperature increases when  $\gamma$  increases but the trend is quite opposite away from the plate.

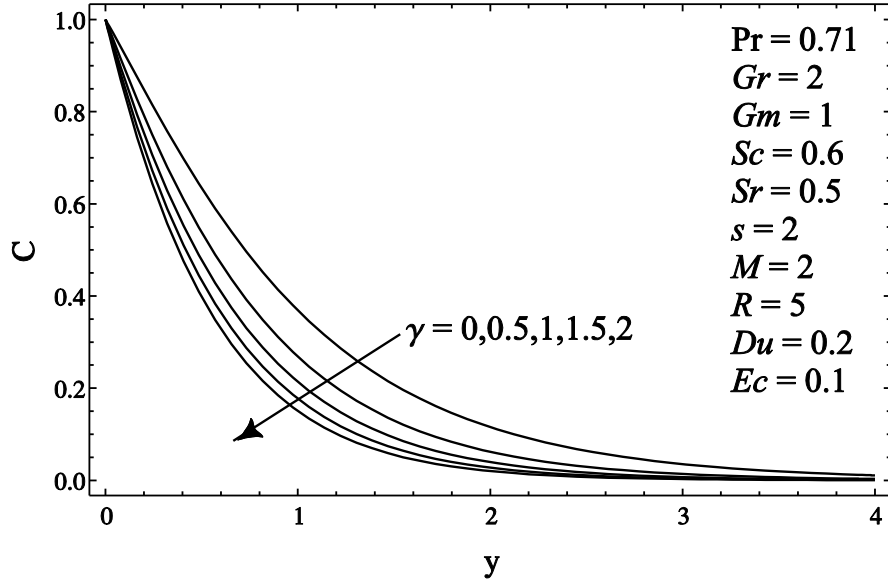


Figure 4.32: Influence of  $\gamma$  on the dimensionless concentration profile.

Table 4.1: Influence of  $M$  on concentration profile  $C(y)$

$y$	$M$			
	0	2	5	10
0	1	1	1	1
0.5	0.47413	0.47755	0.49330	0.51974
1	0.21061	0.21350	0.22962	0.25659
1.5	0.09095	0.09246	0.10549	0.12623
2	0.03878	0.03944	0.04972	0.06483
2.5	0.01645	0.01672	0.02491	0.03617
3	0.00697	0.00707	0.01362	0.02228
3.5	0.00295	0.00299	0.00816	0.01496
4	0.00125	0.00127	0.00528	0.01062

Variations of the Skin friction, Nusselt number and Sherwood number for different physical parameters have been presented in Table 4.4. Numerical values reveal that the chemical reaction parameter  $\gamma$  enhances the skin friction and Sherwood number but reduced the Nusselt number. It has been observed that the skin friction, Nusselt number, as found in [48], and Sherwood number decrease with an increase in Dufour number. Skin friction and Sherwood number decrease with an increase in  $Sr$ , whereas this trend

is quite opposite when  $s$  increases. However, Nusselt number increases when both  $Sr$  and  $s$  increase (as shown in Table 4.4). It can also be noted that with an increase in magnetic field parameter Nusselt number and Sherwood number decreases, whereas the skin friction increases. It further shows that an increase in  $R$  leads to an increase in skin friction, Nusselt number and Sherwood number.

Table 4.2: Influence of  $Du$  on concentration profile  $C(y)$

$y$	$Du$				
	0	0.2	0.4	0.6	0.8
0	1	1	1	1	1
0.5	0.47568	0.47753	0.47936	0.48118	0.48299
1	0.21129	0.21352	0.21574	0.21797	0.22020
1.5	0.09058	0.09250	0.09444	0.09638	0.09834
2	0.03812	0.03949	0.04087	0.04227	0.04369
2.5	0.01589	0.01676	0.01764	0.01853	0.01945
3	0.00659	0.00710	0.00762	0.00816	0.00871
3.5	0.00274	0.00302	0.00331	0.00362	0.00394
4	0.00113	0.00128	0.00145	0.00162	0.00181

Table 4.3: Influence of  $\gamma$  on temperature profile  $\theta(y)$

$y$	$\gamma$				
	0	0.5	1	1.5	2
0	0.54548	0.56273	0.57599	0.58723	0.59719
0.5	0.13617	0.14445	0.15046	0.15533	0.15946
1	0.03810	0.04089	0.04258	0.04374	0.04461
1.5	0.01300	0.01344	0.01349	0.01339	0.01326
2	0.00549	0.00514	0.00477	0.00444	0.00416
2.5	0.00269	0.00218	0.00182	0.00155	0.00136
3	0.00142	0.00098	0.00072	0.00056	0.00045
3.5	0.00077	0.00045	0.00029	0.00020	0.00015
4	0.00042	0.00021	0.00012	0.00007	0.00005

Table 4.4: Skin Friction ( $\tau$ ), Nusselt number ( $Nu$ ) and Sherwood number ( $Sh$ ) effects

$\gamma$	$Du$	$Sr$	$s$	$M$	$R$	$\tau$	$Nu$	$Sh$
0	0.2	0.5	2	2	5	1.84012	2.83325	0.74137
0.5	0.2	0.5	2	2	5	1.89790	2.77706	1.10800
1	0.2	0.5	2	2	5	1.92764	2.73615	1.37081
1.5	0.2	0.5	2	2	5	1.94789	2.70291	1.58438
2	0.2	0.5	2	2	5	1.96625	2.67449	1.77027
1	0	0.5	2	2	5	1.98041	2.86155	1.37940
1	0.2	0.5	2	2	5	1.93173	2.73244	1.37163
1	0.4	0.5	2	2	5	1.88249	2.62176	1.36386
1	0.6	0.5	2	2	5	1.83259	2.52586	1.35608
1	0.8	0.5	2	2	5	1.78194	2.44196	1.34828
1	0.2	0	2	2	5	1.95618	2.68080	1.75932
1	0.2	0.5	2	2	5	1.86649	2.73578	1.37155
1	0.2	1	2	2	5	1.79393	2.79868	0.99129
1	0.2	1.5	2	2	5	1.73869	2.86296	0.61843
1	0.2	2	2	2	5	1.67737	2.95003	0.25289
1	0.2	0.5	0	2	5	0.47563	2.14483	0.63175
1	0.2	0.5	1	2	5	1.11587	2.44572	0.96793
1	0.2	0.5	2	2	5	1.86649	2.73806	1.35768
1	0.2	0.5	4	2	5	3.53964	3.24916	2.24203
1	0.2	0.5	6	2	5	5.29449	3.65413	3.20502
1	0.2	0.5	2	0	5	0.93954	2.85713	1.37731
1	0.2	0.5	2	2	5	1.92253	2.75086	1.36987
1	0.2	0.5	2	5	5	2.65728	2.64741	1.34731
1	0.2	0.5	2	10	5	3.21054	2.57165	1.30335
1	0.2	0.5	2	2	0	0.62003	1.42370	1.07310
1	0.2	0.5	2	2	1	1.19964	1.77307	1.22982
1	0.2	0.5	2	2	5	1.89071	2.75222	1.34488
1	0.2	0.5	2	2	10	1.91209	3.57680	1.37436
1	0.2	0.5	2	2	20	1.91408	4.76568	1.40171

## 4.6 Chapter Summary

In this chapter, Soret and Dufour effects on the heat and mass transfer MHD flow past an impulsively started infinite vertical porous plate with Newtonian heating in the presence of thermal radiation, viscous dissipation and chemical reaction have been examined using Homotopy Analysis Method (HAM). There is an excellent agreement between the exact analytical solution results and the HAM solution results in the absence of viscous dissipation and Dufour effect. The obtained results revealed that the fluid velocity increases by increasing Soret and Dufour numbers. However, thermal boundary layer thickness decreases with an increase in the Soret number whereas it increases with increasing the Dufour number. Moreover, an increase in the Soret and Dufour number causes to decrease in the skin friction and Sherwood number. On the other hand, Nusselt number decreases when Dufour number increases, and it increases with an increase in the Soret number.



## CHAPTER 5

### CONCLUSION

#### 5.1 Conclusion

Free convection heat and mass transfer flow past an infinitely moving vertical porous plate with three types of different flow models namely, (i) heat generation and viscous dissipation (ii) thermal radiation and viscous dissipation effects in the presence of transverse magnetic field and (iii) Soret and Dufour effects with thermal radiation, viscous dissipation and chemical reaction has been studied subjected to Newtonian heating thermal boundary conditions. The governing differential equations are transformed into system of coupled non-linear ordinary differential equations with suitable dimensionless variables. The resulting nonlinear equations are solved by using an analytical technique known as Homotopy Analysis Method (HAM). The HAM solution results are compared with the exact solution results for limiting cases and it is found that the HAM results coincide well with the exact solution results. The effects of the physical parameters on the fluid characteristics are displayed in graphical and tabular forms. It has been observed that, the dimensionless velocity increases as the thermal Grashof number, Eckert number, heat generation parameter, Soret number, Dufour number or mass Grashof number increasing, while it decreases as the Prandtl number, suction parameter, magnetic field parameter, radiation parameter or chemical reaction parameter increasing. The dimensionless temperature increases as the Eckert number, heat generation parameter, magnetic field parameter or Dufour number increasing, while it decreases as the Prandtl number, suction parameter, radiation parameter or Soret number increasing. Similarly, dimensionless concentration increases

as the magnetic field, Soret and Dufour number increasing, while it decreases as the suction parameter, radiation parameter or chemical reaction parameter increasing. Furthermore, practically important quantities such as skin friction, heat and mass transfer rates have also been analyzed numerically. It was found that the skin friction increases as the suction parameter, magnetic field parameter, prandtl number, radiation parameter or chemical reaction parameter increasing, while it decreases as the thermal Grashof number, Eckert number, heat generation parameter, Soret number or Dufour number increasing. The heat transfer rate or Nusselt number increases as the Prandtl number, thermal Grashof number, suction parameter, radiation parameter or Soret number increasing, while it decreases as the Eckert number, heat generation parameter, magnetic field parameter, Dufour number or chemical reaction parameter increasing. Similarly, mass transfer rate or Sherwood number increases as the suction parameter, radiation parameter or chemical reaction parameter increasing, while it decreases as the magnetic field parameter, Soret number or Dufour number increasing.

## **5.2 Recommendations for Future Work**

Free convection flow past an infinite vertical porous plate with Newtonian heating has been studied in this thesis. Heat generation, viscous dissipation, magnetic field, thermal radiation, Soret and Dufour effects have been analyzed on the free convection flow in the presence of Newtonian heating. In the literature, nobody has been studied these effects on the steady free convection flow past an infinite vertical porous plate with Newtonian heating to the best of my knowledge. The hierarchy proposed in this thesis provides an excellent guideline to future research work. The research contributions at the individual chapters of the hierarchy suggest many more aspects of heat and mass transfer under the influence of Newtonian heating. The studied effects, in this thesis, can be examined with two dimension steady free convective flow along a vertical porous plate with Newtonian heating. Furthermore, Hall current effect can be analyzed on one or two dimension steady free convection flow past an infinite vertical porous plate in the presence of Newtonian heating. Above mentioned all effects can also be investigated on unsteady free convection flow past infinite vertical porous plate under the influence of Newtonian heating.

## APPENDIX A

### BOUSSINESQ APPROXIMATION

#### Boussinesq Approximation for Heat and Mass Transfer

The boundary layer equations for steady state two-dimensional incompressible laminar fluid flow are

$$\frac{\partial u'}{\partial x'} + \frac{\partial v'}{\partial y'} = 0 \quad (1)$$

$$\rho \left( u' \frac{\partial u'}{\partial x'} + v' \frac{\partial u'}{\partial y'} \right) = -\frac{\partial P}{\partial x'} + \mu \left( \frac{\partial^2 u'}{\partial x'^2} + \frac{\partial^2 u'}{\partial y'^2} \right) - \rho g \quad (2)$$

$$\rho \left( u' \frac{\partial v'}{\partial x'} + v' \frac{\partial v'}{\partial y'} \right) = -\frac{\partial P}{\partial y'} + \mu \left( \frac{\partial^2 v'}{\partial x'^2} + \frac{\partial^2 v'}{\partial y'^2} \right) \quad (3)$$

$$u' \frac{\partial T'}{\partial x'} + v' \frac{\partial T'}{\partial y'} = \alpha \left( \frac{\partial^2 T'}{\partial x'^2} + \frac{\partial^2 T'}{\partial y'^2} \right) \quad (4)$$

In the boundary layer analysis, the velocity and temperature gradients normal to the surface are much greater than those in the direction parallel to the surface [76], [77], in other words  $y' \sim \delta, x' \sim L$ , and  $\delta \ll L$ , where  $\delta$  is the boundary layer thickness and  $L$  is the characteristic length, is considered. Therefore, the terms of the order of magnitude of  $(\delta/L)^2$  and smaller are being neglected in equations (2)-(4) [76]. It follows from equation (3) for boundary layer flow is:

$$\frac{\partial P}{\partial y'} = 0 \quad (5)$$

Equation (5) indicates that the changes of pressure in the  $y'$  direction can be ignored in boundary layer flows. The transversal momentum equation (2) reduces to the statement that in the boundary layer, the pressure is only a function of longitudinal position,

$$\frac{\partial P}{\partial x'} = \frac{dP}{dx'} = \frac{dP_\infty}{dx'} \quad (6)$$

The boundary layer equations for momentum and energy are

$$\rho \left( u' \frac{\partial u'}{\partial x'} + v' \frac{\partial u'}{\partial y'} \right) = - \frac{dP_\infty}{dx'} + \mu \frac{\partial^2 u'}{\partial y'^2} - \rho g \quad (7)$$

$$u' \frac{\partial T'}{\partial x'} + v' \frac{\partial T'}{\partial y'} = \alpha \frac{\partial^2 T'}{\partial y'^2} \quad (8)$$

where  $dP_\infty/dx'$  is the hydrostatic pressure gradient dictated by the reservoir fluid of density  $\rho_\infty$ , therefore  $dP_\infty/dx' = -\rho_\infty g$  and the momentum equation (7) becomes,

$$\rho \left( u' \frac{\partial u'}{\partial x'} + v' \frac{\partial u'}{\partial y'} \right) = \mu \frac{\partial^2 u'}{\partial y'^2} + (\rho_\infty - \rho)g \quad (9)$$

Equations (1), (8) and (9) must be solved in order to determine  $u', v'$  and  $T'$  in the boundary layer. Through the body force term  $(\rho_\infty - \rho)g$  in the momentum equation (9), the flow is driven by the density field  $\rho(x', y')$  generated by the temperature field  $T'(x', y')$ . Equations (8) and (9) are coupled via the equation of state of the fluid; for example,

$$P = \rho R T' \quad (10)$$

if the fluid behaves according to the ideal gas model [77]. At a level  $x'$ , we have

$$\rho = \frac{P_\infty/R}{T'} \text{ and } \rho_\infty = \frac{P_\infty/R}{T'_\infty} \quad (11)$$

Thus,

$$(\rho - \rho_\infty) = \frac{P_\infty/R}{T'} - \frac{P_\infty/R}{T'_\infty} = \frac{P_\infty/R}{T'} \left( 1 - \frac{T'}{T'_\infty} \right) = \rho \left( 1 - \frac{T'}{T'_\infty} \right) \quad (12)$$

Equation (12) can be written as

$$\frac{\rho_\infty - \rho}{\rho} = \frac{T' - T'_\infty}{T'_\infty}$$

$$\frac{\rho_\infty - \rho}{\rho_\infty} \cdot \frac{\rho_\infty}{\rho} = \frac{T' - T'_\infty}{T'_\infty}$$

$$\frac{\rho_\infty - \rho}{\rho_\infty} \left( \frac{\rho}{\rho_\infty} \right)^{-1} = \frac{T' - T'_\infty}{T'_\infty}$$

$$\frac{\rho_\infty - \rho}{\rho_\infty} \left( 1 - \frac{\rho_\infty - \rho}{\rho_\infty} \right)^{-1} = \frac{T' - T'_\infty}{T'_\infty}$$

which in the limit  $(T' - T'_\infty) \ll T'_\infty$  yields

$$\frac{\rho_\infty - \rho}{\rho} \cong \frac{T' - T'_\infty}{T'_\infty}$$

$$\frac{\rho_\infty}{\rho} - 1 \cong \frac{T' - T'_\infty}{T'_\infty}$$

$$\frac{\rho}{\rho_\infty} \cong \left( 1 + \frac{T' - T'_\infty}{T'_\infty} \right)^{-1}$$

$$\rho \cong \rho_\infty \left[ 1 - \frac{1}{T'_\infty} (T' - T'_\infty) + \dots \right] \quad (13)$$

Equation (13) describes that the density decreases slightly below  $\rho_\infty$  as the local absolute temperature increases slightly above the reservoir absolute temperature  $T'_\infty$ . In general, for fluids that are not necessarily ideal gases, equation (13) can be written as

$$\rho \cong \rho_\infty [1 - \beta(T' - T'_\infty) + \dots] \quad (14)$$

where  $\beta$  is the volumetric expansion coefficient at constant pressure,

$$\beta = -\frac{1}{\rho} \left( \frac{\partial \rho}{\partial T'} \right)_p \quad (15)$$

Implicit in the first order Taylor expansion (14) is the assumption that the dimensionless product  $\beta(T' - T'_\infty)$  is considerably smaller than unity.

The Boussinesq approximation of the boundary layer equations amounts to substituting equation (14) into equation (8) and (9) and, in each case, retaining the dominant term. For example, in the momentum equation (9),  $\rho$  appears in the inertia terms as well as in the body force term; using approximation (14), the inertia terms will be multiplied by the dominant term  $\rho_\infty = \text{constant}$ , whereas

the leading body force term becomes  $\rho_\infty \beta g(T' - T'_\infty)$ . Therefore the momentum equation (9) can be written as

$$u' \frac{\partial u'}{\partial x'} + v' \frac{\partial u'}{\partial y'} = \nu \frac{\partial^2 u'}{\partial y'^2} + g\beta(T' - T'_\infty) \quad (16)$$

where  $g, \beta, T'_\infty$ , and  $\nu = \mu/\rho_\infty$  are constants. Similarly, the thermal diffusivity appearing in the energy equation (8),  $\alpha = k/\rho_\infty c_P$  is assumed constant.

The governing equations result from laws of conservation of mass, of momentum, of energy, and of the diffusing molecular species [81] are simplified for typical free convection flows by the Boussinesq approximations, which apply for small diffusion generated by density variations. This simplification applies to the continuity equation and to the evaluation of the buoyancy force arising from density differences. The set of equations can be written as

$$\frac{\partial u'}{\partial x'} + \frac{\partial v'}{\partial y'} = 0 \quad (17)$$

$$\rho \left( u' \frac{\partial u'}{\partial x'} + v' \frac{\partial u'}{\partial y'} \right) = -\frac{\partial P}{\partial x'} + \mu \left( \frac{\partial^2 u'}{\partial x'^2} + \frac{\partial^2 u'}{\partial y'^2} \right) - \rho g \quad (18)$$

$$\rho \left( u' \frac{\partial v'}{\partial x'} + v' \frac{\partial v'}{\partial y'} \right) = -\frac{\partial P}{\partial y'} + \mu \left( \frac{\partial^2 v'}{\partial x'^2} + \frac{\partial^2 v'}{\partial y'^2} \right) \quad (19)$$

$$u' \frac{\partial T'}{\partial x'} + v' \frac{\partial T'}{\partial y'} = \alpha \left( \frac{\partial^2 T'}{\partial x'^2} + \frac{\partial^2 T'}{\partial y'^2} \right) \quad (20)$$

$$u' \frac{\partial C'}{\partial x'} + v' \frac{\partial C'}{\partial y'} = D_m \left( \frac{\partial^2 C'}{\partial x'^2} + \frac{\partial^2 C'}{\partial y'^2} \right) \quad (21)$$

The Boussinesq approximation concerns the combination  $-\rho g - \partial P/\partial x'$  in the momentum equation (18). For external free convection flows [77], the local hydrostatic value  $dP/dx' = -\rho_\infty g$ , and the pressure difference in the convection region associated with motion.

Consider the term  $-dP/dx' - \rho g = (\rho_\infty - \rho)g$

A series expansion of  $(\rho_\infty - \rho)$  in terms of  $T', P$  and  $C'$  at a given elevation indicates that the  $P$  effect may be neglected and that only the linear term of the temperature effect will remain in the  $\beta(T' - T'_\infty) \ll 1$ , where  $\beta = -(1/\rho)(\partial\rho/\partial T')_{P,C'}$  is the volumetric coefficient of thermal expansion. A

similar argument indicates that only the linear term of the concentration effect need be retained for  $\beta^*(C' - C'_\infty) \ll 1$ , where  $\beta^* = -(1/\rho)(\partial\rho/\partial C')_{p,T'}$  is the volumetric coefficient of expansion with concentration [81]. Thus, the term  $g(\rho_\infty - \rho)$  is simplified to the following:

$$g(\rho_\infty - \rho) = g\rho\beta(T' - T'_\infty) + g\rho\beta^*(C' - C'_\infty).$$

Now, the set of governing equations for free convective heat and mass transfer laminar flow becomes

$$\frac{\partial u'}{\partial x'} + \frac{\partial v'}{\partial y'} = 0 \quad (22)$$

$$u' \frac{\partial u'}{\partial x'} + v' \frac{\partial u'}{\partial y'} = \nu \frac{\partial^2 u'}{\partial y'^2} + g\beta(T' - T'_\infty) + g\beta^*(C' - C'_\infty) \quad (23)$$

$$u' \frac{\partial T'}{\partial x'} + v' \frac{\partial T'}{\partial y'} = \alpha \frac{\partial^2 T'}{\partial y'^2} \quad (24)$$

$$u' \frac{\partial C'}{\partial x'} + v' \frac{\partial C'}{\partial y'} = D_m \frac{\partial^2 C'}{\partial y'^2} \quad (25)$$

## REFERENCES

- [1] L. M. Jiji, *Heat Conduction*, 3<sup>rd</sup> Ed., Springer-Verlag Berlin Heidelberg, 2009.
- [2] L. M. Jiji, *Heat convection*, 3<sup>rd</sup> Ed., Springer-Verlag Berlin Heidelberg, 2009.
- [3] R. Siegel, J. R. Howell, and M. P. Menguc, *Thermal Radiation Heat Transfer*, 5<sup>th</sup> Ed., Taylor & Francis, 2010.
- [4] M. F. Modest, *Radiative Heat Transfer*, 3<sup>rd</sup> Ed., Elsevier Science, 2013.
- [5] Y. J. Kim, "Unsteady convection flow of micropolar fluids past a vertical porous plate embedded in a porous medium," *Acta Mech.* vol. 148, pp. 105-116, 2001.
- [6] B. Jaiswal and V. Soundalgekar, "Oscillating plate temperature effects on a flow past an infinite vertical porous plate with constant suction and embedded in a porous medium," *Heat Mass Trans.*, vol. 37, pp. 125-131, 2001.
- [7] Y. J. Kim and A. G. Fedorov, "Transient mixed radiative convection flow of a micropolar fluid past a moving, semi-infinite vertical porous plate," *Inter. J. Heat Mass Trans.*, vol. 46, pp. 1751-1758, 2003.
- [8] O. D. Makinde, "Free convection flow with thermal radiation and mass transfer past a moving vertical porous plate," *Inter. Comm. Heat Mass Trans.*, vol. 32, pp. 1411-1419, 2005.
- [9] J. Cheng, S. Liao, and I. Pop, "Analytic series solution for unsteady mixed convection boundary layer flow near the stagnation point on a vertical surface in a porous medium," *Trans. porous med.*, vol. 61, pp. 365-379, 2005.
- [10] M. Seddeek and F. A. Salama, "The effects of temperature dependent viscosity and thermal conductivity on unsteady MHD convective heat transfer past a semi-infinite vertical porous moving plate with variable suction," *Comp. Mater. Sci.*, vol. 40, pp. 186-192, 2007.
- [11] M. Alam, M. Rahman, and M. Sattar, "Effects of variable suction and thermophoresis on steady MHD combined free-forced convective heat and mass transfer flow over a semi-infinite permeable inclined plate in the presence of thermal radiation," *Inter. J. Ther. Sci.*, vol. 47, pp. 758-765, 2008.



- [12] F. Ibrahim, A. Elaiw, and A. Bakr, "Effect of the chemical reaction and radiation absorption on the unsteady MHD free convection flow past a semi infinite vertical permeable moving plate with heat source and suction," *Commun. Nonlinear. Sci.*, vol. 13, pp. 1056-1066, 2008.
- [13] R. A. DAMSEH and B. A. SHANNAK, "Visco-elastic fluid flow past an infinite vertical porous plate in the presence of first-order chemical reaction," *Appl. Math. Mech. -Engl. Ed.*, vol. 31, pp. 955–962, 2010.
- [14] M. C. Knirsch, C. Alves dos Santos, A. A. Martins de Oliveira Soares Vicente, and T. C. Vessoni Penna, "Ohmic heating—a review," *Trends in Food Science & Technology*, vol. 21, pp. 436-441, 2010.
- [15] S. Liao, "Beyond perturbation: introduction to the homotopy analysis method", *Champan Hall CRC*, Boca Raton 2003.
- [16] S. Liao, "Notes on the homotopy analysis method: some definitions and theorems," *Commun. Nonlinear Sci.*, vol. 14, pp. 983-997, 2009.
- [17] S. Abbasbandy, E. Shivanian, and K. Vajravelu, "Mathematical properties of  $\hbar$ -curve in the frame work of the homotopy analysis method," *Commun. Nonlinear Sci.*, vol. 16, pp. 4268-4275, 2011.
- [18] S. Abbasbandy and M. Jalili, "Determination of optimal convergence-control parameter value in homotopy analysis method," *Num. Algor.*, pp. 1-13, 2013.
- [19] R. A. Van Gorder and K. Vajravelu, "On the selection of auxiliary functions, operators, and convergence control parameters in the application of the homotopy analysis method to nonlinear differential equations: a general approach," *Commun. Nonlinear Sci.*, vol. 14, pp. 4078-4089, 2009.
- [20] S. J. Ramazannia Toloti and J. Saeidian, "Comments on “R.A. Van Gorder and K. Vajravelu, Commun. Nonlinear Sci. Numer. Simul. 14 (2009) 4078–4089”," *Commun. Nonlinear Sci.*, vol. 17, pp. 1085-1088, 2012.
- [21] M. Turkyilmazoglu, "Solution of the Thomas–Fermi equation with a convergent approach," *Commun. Nonlinear Sci.*, vol. 17, pp. 4097-4103, 2012.
- [22] Y. Zhao, Z. Lin, Z. Liu, and S. Liao, "The improved homotopy analysis method for the Thomas–Fermi equation," *Appl. Mathe. Comp.*, vol. 218, pp. 8363-8369, 2012.

- [23] B. GHANBARI, "On the Convergence of the Homotopy Analysis Method for Solving Fredholm Integral Equations", vol. 10, 2013.
- [24] A. K. Alomari, M. S. M. Noorani, and R. Nazar, "Comparison between the homotopy analysis method and homotopy perturbation method to solve coupled Schrodinger-KdV equation," *J. Appl. Mathe. Comp.*, vol. 31, pp. 1-12, 2009.
- [25] S. Abbasbandy, "Homotopy analysis method for heat radiation equations," *Inter. Communi. Heat Mass Trans.*, vol. 34, pp. 380-387, 2007.
- [26] Y. Liu, S. Liao, and Z. Li, "Symbolic computation of strongly nonlinear periodic oscillations," *J. Symb. Comput.*, vol. 55, pp. 72-95, 2013.
- [27] S. Srinivas and R. Muthuraj, "Effects of thermal radiation and space porosity on MHD mixed convection flow in a vertical channel using homotopy analysis method," *Communi. Nonlinear Sci.*, vol. 15, pp. 2098-2108, 2010.
- [28] L. Zheng, N. Liu, and X. Zhang, "Maxwell Fluids Unsteady Mixed Flow and Radiation Heat Transfer Over a Stretching Permeable Plate With Boundary Slip and Nonuniform Heat Source/Sink," *J. heat trans.*, vol. 135, 2013.
- [29] M. A. Hossain, K. Khanafer, and K. Vafai, "The effect of radiation on free convection flow of fluid with variable viscosity from a porous vertical plate," *Inter.J. Ther. Sci.*, vol. 40, pp. 115-124, 2001.
- [30] M. Abd El-Naby, E. M. Elbarbary, and N. Y. AbdElazem, "Finite difference solution of radiation effects on MHD unsteady free-convection flow over vertical porous plate," *Appl. Mathe. Comput.*, vol. 151, pp. 327-346, 2004.
- [31] M. A. Samad and M. Mansur-Rahman, "Thermal radiation interaction with unsteady MHD flow past a vertical porous plate immersed in a porous medium," *J. Naval Arch. Marine Eng.*, vol. 3, pp. 7-14, 2006.
- [32] J. Z. Jordán, "Network simulation method applied to radiation and viscous dissipation effects on MHD unsteady free convection over vertical porous plate," *Appl. Mathe. Model.*, vol. 31, pp. 2019-2033, 2007.
- [33] O. D. Makinde and A. Ogulu, "The effect of thermal radiation on the heat and mass transfer flow of a variable viscosity fluid past a vertical porous plate permeated by a transverse magnetic field," *Chem. Eng. Commun.*, vol. 195, pp. 1575-1584, 2008.

- [34] R. Mohamed and S. Abo-Dahab, "Influence of chemical reaction and thermal radiation on the heat and mass transfer in MHD micropolar flow over a vertical moving porous plate in a porous medium with heat generation," *Inter. J. Ther. Sci.*, vol. 48, pp. 1800-1813, 2009.
- [35] D. Pal and B. Talukdar, "Perturbation analysis of unsteady magnetohydrodynamic convective heat and mass transfer in a boundary layer slip flow past a vertical permeable plate with thermal radiation and chemical reaction," *Commun. Nonlinear Sci.*, vol. 15, pp. 1813-1830, 2010.
- [36] O. Makinde, "MHD mixed-convection interaction with thermal radiation and nth order chemical reaction past a vertical porous plate embedded in a porous medium," *Chem. Eng. Commun.*, vol. 198, pp. 590-608, 2010.
- [37] E. R. G. Eckert and R. M. Drake, "Analysis of Heat and Mass Transfer," McGraw-Hill, New York, 1972.
- [38] A. Postelnicu, "Influence of chemical reaction on heat and mass transfer by natural convection from vertical surfaces in porous media considering Soret and Dufour effects," *Heat Mass Trans.*, vol. 43, pp. 595-602, 2007.
- [39] M. Mansour, N. El-Anssary, and A. Aly, "Effects of chemical reaction and thermal stratification on MHD free convective heat and mass transfer over a vertical stretching surface embedded in a porous media considering Soret and Dufour numbers," *Chem. Eng. J.*, vol. 145, pp. 340-345, 2008.
- [40] A. J. Chamkha and A. Ben-Nakhi, "MHD mixed convection–radiation interaction along a permeable surface immersed in a porous medium in the presence of Soret and Dufour's effects," *Heat Mass trans.*, vol. 44, pp. 845-856, 2008.
- [41] M. Partha, "Thermophoresis particle deposition in a non-Darcy porous medium under the influence of Soret, Dufour effects," *Heat Mass Trans.*, vol. 44, pp. 969-977, 2008.
- [42] O. A. Bég, A. Bakier, and V. Prasad, "Numerical study of free convection magnetohydrodynamic heat and mass transfer from a stretching surface to a saturated porous medium with Soret and Dufour effects," *Comput. Mater. Sci.*, vol. 46, pp. 57-65, 2009.

- [43] M. Partha, "Suction/injection effects on thermophoresis particle deposition in a non-Darcy porous medium under the influence of Soret, Dufour effects," *Inter. J. Heat Mass Trans.*, vol. 52, pp. 1971-1979, 2009.
- [44] A. Mahdy, "Soret and Dufour effect on double diffusion mixed convection from a vertical surface in a porous medium saturated with a non-Newtonian fluid," *J. Non-Newton. Fluid.*, vol. 165, pp. 568-575, 2010.
- [45] B. R. Kumar and S. K. Murthy, "Soret and Dufour effects on double-diffusive free convection from a corrugated vertical surface in a non-Darcy porous medium," *Trans. porous med.*, vol. 85, pp. 117-130, 2010.
- [46] B.-C. Tai and M.-I. Char, "Soret and Dufour effects on free convection flow of non-Newtonian fluids along a vertical plate embedded in a porous medium with thermal radiation," *Inter. Commun Heat Mass Trans.*, vol. 37, pp. 480-483, 2010.
- [47] S. Vempati and A. Laxmi-Narayana-Gari, "Soret and Dufour effects on unsteady MHD flow past an infinite vertical porous plate with thermal radiation," *Appl. Mathe. Mech.*, vol. 31, pp. 1481-1496, 2010.
- [48] P. O. Olanrewaju and O. D. Makinde, "Effects of thermal diffusion and diffusion thermo on chemically reacting MHD boundary layer flow of heat and mass transfer past a moving vertical plate with suction/injection," *Arab. J. Sci. Eng.*, vol. 36, pp. 1607-1619, 2011.
- [49] R. Kandasamy, T. Hayat, and S. Obaidat, "Group theory transformation for Soret and Dufour effects on free convective heat and mass transfer with thermophoresis and chemical reaction over a porous stretching surface in the presence of heat source/sink," *Nucl. Eng. Des.*, vol. 241, pp. 2155-2161, 2011.
- [50] P. Puvi Arasu, P. Loganathan, R. Kandasamy, and I. Muhaimin, "Lie group analysis for thermal-diffusion and diffusion-thermo effects on free convective flow over a porous stretching surface with variable stream conditions in the presence of thermophoresis particle deposition," *Nonlinear Anal. Hybrid Sys.*, vol. 5, pp. 20-31, 2011.
- [51] C.-Y. Cheng, "Soret and Dufour effects on free convection boundary layers of non-Newtonian power law fluids with yield stress in porous media over a

- vertical plate with variable wall heat and mass fluxes," *International Commun. Heat Mass Trans.*, vol. 38, pp. 615-619, 2011.
- [52] V. Ramachandra Prasad, B. Vasu, and O. A. Bég, "Thermo-diffusion and diffusion-thermo effects on MHD free convection flow past a vertical porous plate embedded in a non-Darcian porous medium," *Chem. Eng. J.*, vol. 173, pp. 598-606, 2011.
- [53] O. Makinde and P. Olanrewaju, "Unsteady mixed convection with Soret and Dufour effects past a porous plate moving through a binary mixture of chemically reacting fluid," *Chem. Eng. Commun.*, vol. 198, pp. 920-938, 2011.
- [54] M. Q. Al-Odat and A. Al-Ghamdi, "Numerical investigation of Dufour and Soret effects on unsteady MHD natural convection flow past vertical plate embedded in non-Darcy porous medium," *Appl. Mathe. Mech.*, vol. 33, pp. 195-210, 2012.
- [55] M. Turkyilmazoglu and I. Pop, "Soret and heat source effects on the unsteady radiative MHD free convection flow from an impulsively started infinite vertical plate," *Inter. J. Heat Mass Trans.*, vol. 55, pp. 7635-7644, 2012.
- [56] T. Hayat, M. Awais, S. Asghar, and S. Obaidat, "Unsteady Flow of Third Grade Fluid With Soret and Dufour Effects," *J. Heat Trans.*, vol. 134, p. 062001, 2012.
- [57] J. Prakash, D. Bhanumathi, A. G. Vijaya Kumar, and S. V. K. Varma, "Diffusion-Thermo and Radiation Effects on Unsteady MHD Flow Through Porous Medium Past an Impulsively Started Infinite Vertical Plate with Variable Temperature and Mass Diffusion," *Trans. Porous Med.*, vol. 96, pp. 135-151, 2013.
- [58] D. Pal and H. Mondal, "Influence of thermophoresis and Soret–Dufour on magnetohydrodynamic heat and mass transfer over a non-isothermal wedge with thermal radiation and Ohmic dissipation," *J. Magn. Magn. Mater.*, vol. 331, pp. 250-255, 2013.
- [59] B. K. Sharma, S. Gupta, V. V. Krishna, and R. Bhargavi, "Soret And Dufour effects on an unsteady MHD mixed convective flow past an infinite vertical plate with Ohmic dissipation and heat source," *Afrika Matem.*, pp. 1-23, 2013.

- [60] M. Turkeyilmazoglu, "The analytical solution of mixed convection heat transfer and fluid flow of a MHD viscoelastic fluid over a permeable stretching surface," *Inter. J. Mech. Sci.*, vol. 77, pp. 263-268, 2013.
- [61] J. Merkin, "Natural-convection boundary-layer flow on a vertical surface with Newtonian heating," *Inter. J. Heat Fluid.*, vol. 15, pp. 392-398, 1994.
- [62] R. Chaudhary and P. Jain, "Unsteady free convection boundary-layer flow past an impulsively started vertical surface with Newtonian heating," *Rom. J. Phy.*, vol. 51, pp. 911-925, 2006.
- [63] M. Salleh, R. Nazar, and I. Pop, "Forced convection boundary layer flow at a forward stagnation point with Newtonian heating," *Chem. Eng. Commun.*, vol. 196, pp. 987-996, 2009.
- [64] P. Mebine and E. M. Adigio, "Unsteady free convection flow with thermal radiation past a vertical porous plate with Newtonian heating," *Turk. J. Phy.*, vol. 33, pp. 109-119, 2009.
- [65] M. Salleh, R. Nazar, and I. Pop, "Modeling of free convection boundary layer flow on a solid sphere with Newtonian heating," *Acta Appl. Mathe.*, vol. 112, pp. 263-274, 2010.
- [66] M. Narahari and M. Y. Nayan, "Free convection flow past an impulsively started infinite vertical plate with Newtonian heating in the presence of thermal radiation and mass diffusion," *Turk. J. Eng. Env. Sci.*, vol. 35, pp. 187-198, 2011.
- [67] R. N. M. Z. Salleh , N. M. Arifin , I. Pop ,J. H. Merkin, "Forced-convection heat transfer over a circular cylinder with Newtonian heating," *J. Eng. Math.*, vol. 69, pp. 101-110, 2011.
- [68] G. Singh and O. D. Makinde, "Computational Dynamics of MHD Free Convection Flow along an Inclined Plate with Newtonian Heating in the Presence of Volumetric Heat Generation," *Chem. Eng. Commun.*, vol. 199, pp. 1144-1154, 2012.
- [69] M. Narahari and B. K. Dutta, "Effects of thermal radiation and mass diffusion on free convection flow near a vertical plate with Newtonian heating," *Chem. Eng. Commun.*, vol. 199, pp. 628-643, 2012.

- [70] S. Das, C. Mandal, and R. Jana, "Radiation effects on unsteady free convection flow past a vertical plate with Newtonian heating," *Inter. J. Compu. Appl.*, vol. 41, pp. 36-41, 2012.
- [71] Youn J. Kim, "Unsteady MHD convection flow of polar fluids past a vertical moving porous plate in a porous medium," *Inter. Commun. Heat Mass Trans.*, vol. 44, pp. 2791-2799, 2001.
- [72] D. Lesnic, D. Ingham, and I. Pop, "Free convection boundary-layer flow along a vertical surface in a porous medium with Newtonian heating," *Inter. J. Heat Mass Trans.*, vol. 42, pp. 2621-2627, 1999.
- [73] R. Chaudhary and P. Jain, "An exact solution to the unsteady free-convection boundary-layer flow past an impulsively started vertical surface with Newtonian heating," *J. Eng. Phy. Thermo.*, vol. 80, pp. 954-960, 2007.
- [74] M. Narahari and A. Ishak, "Radiation effects on free convection flow near a moving vertical plate with Newtonian heating," *J. Appl. Sci.*, vol. 11, pp. 1096-1104, 2011.
- [75] O. D. Makinde, "Effects of viscous dissipation and Newtonian heating on boundary-layer flow of nanofluids over a flat plate," *Inter. J. Num. Heat Fluid*, vol. 23, pp. 1291-1303, 2013.
- [76] P. H. Oosthuizen and D. Naylor, "An introduction to convective heat transfer analysis", McGraw Hill, New York, 1999.
- [77] A. Bejan, "Convection Heat Transfer", 3<sup>rd</sup> Ed., Wiley, 2004.
- [78] V. J. Rossow, *On flow of electrically conducting fluids over a flat plate in the presence of a transverse magnetic field*: NASA, Report No. 1358, 489, 1958.
- [79] A. A. Raptis and V. M. Soundalgekar, "MHD flow past a steadily moving infinite vertical porous plate with constant heat flux," *Nuc. Eng. Des.*, vol. 72, pp. 373-379, 1982.
- [80] A. Raptis, N. Kafousias, and G. Tzivanidis, "Hydromagnetic free convection effects on the oscillatory flow of an electrically conducting rarefied gas past an infinite vertical porous plate," *Nuc. Eng. Des.*, vol. 73, pp. 53-68, 1982.
- [81] B. Gebhart and L. Pera, "The nature of vertical natural convection flows resulting from the combined buoyancy effects of thermal and mass diffusion," *Int. J. Heat Mass Trans.*, vol. 14, pp. 2025-2050, 1971.

